UNIVERSITEIT VAN PRETORIA
UNIVERSITY OF PRETORIA
YUNIBESITHI YA PRETORIA

ON THE ENERGY AND SEPARATION EFFICIENCY OF DENSE MEDIUM CYCLONE COAL BENEFICIATION PROCESSES

by

Lijun Zhang

Submitted in partial fulfillment of the requirements for the degree
Philosophiae Doctor (Electrical Engineering)

in the

Department of Electrical, Electronic and Computer Engineering
Faculty of Engineering, Built Environment and Information Technology

UNIVERSITY OF PRETORIA

April 2016

SUMMARY

ON THE ENERGY AND SEPARATION EFFICIENCY OF DENSE MEDIUM CYCLONE COAL BENEFICIATION PROCESSES

by

Lijun Zhang

Promoter(s):	Prof. Xiaohua Xia
Department:	Electrical, Electronic and Computer Engineering
University:	University of Pretoria
Degree:	Philosophiae Doctor (Electrical Engineering)
Keywords:	Coal beneficiation, dense medium cyclone, energy efficiency, separation efficiency, pumped-storage system, feed-forward control, closed loop control, dual loop control, sampled and delayed measurements.

In light of the energy shortage and environmental pollution, improving the energy efficiency of energy-intensive industrial processes is a research topic of increasing importance. The mining industry is one such heavy energy user. In particular, pumping systems are responsible for a noticeable portion of the total energy usage and they are identified as an area of potentially high energy efficiency improvement. This thesis studies one of the most important processes in coal mining industry, dense medium cyclone (DMC) coal beneficiation process, in terms of energy and separation efficiency improvement. The pumping system used in the DMC process is studied to reduce its energy consumption and associated costs. The DMC coal cleaning process is investigated to improve its separation efficiency with the aim of efficient coal utilization and therefore conservation of the non-renewable coal resource. Energy efficiency and separation efficiency are first studied individually before an integrated solution to both of them is designed.

For energy efficiency improvement, a pumped-storage system (PSS) is introduced to the existing pumping system supplying dense medium to the DMC process. This PSS essentially introduces a structural change to the existing medium circulation in the DMC circuit to save energy. The main

idea of introducing PSS to the DMC coal preparation process is to prevent energy wastage due to the industrial practice of constant medium over-pumping. The PSS adds additional medium circulation loops in the DMC coal washing plant to pump over-pumped medium back to the DMC process with a smaller pump. Optimal operation of the PSS requires dealing with multi-pumps and medium storage equipment, which is a challenging task. To achieve optimal operation, a mathematical model of the PSS is developed and the optimal operation of the pumps is formulated into a binary integer programming problem. The solution of the formulated operation problem is then used in economic analysis of the PSS with life cycle cost and payback period techniques to determine its financial effectiveness and viability. According to a case study based on a real-world coal beneficiation plant, it is concluded that the PSS is a financially favorable solution to reduce energy consumption and cost.

In terms of separation efficiency, current industrial practice uses rule-of-thumb and empirically based controls to adjust the density of the medium used to enhance separation in the DMC. There is no model-based controller that is able to improve separation efficiency of the DMC process. Two controllers based on advanced control technology are designed in this thesis to promote separation efficiency of the DMC coal cleaning process. The first one is a feed-forward controller, which optimizes the medium density according to sampled measurements from the ROM coal because many coal washing plants do not measure the composition of the fines yield from the DMC output because of its high cost. This feed-forward controller is essentially an open loop controller and it is designed according to a mass balance model of the DMC using a model predictive control method. To improve the performance of the DMC circuit achieved by the feed-forward controller further, the second controller is designed. This is done by taking advantage of feedback measurements from the output of the DMC to design a closed-loop controller. Some of the coal preparation plants are sending samples from the output of their DMC process to laboratories to analyze the fine coal composition and some of them are planning to invest in on-site measurement devices for this purpose. The closed-loop controller aims to make use of these measurements to improve the performance of the DMC process. In the design of this closed-loop controller, delays in the measurements of fine coal quality are considered. The closed-loop control introduces a change to the control obtained by the feed-forward control according to sampled and delayed measurements from the output of the DMC to improve the performance of the DMC process, making it robust against model plant mismatch (MPM) and external disturbances, which are inevitable in the DMC circuit. Case studies are also conducted to validate the effectiveness of the two controllers that are designed. It is then concluded that closed-loop control is superior to the open loop feed-forward controller in the presence of MPM and external disturbances, as expected. However, it is

obvious that both of the controllers can find their best application in the coal mine according to the specific situation.

Finally, the interplay between the energy and separation efficiency is studied and an integrated control system is designed. The new control system exhibits a dual closed-loop control architecture and features: simultaneous improvement of energy efficiency and separation efficiency; medium density profile optimization by the outer loop controller and direct control of actuators used for the medium density adjustment by the inner loop controller; incorporation of the PSS scheme in the controller design to improve energy efficiency; and use of a model predictive control method to control the DMC process optimally with the ability of looking ahead. In other words, the integrated control system designed is a complete solution to the DMC coal beneficiation process for both energy efficiency and separation efficiency improvement. It combines the benefits of the PSS for energy efficiency and the controllers designed for separation efficiency. In addition, it further extends the controller designed for separation efficiency by including the PSS and magnetite recovery circuit in the controller design, enabling direct manipulation of the actuators used to formulate the medium solutions by the control system that has been designed.

OPSOMMING

AANGAANDE DIE ENERGIE- EN SKEIDINGSDOELTREFFENDHEID VAN DIGTE-MEDIUM-SIKLOONSTEENKOOLVEREDELINGPROSESSE

deur

Lijun Zhang

Promotor(s):	Prof. Xiaohua Xia
Departement:	Elektriese, Elektroniese en Rekenaar-Ingenieurswese
Universiteit:	Universiteit van Pretoria
Graad:	Philosophiae Doctor (Elektriese Ingenieurswese)
Sleutelwoorde:	Steenkoolveredeling, digtemediumsikloon, energiedoeltreffendheid, skeidingdoeltreffendheid, pompbergingstelsel, vooruitvoeringkontrole, geslote-luskontrole, dubbelluskontrole, steekproef- en vertraagde metings.

Teen die agtergrond van die energietekort en omgewingsbesoedeling is die verbetering van die energiedoeltreffendheid van energie-intensiewe industriële prosesse ’n navorsingsonderwerp van toenemende belang. Die mynindustrie is een van hierdie groot energieverbruikers. Veral pompstelsels is verantwoordelik vir ’n beduidende deel van die totale energieverbruik en word gesien as een van die gebiede met groot potensiaal vir die verbetering van energiedoeltreffendheid. Hierdie tesis bestudeer een van die belangrikste prosesse in die steenkoolmynindustrie, naamlik die digtemediumsikloonkoolveredelingproses (DMC-proses), wat betref die verbetering van energie- en skeidingdoeltreffendheid. Die pompstelsel wat in die DMC-proses gebruik word, word bestudeer om die energieverbruik daarvan en die gepaardgaande koste te verminder. Die DMC-koolskoonmaakproses word ondersoek om die skeidingdoeltreffendheid daarvan te verbeter met die oog op effektiewe gebruik van steenkool en dus bewaring van die nie-hernubare steenkoolbron. Die energiedoeltreffendheid en skeidingsdoeltreffendheid word eers apart bestudeer voordat ’n geïntegreerde oplossing vir albei ontwerp word.

'n Pompbergingstelsel (PSS) word ingevoeg by die bestaande pompstelsel wat digte medium aan die DMC-proses verskaf, met die oog op die verbetering van energiedoeltreffendheid. Hierdie PSS bring 'n strukturele verandering teweeg in die bestaande mediumsirkulasie in die DMC-kringloop om energie te bespaar. Die hoofdoel met die invoeging van die PSS in die DMC-steenkoolvoorbereidingproses is om vermorsing van energie deur die industriële praktyk van konstante oorpomp van die medium te voorkom. Die PSS voeg addisionele mediumsirkulasielusse in die DMC-steenkoolwas-aanleg by om te veel medium wat oorgepomp is, na die DMC-proses terug te pomp met 'n kleiner pomp. Optimale werkverrigting van die PSS vereis die hantering van multi-pompe en mediumbergingtoerusting, wat 'n uitdagende taak is. Om optimale werkverrigting te verkry, word 'n wiskundige model van die PSS ontwikkel en die optimale werking van die pompe word in 'n binêre heeltalprogramprobleem geformuleer. Die oplossing van die geformuleerde werkverrigtingprobleem word dan gebruik in 'n ekonomiese analise van die PSS met leefsikluskoste en terugbetaaltydperktegnieke om die finansiële doeltreffendheid en lewensvatbaarheid daarvan te bepaal. Na aanleiding van 'n gevallestudie gegrond op 'n werklike steenkoolveredelingaanleg, is tot die gevolgtrekking gekom dat PSS 'n finansieel voordelige oplossing is om energieverbruik en-koste doeltreffend te verminder.

Wat skeidingdoeltreffendheid betref, gebruik nywerhede praktiese en empiries-gebaseerde kontroles om die digtheid van die medium wat gebruik word, aan te pas om skeiding in die DMC te verbeter. Daar is 'n tekort aan model-gebaseerde beheerders wat in staat is om die skeidingsdoeltreffendheid van die DMC-proses te verbeter. Twee beheerders wat op gevorderde beheertegnologie gebaseer is, word in hierdie tesis ontwerp om die skeidingsdoeltreffendheid van die DMC-steenkoolskoonmaakproses te vebeter. Die eerste is 'n vooruitvoerderbeheerder wat die medium-digtheid optimeer volgens monstermetings van die onbehandelde steenkool omdat baie steenkoolwasaanlegte nie die samestelling van die fyn steenkoolopbrengs van die DMC-uitset meet nie omrede die hoë koste. Die vooruitvoerderbeheerder is in werklikheid 'n ooplusbeheerder en is ontwerp volgens 'n massabalansmodel van die DMS deur die gebruik van die modelvoorspellingbeheermetode. Om die werkverrigting van die DMC-stroombaan wat deur die vooruitvoerderbeheerder bereik word verder te verbeter, word die tweede beheerder ontwerp. Dit word gedoen deur terugvoermetings van die uitset van die DMC te benut om 'n geslotelus-beheerder te ontwerp. Sommige steenkoolvoorbereidingaanlegte stuur monsters van die uitset van hulle DMC-proses aan laboratoriums om die samestelling van die fyn steenkool te ontleed en sommige beplan om vir hierdie doel in toestelle te belê. Die doel met die geslote-lusbeheerder is om hierdie metings te gebruik om die werkverrigting van die DMC-proses te verbeter. In die ontwerp van hierdie geslote-lusbeheerder word vertragings in die meting van die

kwaliteit van fyn steenkool in ag geneem. Die geslote-lusbeheerder veroorsaak ’n verandering in die kontrole wat verkry word deur vooruitvoerkontrole volgens steekproefneming en vertraagde metings van die uitset van die DMC om die werkverrigting van die DMC-proses te verbeter deur dit robuust te maak teen model-aanlegwanaanpasing (MPM) en eksterne versteurings, wat onvermydelik is vir die DMC-stroombaan. Gevallestudies word ook onderneem om die doeltreffendheid van die twee beheerders wat ontwerp is, te bevestig. Die gevolgtrekking is dan dat gesloteluskontrole beter is as die ooplus-vooruitvoerderbeheerder in die aanwesigheid van MPM en eksterne versteurings, soos verwag word. Dit is nietemin duidelik dat albei beheerders ten beste in steenkoolmyne aangewend kan word volgens die bepaalde situasie.

Ten slotte word die wisselwerking tussen energie en skeidingdoeltreffendheid bestudeer en ’n geïntegreerde kontrolestelsel word ontwerp. Die nuwe kontrolestelsel het ’n tweeledige geslote-lusbeheerargitektuur en -kenmerke: gelyktydige verbetering van energiedoeltreffendheid en skeiding-doeltreffendheid; mediumdigtheidprofieloptimering deur die buitenste luskontroleerder en direkte kontrole van drywers wat vir die mediumdigtheidaanpasing gebruik word deur die binneste lusbeheer-der; en gebruik van die gevorderde modelvoorspellingkontrolemetode om die DMC-proses optimaal te beheer met die vermoë om vooruit te sien. Met ander woorde, die geïntegreerde kontrolestelsel wat ontwerp is, is ’n volledige oplossing vir die DMC-steenkoolveredelingproses wat sowel verbeterde en-ergiedoeltreffendheid as skeidingsdoeltreffendheid betref. Dit kombineer die voordele van die PSS vir energiedoeltreffendheid en die beheerders wat vir skeidingsdoeltreffendheid ontwerp is. Daarbenewens verbeter dit die beheerder wat vir skeidingsdoeltreffendheid ontwerp is verder deur die insluiting van die PSS en magnetietherwinningbaan in die ontwerp van die beheerder, wat direkte manipulasie moontlik maak van die drywers wat gebruik word vir die formulering van die mediumoplossings deur die kontrolestelsel wat ontwerp is.

ACKNOWLEDGMENT

Upon finishing this thesis, I cannot stop thinking about those who have guided me, helped me, supported me, and encouraged me throughout the entire period of my PhD study.

I first would like to express my special appreciation and thanks to my supervisor, Prof. Xiaohua Xia, who has been a tremendous mentor for me. As a world-known scientist in the field of both control and energy systems, he was the first reason I decided to come to South Africa for my doctoral study back in 2012. As the years passed, Prof. Xia not only guided me in terms of conducting research, but also supported me in many other aspects of my life, like a father. He offered me numerous opportunities and guidance in research projects and my academic career. Thanks to him, I was able to be part of the Measurement and Verification team at the University of Pretoria, which is contracted by Eskom, the largest utility company in South Africa, to determine energy savings from energy conservation measures. This offered me opportunities of building connections with the energy industry in the country and gain practical experience in the field of energy engineering. Also thanks to him, I was appointed as a permanent lecturer in the department where I am studying. I am sincerely grateful for his training/supervision/help in many aspects, such as scientific research, practical project handling, industrial involvement, and teaching and student supervision.

I would also like to thank Prof. Jiangfeng Zhang from the University of Strathclyde, Glasgow Scotland and Prof. Xiangtao Zhuan from Wuhan University, Wuhan, China. Prof. Zhang offered me lots of important advice in my early days at the University of Pretoria, and shared many experiences in performance reporting about energy efficiency and demand side management and undergraduate teaching. Prof. Zhuan was the supervisor of my Master's study and he introduced me to Prof. Xia during my study at Wuhan University. I would like to thank him especially for the guidance he offered during my Master's study, which was the first step in my later academic career.

I had a great time in the past years in South Africa also because of the company of many of excellent friends. I met some of them in South Africa and some of them back in China. I would like to thank especially Dr. Xianming Ye and his wife. They have helped me so many times that I cannot even count. I still remember the first day when I arrived South Africa; it was they who picked me up at the Gautrain station and helped me with flat rental, furniture purchase, etc. They helped me in many ways

during the easy times and bad times. For all the new friends that I have met in South Africa, including Ming Zhang, Dr. Donghui Wei and his family, Nan Wang and his family, Bo Wang, Dr. Xueliang Cai's family, Dr. Zhou Wu, Dr. Bing Zhu, and Jun Mei, etc. I would like to thank them all for their kindness and company in the years we spent together. I know there is a long list and I wouldn't be able to mention everyone here. So, I would like to express my gratefulness to all of my friends. It was you who made my life joyful.

Thanks are extended to the students whom I have supervised, among others Michael Chennells, Arnab Chatterjee, Maria Michael, and Lesiba Mokgonyana. They have all done a great job during their study, which made my early student supervision experience pleasant and fruitful. I have learned a lot from them.

Lastly but most importantly, I want to thank my family for their unwavering love and support. I know I have come a long way in the journey of pursuing my studies and academic career since I was a young boy. Many years have passed and if something remained the same in this course, it's the love of my family. They have always been supportive of my decisions, even it meant that I would not be able to go home and visit them often. I am forever indebted to my family members. In particular, I would like to express extensive gratitude to my wife, Yuling Fan, for her support, understanding and love. She was only my girlfriend when I decided to further my studies in a foreign country, South Africa. I thank her for coming together with me to this unfamiliar place. Thanks also for her caring, patience and selfless love through the days of laughter and tears. It is she who made my life happy and meaningful in many ways and it is she who made this thesis possible.

Lijun Zhang
University of Pretoria, South Africa
April 2016

PUBLICATIONS

PUBLICATIONS RELEVANT TO THIS THESIS

Two journal papers and four conference papers on the topic of this thesis have been published.

[J1] L. Zhang, X. Xia, and J. Zhang, "Medium density control for coal washing dense medium cyclone circuits," *IEEE Transactions on Control Systems Technology*, vol. 23, no. 3, pp. 1117–1122, 2015.

[J2] L. Zhang, X. Xia, and J. Zhang, "Improving energy efficiency of cyclone circuits in coal beneficiation plants by pump-storage systems," *Applied Energy*, vol. 119, pp. 306 – 313, 2014.

[C1] L. Zhang, X. Xia, and B. Zhu, "Magnetite and water addition control for a dense medium coal washing circuit," in *Chinese Automation Congress (CAC), 2015*, Wuhan, China, pp. 1744–1749, 27–29 Nov 2015.

[C2] L. Zhang and X. Xia, "Coal washing plant cyclone module control with a pump-storage system," in *2015 34th Chinese Control Conference*, Hangzhou, China, pp. 1185–1190, 28–30 July 2015.

[C3] L. Zhang and X. Xia, "A model predictive control for coal beneficiation dense medium cyclones," in *19th World Congress of the International Federation of Automatic Control*, vol. 19, Cape Town, South Africa, pp. 9810–9815, 24-29 August 2014.

[C4] L. Zhang and X. Xia, "An optimization model for reducing energy usage of coal washing plants," in *2014 International Conference on Applied Energy*, Taipei, Taiwan, 30 May - 02 June 2014.

PUBLICATIONS ON OTHER TOPICS

Five journal papers and two conferences papers have been published during the same period of my PhD study.

[J1] A. Chatterjee, L. Zhang, and X. Xia, "Optimization of mine ventilation fan speeds according to ventilation on demand and time of use tariff," *Applied Energy*, vol. 146, pp. 65 – 73, 2015.

[J2] L. Zhang and X. Zhuan, "Optimal operation of heavy-haul trains equipped with electronically controlled pneumatic brake systems using model predictive control methodology," *IEEE Transactions on Control Systems Technology*, vol. 22, no. 1, pp. 13–22, 2014.

[J3] X. Ye, X. Xia, L. Zhang, and B. Zhu, "Optimal maintenance planning for sustainable energy efficiency lighting retrofit projects by a control system approach," *Control Engineering Practice*, vol. 37, no. 0, pp. 1 – 10, 2015.

[J4] L. Zhang and X. Zhuan, "Development of an optimal operation approach in MPC framework for heavy haul trains," *IEEE Transactions on Intelligent Transportation Systems*, vol. 16, no. 3, pp. 1391–1400, 2015.

[J5] L. Zhang and X. Zhuan, "Braking-penalized receding horizon control of heavy-haul trains," *IEEE Transactions on Intelligent Transportation Systems*, vol. 14, no. 4, pp. 1620–1628, 2013.

[C1] L. Zhang and X. Xia, "An integer programming approach for truck-shovel dispatching problem in open pit mines," in *7th International Conference on Applied Energy*, Abu Dhabi, UAE, 28–31 March 2015.

[C2] A. Chatterjee, X. Xia, and L. Zhang, "Optimisation of mine ventilation fan speeds on demand," in *2014 International Conference on the Industrial and Commercial Use of Energy*, Cape Town, South Africa, 18–20 August 2014.

LIST OF ABBREVIATIONS

ROM	Run-of-mine
DMC	Dense medium cyclone
MPC	Model predictive control
DCLC	Dual closed-loop control
TOU	Time-of-Use
CFD	Computational fluid dynamics
PSS	Pumped-storage system
R	South African currency rand
DOE-SA	Department of Energy, Republic of South Africa
NT-SA	National Treasury, Republic of South Africa
CO_2	Carbon dioxide
EEDSM	Energy efficiency and demand side management
LCC	Life cycle cost
MPM	Model plant mismatch
P1	Corrected medium pump
P2	Returned medium pump
S1	Corrected medium sump
S2	Returned medium sump
S3	Re-mix sump

TABLE OF CONTENTS

LIST OF FIGURES

LIST OF TABLES

LIST OF SYMBOLS

α	ratio at which the slurry inside the DMC is splited into two streams
β	percentage of the magnetite that reaches the magnetic separator
Δh	height of S3
ΔP	pressure drop across the valve
Δu	change of control action obtained by the closed-loop controller
δ	vector with uniformly distributed random numbers on $[0, 1]$
$\Delta\rho_m$	limit on the rate of change of ρ_m
η_p	combined energy efficiency of the pump and its drive
η_s	separation efficiency of the magnetic separator
ρ_m	density of the dense medium
ρ_m^b	bulk density of the magnetite
ρ_m^l	lower limit of ρ_m
ρ_m^u	upper limit of ρ_m
ρ_o	density of the slurry that reports to the overflow of the DMC
ρ_u	density of the slurry that reports to the underflow of the DMC

ρ_{ash} density of ash content

ρ_c vector $[\rho_{ash}, \rho_S, \rho_{H_2O}, \rho_{vol}]^T$

ρ_{H_2O} density of water

ρ_{mb} density of the the mixed slurry

ρ_m^p density of magnetite particles

ρ_{rm} density of the condensed magnetite from the outlet of the magnetic separator

ρ_S density of sulfur

ρ_{vol} density of volatile matter

ρ_w density of water in the dense medium

C_s electricity cost savings of the PSS

C_w valve coefficient

CC capital cost of the PSS options

d annual deprecation ratio of the facilities

$d(k)$ modeling error

d_T diameter of S3 in case of a cylindrical sump

E energy consumption of the existing corrected medium pump

E_B energy consumption of the benchmark controller

E_s energy savings of the PSS

E_{DCLC} energy consumption of the dual closed-loop controller

E_{PSS}^{day} daily kWh energy consumption of the pumps in the PSS

g	gravitational acceleration
h_0	differential head of the existing corrected medium pump
h_1	differential head of P1
h_2	differential head of P2
k	current sampling instant kT_s
k_e	weighting factor
K_o	DMC specific constant
k_p	weighting factor
K_u	DMC specific constant
$K_{o,c}$	DMC specific constant vector
$K_{o,m}$	DMC specific constant
$K_{u,c}$	DMC specific constant vector
$K_{u,m}$	DMC specific constant
l_w	valve position
m	maintenance ratio
m_m	mass flow rate of magnetite reaching the magnetic separator
MC	maintenance cost of the PSS options
N	speed of the screw conveyor
n	project lifetime in years
N_c	control horizon of the closed-loop MPC

n_c	number of DMC modules in the plant
N_c^{in}	control horizon of the inner loop controller
N_p	optimization horizon of the closed-loop MPC
N_p^{in}	optimization horizon of the inner loop controller
n_y	last year with a negative cumulative cash flow
OC	operating cost of the PSS options
$p(t)$	The electricity price at time t
q	annual increase of electricity price
Q_0	screw conveyor related constant
Q_1	volume flow rate of P1
Q_2	volume flow rate of P2
Q_m	required medium volume flow rate to the medium splitter
Q_m^p	flow rate of magnetite particles in the dense medium
Q_{cm}	flow rate of medium to the DMC
Q_{mb}	flow rate of the mixed slurry feeding to the DMC
Q_{mm}	flow rate of magnetite added by the screw conveyor
Q_{rm}	flow rate of the condensed medium
Q_w	flow rate of water in the dense medium
QI	performance indicator of the separation efficiency
r	discount rate

r_m^V	percentage at which the medium pumped to the splitter is returned to the PSS circuit
SV	salvage value of the PSS options
T	time duration of a day
T_s	sampling period of the outer loop controllers
T_s^{in}	sampling period of the inner loop controller
$u(k)$	control action at time k
u^0	control action obtained by the feed forward controller
$u_1(t)$	on/off status of P1 at time t
$u_2(t)$	on/off status of P2 at time t
V_2	volume of medium in S2
V_2^{max}	capacity of S2
V_2^{min}	minimum volume of medium allowed in S2
V_3	volume of medium in S3
V_3^{max}	capacity of S3
V_3^{min}	minimum volume of medium allowed in S3
V_m	volume of the re-mix box
V_o	volume of slurry that reports to the overflow of the DMC
V_s	volume of slurry inside the DMC
V_u	volume of slurry that reports to the underflow of the DMC
V_{cor}	volume of medium in the corrected medium sump

V_{mb} The volume of the DMC feed sump

W_i mass flow rate of the slurry to the DMC

W_{ore} mass flow rate of the ROM coal

$x(k)$ state of the DMC at time k

x^0 state of the DMC reached by the feed forward controller

$x_r(k)$ desired carbon percentage in the fine coal at time k

$x_{i,ash}$ mass percentage of ash in the mixed slurry feeding to the DMC

$x_{i,C}$ mass percentage of carbon content in the slurry feeding to the DMC

$x_{i,c}$ vector $[x_{i,ash}, x_{i,S}, x_{i,H_2O}, x_{i,vol}]^T$

x_{i,H_2O} mass percentage of moisture in the mixed slurry feeding to the DMC

$x_{i,m}$ mass percentage of dense medium in the mixed slurry feeding to the DMC

$x_{i,S}$ mass percentage of sulfur in the mixed slurry feeding to the DMC

$x_{i,vol}$ mass percentage of volatile matter in the mixed slurry feeding to the DMC

$x_{o,ash}$ mass percentage of ash in the DMC overflow

$x_{o,c}$ vector $[x_{o,ash}, x_{o,S}, x_{o,H_2O}, x_{o,vol}]^T$

$x^0_{o,C}$ mass percentage of carbon content in the fines reached by the feed forward controller

$x^l_{o,C}$ lower limit of carbon percentage in the fines

$x^u_{o,C}$ upper limit of carbon percentage in the fines

x_{o,H_2O} mass percentage of moisture in the DMC overflow

$x_{o,m}$ mass percentage of dense medium in the DMC overflow

$x_{o,S}$ mass percentage of sulfur in the DMC overflow

$x_{o,vol}$ mass percentage of volatile matter in the DMC overflow

$x_{ore,ash}$ mass percentage of ash in the ROM coal

$x_{ore,c}$ vector $[x_{ore,ash}, x_{ore,S}, x_{ore,H_2O}, x_{ore,vol}]^T$

x_{ore,H_2O} mass percentage of moisture in the ROM coal

$x_{ore,S}$ mass percentage of sulfur in the ROM coal

$x_{ore,vol}$ mass percentage of volatile matter in the ROM coal

$x_{u,ash}$ mass percentage of ash in the DMC underflow

$x_{u,c}$ vector $[x_{u,ash}, x_{u,S}, x_{u,H_2O}, x_{u,vol}]^T$

x_{u,H_2O} mass percentage of moisture in the DMC underflow

$x_{u,m}$ mass percentage of dense medium in the DMC underflow

$x_{u,S}$ mass percentage of sulfur in the DMC underflow

$x_{u,vol}$ mass percentage of volatile matter in the DMC underflow

CHAPTER 1 INTRODUCTION

1.1 THE DMC FINE COAL CLEANING PROCESS

Efficient utilization of fossil fuel resources is gaining increasing attention in order to mitigate the carbon footprint in the global environment. In particular, cleaner use of coal is of vital importance in this regard because coal is still the largest contributor to electricity generation [1]. This thesis deals with fine coal cleaning processes that remove undesirable impurities from run-of-mine (ROM) coal to reduce pollutant emission and improve the efficiency of coal combustion processes.

ROM coal has different impurities such as ash and sulfur contents, depending on the geologic conditions and mining techniques employed [2]. Cleaning the ROM coal to remove excessive impurities for efficient and environmentally safe utilization is the main task of coal preparation processes [3, 4]. Better cleaning efficiency of the coal washing plant means more efficient utilization of the coal resource and less toxic gas emission during the burning process of the product, coal.

In particular extraneous, non-combustible materials, such as sulfur and ash, are the root cause of emission of SO_x, NO_x, and particulate matter. Removal of such impurities reduces transportation cost per unit of heat and guarantees consistent heat value of coal supplied to customers, whose plant efficiency usually depends on the quality of its incoming coal [5]. For instance, the properties and the quantities of the impurities in coal are of major concern in the design and operation of coal-fired steam generating equipment that is extensively used by utilities for power generation. Therefore, the separation efficiency of coal cleaning processes has a direct influence on many power generating plants and industrial processes that use coal as their primary source of power.

Different cleaning methods are employed to remove impurities in ROM coal, such as advanced

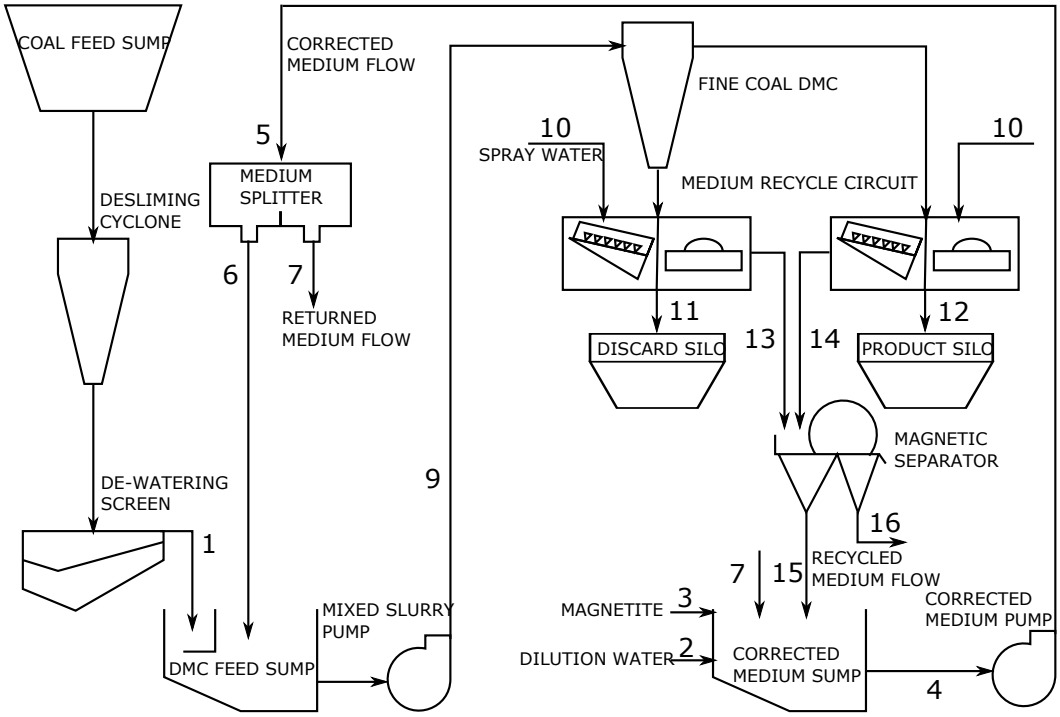

Figure 1.1. Typical DMC coal cleaning circuit

floatation [6, 7, 3, 8], dense medium vessels and compound spirals [9, 10, 11], etc. The most popular and productive coal cleaning technique for fine coal cleaning is the dense medium cyclone (DMC) washing process that features high separation efficiency at high tonnages [12]. DMCs are essentially gravity-based separation equipment in which particles with different densities are classified and beneficiated. The basic working principle of a DMC is that, with the help of dense medium that has a density between that of the fine coal and the rejects, the lighter coal particles float while the heavier rejects sink, causing the fine coal product and reject to discharge at the overflow and underflow of the cyclone, respectively [13]. A typical DMC based coal cleaning circuit is shown in Fig. 1.1, in which the material flows are numbered for the sake of clarity. The same number indicates the same material flow. Before entering the DMC process, the ROM coal is first processed by a de-sliming cyclone and de-watering screen, after which it (flow stream marked as 1 in Fig. 1.1) is fed to the DMC feed sump where it is blended with the dense medium (flow stream 6). This mixed coal and medium slurry (flow stream 9) is then fed to the DMC for separation. In the DMC, the carbon content and impurities of the ROM coal are separated and exit at the top and bottom of the DMC, respectively. These two streams of slurries from the output of the DMC are subject to drain and rinse screens to remove magnetite from the product and the discard. The final outputs are stored in the product silo and discard silo respectively for further processing and the diluted medium slurries (flow streams 13 and 14) are then collected and

sent to a magnetic separator for magnetite recovery.

The recovered medium (flow stream 15) is in the form of condensed medium and fed to a corrected medium sump, where extra magnetite and water are added to formulate the required medium solution with proper density. The whole process starts with the in-flows, flow streams 1, 2 and 3, to the DMC circuit and ends at flow stream 15, which enters the corrected medium sump. This process is repeated constantly with new ROM coal being beneficiated.

Although DMC cleaning processes are widely used and efficient in coal beneficiation, they are very energy-intensive. Reducing the energy consumption of these processes is an urgent task for coal mines. Especially since many coal mines and their preparation plants were built a long time ago when the price of electricity was low. These mines are losing revenue today because of the alarmingly increased electricity price, which forces them to investigate options to decrease consumption.

In summary, improving both separation efficiency and energy efficiency of the DMC coal beneficiation process is a concern of high priority for modern coal preparation plants. In this thesis, this problem is investigated in detail and solutions yielding separation efficiency and energy efficiency improvement are proposed. These solutions are then combined to offer a complete solution to coal washing plants in terms of energy and separation efficiency.

1.2 LITERATURE REVIEW

1.2.1 Energy efficiency

With growing concern about the environment and energy security across the globe, research in these areas is becoming more and more popular. Ever-increasing electricity demands mean that many countries are facing threats of energy shortage, such as electricity blackouts that result in enormous economic losses [14]. To avoid such blackouts, studies are done in the field of rolling blackouts [15], demand response programs [16], etc. Reducing energy consumption by energy efficiency and demand side management (EEDSM) technologies has proven to be an effective and rapid remedy to bridge the gap between electricity supply and demand [17, 18, 19, 20, 21]. Specifically, application of EEDSM to energy-intensive and/or large-scale systems usually leads to remarkable results in terms of

consumption reduction, grid strain relief and emission reduction [22, 17]. For highly energy-intensive mining processes, a small percentage of energy efficiency improvement usually translates to noticeable energy and economic benefits [17].

This is of particular interest for economies that depend heavily on the mining industry. South Africa such an economy. According to Eskom, the public electricity utility in South Africa, the mining industry consumes about 15% of Eskom's annual output[1]. Moreover, electricity contributed 56% to the mining industry's energy usage from 2002 to 2009 in South Africa, according to available statistics[2]. This implies that reducing electricity consumed by the coal mines contracted to power stations can offer a great opportunity for alleviating grid pressure and improving the country's energy scenario.

Many coal washing plants in South Africa were built many years ago when electricity demand was low. The overall design adopted at that time was about limiting capital expenditure and operational downtime rather than focusing on energy efficiency. However, this needs to be reconsidered in view of the changes in the country's energy scenario. The South African Department of Energy (DOE-SA) has compiled an integrated resource plan for electricity to promote energy efficiency and emission reduction in industrial processes and improve the efficiency of coal-fired power plants in the last decade [23]. In addition to that, the National Treasury of South Africa (NT-SA) has published a policy paper on carbon tax, which imposes a carbon tax starting at R40 per tonne of CO_2 equivalent emission in 2015 and will escalate this rate to R117/ton in 2025 [23, 24]. In light of these new regulations, improving the energy efficiency of the coal mining processes and that of coal-fired power plants (which supply almost 96% of the total generating capacity in South Africa [25]) is gaining more and more attention.

In addition, because of the fast increase in the electricity price, the energy efficiency of such mining processes has been brought to the attention of plant managers. In particular, pumping systems in mines usually operate at very low energy efficiency because the pumps used are usually over-sized and their operation only considers operational safety. Therefore, there is a great opportunity for reducing energy consumption of DMC coal processing plants by energy-efficient pumping systems. This corresponds to one of the most important areas in the mining industry in terms of energy efficiency improvement,

[1] Eskom 2011, Towards an energy efficient mining sector.
[2] Statistics South Africa 2012, D0405.1.1-Energy accounts for South Africa, 2002-2009 (Discussion document).

namely pumping systems, which have been assessed to be able to save 14% of the total electricity costs of a mine if proper energy efficiency solutions are applied[3].

For the DMC circuitry in consideration, the dense medium is pumped from the bottom of the plant to the DMC module, which is usually 30–80 meters high above the ground (see Fig. 1.1 where the dense medium is pumped up to the medium splitter by the corrected medium pump). The pumping energy required therefore contributes a large proportion of the DMC's operating cost. Moreover, the corrected medium pump is usually over-sized in many coal beneficiation plants. For instance, an energy audit conducted for a South African coal preparation plant revealed that only 25% of the medium pumped to the DMC module entered the DMC separation process while the other 75% simply flowed back to the corrected medium sump. Therefore, the pumping system supplying medium to the DMC process was running at a staggering 75% over-pumping rate. In view of this, reducing energy waste of the pumping system offers good potential for energy efficiency improvement.

Inspired by the application of a pumped-storage system (PSS) in industrial systems for energy efficiency improvement, it is proposed in this thesis to introduce a PSS to the DMC circuit to reduce energy wastage. It has been found that application of PSS to coal washing plants has not been studied in the literature, although application of PSS in power plants has been extensively reported, such as [26, 27]. Therefore, introducing PSS to the process requires schematic change to the plant, mathematical modeling of the PSS system, and operational control of the reconfigured pumping system. Introduction of a PSS to the DMC circuit essentially creates a multi-pump system, whose operation must be optimized to achieve the desired energy efficiency improvement. In addition, optimal operation of the pumping system will result in economic benefits in light of the time-based electricity tariffs that prevail today. In this respect, the operation of multi-pumps is complex and still under investigation by many researchers, although switching control of a single pump is not technically expensive [28, 29]. The current practice for controlling such a system resorts to rule-based methods [30, 31]. In recent years, mathematical techniques have been introduced to solve this problem, such as the optimization of pumping stations and air conditioning systems undertaken in 2012 and 2013 [32, 33, 28, 34, 29].

In pump station studies, [33] presented an improved dynamic programming method for single-pump operation in a pumping station in order to reduce energy cost. [28] extended the results of [33] to multi-pump operation with pump switching cost considered. The focus of [33] and [28] is to reduce

[3]U.S. Department of Energy 2007, Mining Industry Energy Bandwidth Study.

the computation time incurred with the pump operation scheduling problem. In [34], multi-pump control of a pump station with the objective of minimizing pump switching frequency is presented. It gives a two-stage control strategy that first determines the number of pumps that should be running and then decides which pump specifically to turn on (off). The pump operation only has ten states and thus the algorithm is a kind of switching control between different states.

Similarly, a decision-making procedure is proposed in [32] and the pump operation scheduling of a water distribution system is investigated in [29] to reduce energy consumption.

The operation problem is essentially a switching control problem, which is mainly solved either by a dynamic programming method [33, 28] or heuristic decision-making methods [32, 34] in those studies. The introduction of time-based electricity tariffs that aim to reduce peak load and relief grid pressure further imposes difficulties for the optimal operation of such multi-pump systems.

In summary, based on findings from the literature and the energy audit of a South African coal washing plant, a PSS is introduced to the DMC fine coal cleaning circuit to improve its energy efficiency. The structural configuration, optimal operation control and economic benefits of the PSS for a DMC coal beneficiation plant are investigated with the goal of reducing energy consumption and hence the cost of the plant. Details of the PSS are presented in Chapter 2 of this thesis.

1.2.2 Separation efficiency

The effectiveness of the DMC coal cleaning process directly determines the quality of the yield fine coal from the coal preparation plant. Improving the effectiveness of the cleaning process is therefore of extreme importance because the market is seeking cleaner coal to comply with tighter environmental regulations promoting sustainable and environmentally friendly development.

As mentioned earlier, the impurities carried in the ROM coal and fine coal, if not cleaned effectively, are the root cause of environmental pollution, high transportation cost and decreased efficiency of coal-fired power generating units and industrial processes. In other words, the non-carbon contents have a deterministic effect on the quality (e.g. heating value) of the coal if the coal is not cleaned thoroughly [35, 36]. For instance, the carbon content in coal that has not been cleaned well cannot

be fully burnt, which results in waste of coal resources and lower efficiency of the process using this coal.

From the viewpoint of coal processing companies, they are forced to improve the quality of their products and reduce energy consumption owing to market competition and the sharp increase in the energy price today. To obtain high-quality coal, the percentage of fixed carbon content in the fines is usually monitored and used as an indicator of the quality of the fine coal [37, 38] since removing all the non-carbon components cannot be easily realized in practice.

To achieve the target of removing impurities from ROM coal, a well-designed control system is essential. This is the same for any industrial system, as discussed in [39, 40, 41, 42]. This is no different for the mining industry, as shown in numerous publications such as [43, 44, 45, 46, 47]. For the DMC coal beneficiation process, the quality of the coal yielded is controlled by the relative density of the dense medium used to enhance the separation. The density of the medium plays the key role in determining the quality of the yield from the DMC circuit and a proper controller is required to adjust this density. As the characteristics of the ROM coal vary, this controller is of essential importance to the DMC coal cleaning process and must have the ability to adapt the medium density according to variations in the quality of the ROM coal.

Current industrial practice and studies in literature control the DMC process by adjusting the relative density of the medium according to rules-based approaches [48] or applying control theory to an empirical DMC model obtained by data fitting using experimental operational data from the process [49, 50]. Drawbacks of the empirical approaches are twofold. Firstly, detailed information on different compositions (fixed carbon, ash, sulfur, etc.) in the fine product is unknown because of the nature of the curve-fitted model, which roughly predicts the probability of particles with a certain density report to the overflow of the DMC. Secondly, the structure and parameters of the cyclone model are process-specific and have no clear physical meanings, which makes it difficult to fine-tune the controller that has been designed.

In view of this, a properly designed, model-based control system for the DMC processes to improve their performance is required. To achieve this, mathematical modeling of the characteristics of the DMC and the medium supplying circuit is a prerequisite. As for the model of the medium supplying circuit, a mass balance based model is presented in this study because no study has been reported in

literature to model and control the DMC circuit. For the DMC model, it is found that mainly two types of models have been developed. The first one is empirical models [51, 52] that predicts the probability of reporting to the fines (rejects) for particles with different densities by polynomial equations fitted to experimental data. Shortcomings of this kind of model is that the percentages of different components in the fines and rejects are not calculated and the equations are static (the state of operation of the DMC is not considered) and DMC-specific. Designing a controller according to them is impossible because those equations do not consider the density of medium used [52]. The second type of DMC model developed is based on the computational fluid dynamics (CFD) method [53, 54, 55, 56, 57]. In these CFD models, the continuous fluid dynamics in the DMC is calculated by solving Navier-Stokes equations using commercial software such as FLUENT [53]. The specific movement of coal particles in a DMC was investigated in studies done by Chu et al. [54, 55, 56] that combined the CFD and the discrete element method [58]. The quality of clean coal from the DMC can be determined after solving the model. However, the CFD-based models are very time-consuming to solve, which prohibits their practical application to control system design [59, 12]. This type of model is usually used to help in the designing process of DMCs before they are manufactured [60, 61].

The DMC model most suitable for controller design found in the literature is presented in [62], in which the DMC process is modeled based on its mass flow balance. The variables in the model have clear physical meanings and the parameters are practically identifiable using plant data. In addition, the time required to solve it is acceptable for practical application. Therefore, this model is employed for the controller design presented in this thesis.

In addition to the modeling of the DMC and medium supplying circuit, there is a challenge of dealing with the problem of lack of measurements in the controller design. In current practice of the coal cleaning plants, only sampled and delayed measurements are available to the control system of the DMC circuit [63]. To be specific, compositions of the ROM are sampled and measured according to the geographical location from where the ROM is extracted. This is essentially a sampled and delayed measurement available for the control system as feed-forward measurement. The fine coal quality is also not measured continuously. Fine coal obtained after the DMC processes is usually sampled and sent to a laboratory to analyze its composition because measurement facilities for this purpose are very costly and not available on the site of the plant. This measurement practice, however, causes long delays. The typical time required from the instant the sample is taken to the analysis results reach the mine could be hours. This delay, together with the fact that the coal quality is not continuously

measured (sampled), poses challenges to the control system design.

In summary, according to the current practice of coal washing plants and research reported in the literature, there is a need to develop a proper control system to adjust the density of the dense medium supplied to the DMC module, making use of sampled and delayed measurements, to improve the performance of the DMC coal cleaning process in terms of separation efficiency.

Therefore, two controllers, namely one open loop controller and one closed-loop controller, are designed in this thesis to deal with separation efficiency improvement of the DMC fine coal cleaning process using advanced model predictive control (MPC) method. Details of these two controllers are given in Chapter 3 and Chapter 4.

In addition, an integrated control system that considers the interplay of energy efficiency and separation efficiency of the DMC process is designed in Chapter 5. This integrated control system combines the benefits of the PSS for energy efficiency improvement and closed-loop control for separation efficiency improvement to provide a unified energy and separation efficiency improvement solution to the DMC coal beneficiation process. Furthermore, the integrated control system is designed according to a dual loop control architecture with the outer loop optimizing the density profile of the medium and the inner loop directly controlling the water and magnetite addition actuators in the DMC circuit to formulate the required medium solution, taking advantage of mathematical models of the magnetite recovery circuit and that of the PSS.

Following the formulation/design of the proposed PSS and control systems, simulations based on a South African coal beneficiation plant are conducted to validate the effectiveness and financial viability.

1.3 RESEARCH MOTIVATION AND OBJECTIVES

Motivations for undertaking this research can be categorized into two aspects:

- Firstly, energy shortage and carbon emission are two of the the most pressing problems world-wide. Energy shortage is one of the factors limiting economic growth, especially in developing

countries where the electricity supply is falling behind the demand increase due to economic development. Carbon emission is now causing environmental problems such as global warming and possibly global drought. Therefore, this research tries to help bridge the gap between electricity supply and demand in one of the world's most energy-intensive industries, the mining industry, by means of energy efficiency improvement of the coal preparation processes.

- Secondly, efficient utilization of non-renewable resources, such as fossil fuels, is essential in view of resource conservation and sustainable development. To promote efficient utilization and therefore conservation of coal, effective removal of impurities carried in the ROM coal is essential. The efficiency of the combustion process of fine coal depends directly on the quality of the coal, which is characterized by the compositions contained in the fine coal. In addition, energy consumption and thus the cost of transporting the coal from the mine to the process where the coal is burned is also affected by the quality of the fine coal. Additional energy and cost are required to transfer the impurities carried in the coal if the coal is not well cleaned. In other words, the quality of fine coal from the coal preparation plant is the key factor that has a deterministic effect on the transportation efficiency, combustion efficiency, and efficiency of industrial processes that use coal as fuel. Therefore, improving the effectiveness of the coal beneficiation process is of pivotal importance. With this purpose in mind, control systems that are able to improve the separation/cleaning efficiency of the DMC fine coal washing circuit are designed.

The overall objectives of this research are:

- To improve the energy efficiency of the DMC coal beneficiation process in order to reduce energy waste and thus to alleviate grid strain and reduce carbon emission.

- To improve the separation efficiency of the DMC coal cleaning process to facilitate efficient coal utilization in order to promote coal reservation, to reduce energy consumption and associated costs in the transportation of coal with the ultimate goal of promoting green development featuring low emission and low consumption.

- To design an integrated control system that is able to improve both energy efficiency and separation efficiency of the DMC fine coal washing process simultaneously.

1.4 CONTRIBUTION AND LAYOUT OF THESIS

The main contributions of this thesis have been published in two journal articles and another has been submitted for publication. Several conference contributions have also been published and listed in the section on publication. The contributions are briefly summarized below. This summary also serves as a layout description of this thesis.

- Introduction of a PSS to the DMC coal cleaning process to improve its energy efficiency;
- Mathematical modeling, operating strategy design, and economic analysis of the PSS introduced;
- Design of two controllers, including an open loop feed-forward controller and a closed-loop controller, to improve separation efficiency of the DMC coal cleaning process with sampled and delayed measurements;
- Design of an integrated dual closed-loop control system to improve both the energy efficiency (making use of the PSS) and the separation efficiency of the DMC coal washing process; and
- Showcasing of successful application of advanced control techniques feedback decoupling, feedback linearization and MPC.

The layout of this thesis follows the order of improving energy efficiency, separation efficiency, and simultaneous improvement of both energy efficiency and separation efficiency of the DMC coal beneficiation process. Each chapter is an extended version of one journal article.

In particular, Chapter 2 introduces a PSS scheme to improve energy efficiency of the DMC process. The configuration and operational strategy of the PSS are designed first, followed by an economic analysis of the viability and benefits of the PSS.

After that, a feed-forward controller is designed in Chapter 3, where the geologically sampled measurements from the ROM coal are used by the open loop controller as feed-forward information to optimize the density profile of the medium to improve the separation efficiency of the DMC process in

view of the varying quality of the feed coal. Closed-loop measurements are not assumed at this stage because of the lack of an on-site measurement device in DMC coal beneficiation plants.

Moving a step further from this open loop feed-forward controller, a closed-loop controller is designed in Chapter 4 to improve the separation efficiency of the DMC process further. The controller is designed in such a way that it can take sampled and delayed measurements on the compositions of the fine coal yield from the output of the DMC as feedback measurements to close the loop. In particular, the feedback measurements can be obtained either from laboratory tests or on-site measurement equipment that has been introduced (both giving sampled and delayed measurements).

Taking advantage of the PSS for energy efficiency improvement and controllers designed for separation efficiency improvement, an integrated control system is proposed in Chapter 5 to improve the two efficiencies simultaneously. The interplay between energy and separation efficiency that was not considered in Chapters 2-4 is accounted for in the design of the integrated control system. The integrated control system therefore provides a complete solution to the DMC coal cleaning process in terms of both energy and separation efficiency improvement.

Finally, some general conclusions are drawn in Chapter 6, together with some ideas for future research.

CHAPTER 2 A PUMPED-STORAGE SYSTEM FOR ENERGY EFFICIENCY

2.1 CHAPTER OVERVIEW

This chapter presents a pumped-storage scheme (PSS) to improve energy efficiency of the DMC coal cleaning process by means of structural change of the plant to prevent the over-pumped medium from flowing back to the bottom of the plant. In particular, a unified PSS scheme, which can be adopted into two practical options, is presented in Section 2.3, followed by mathematical modeling of the PSS in Section 2.4. The optimal operation problem of the PSS is formulated in Section 2.5 and a life cycle cost (LCC) analysis of the proposed PSS scheme is shown in Section 2.6. Lastly, a case study based on operational data from a South African coal preparation plant is presented in Section 2.7 before a conclusion is drawn in Section 2.8.

2.2 INTRODUCTION

The PSS that is introduced aims to provide the plant with a medium re-circulation ability that allows the over-pumped medium to be pumped back to the distributor without flowing back down to the bottom of the plant. In this way energy consumption and the associated costs are reduced. Two different configurations of the PSS were proposed for the coal beneficiation plant in [64]. A unified representation of the two options is presented in this chapter. A mathematical model of the PSS is established and the corresponding operational strategy under a time-based electricity tariff is formulated into an binary integer optimization problem. In addition, the economic benefits of the proposed PSS options are investigated to validate their viability based on the results obtained from the optimal operating strategy. In order to determine energy savings resulting from the introduced PSS only, the

PSS circuit is isolated from the rest of the DMC circuit according to the International Performance Measurement and Verification Protocol [65]. In particular, density control of the medium is not considered, as this falls outside the PSS boundary. Therefore, the medium density is assumed to be constant throughout all analysis. Only energy savings due to the PSS are reported in the results.

2.3 CONFIGURATION OF THE PSS

The medium circulation in the DMC coal cleaning process shown in Fig. 1.1 is re-arranged to clearly depict the paths of the medium flows in Fig. 2.1, in which the flow stream numbered 7 is the portion of medium that is directed to flow back to the corrected medium sump without entering the DMC cleaning process.

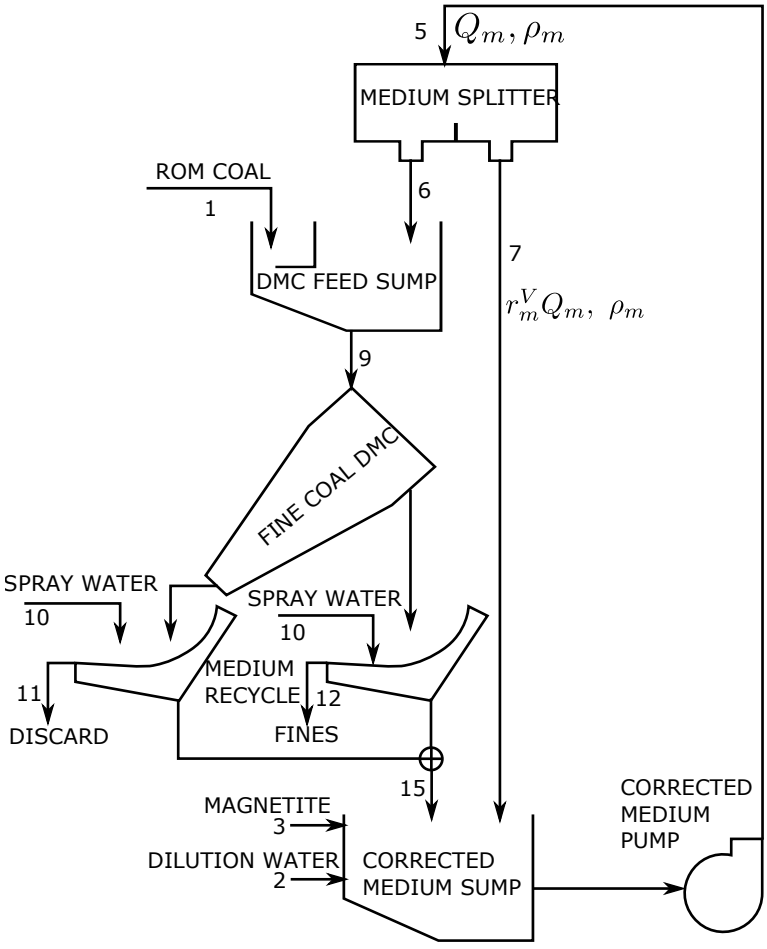

Figure 2.1. Medium circulation in the DMC coal cleaning process

The PSS introduces an additional medium circulation loop to pump the returned medium back up to the medium splitter, as shown in Fig. 2.2. In addition, the PSS is designed in such a way that the amount of medium supplied to the DMC is not affected. The reason for this is that the plant owners are unwilling to risk a quality drop in the yield of the DMC circuit due to insufficient medium supply. Therefore, the proposed approach does not change the medium supply rate to the medium splitter, *i.e.*, the flow rate of the dense medium pumped to the splitter is kept the same as that of the existing system. Instead, the dense medium circuit is changed in configuration and operation to reduce energy costs. The configuration of the PSS is clearly shown in the area surrounded by the red (dotted) line in Fig. 2.2. The medium circulation loop indicated by the flow streams 5→7→8→5 is created by the PSS, which prevents the medium returned by the medium splitter from flowing back to the corrected medium sump. The returned medium is stored in an additional returned medium sump and pumped back up to the medium splitter for re-use by the newly introduced medium pump P2, as shown in Fig. 2.2. It can be seen that the differential head of this added pump P2 can be much less than that of the existing corrected medium pump, therefore the power and energy consumption of the pumping system for medium supply to the DMC module can be reduced.

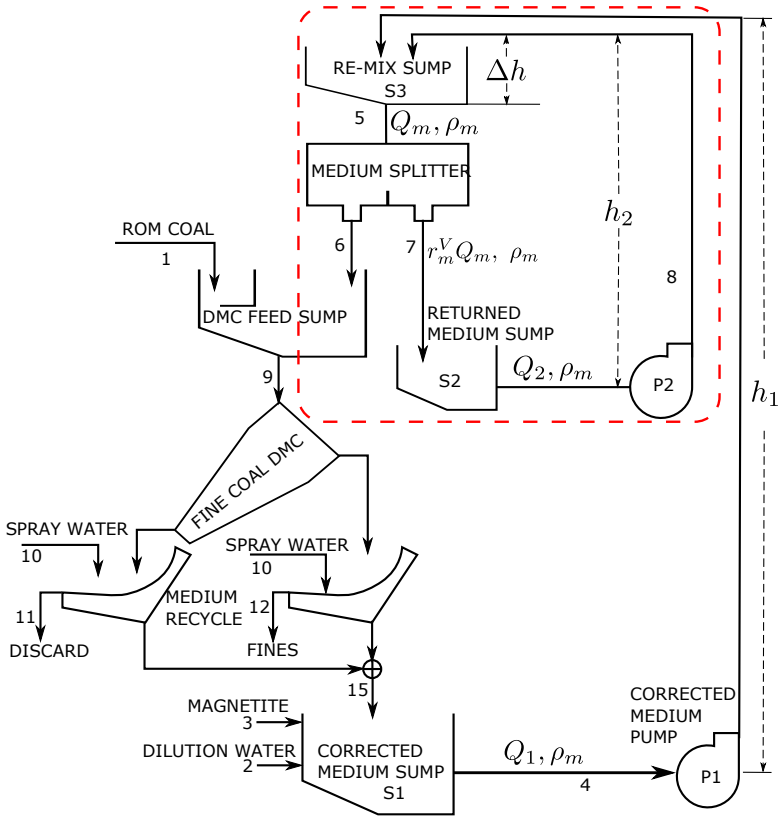

Figure 2.2. PSS configuration for the DMC circuit

2.4 MATHEMATICAL MODELING OF THE PSS

Modeling of the PSS scheme is done with reference to Fig. 2.2, where the corrected medium sump and corrected medium pump are denoted S1 and P1, respectively. The returned medium sump, re-mix sump and returned medium pump introduced by the PSS are denoted S2, S3 and P2, respectively.

Without losing generality, the following assumptions are made in the modeling process:

- There is no medium leakage along the pipes.
- The pumps in the PSS are properly sized and are of the same class of efficiency.
- There is always enough medium in the corrected medium sump to support the DMC beneficiation process.

2.4.1 System dynamics

The volume dynamics of the medium storing sumps in the PSS scheme are modeled according to mass balance as follows:

$$\begin{aligned} \frac{dV_2}{dt} &= r_m^V Q_m - Q_2 u_2(t), \\ \frac{dV_3}{dt} &= Q_1 u_1(t) + Q_2 u_2(t) - Q_m, \end{aligned} \tag{2.1}$$

where V_2 and V_3 are the volumes of medium in S2 and S3, respectively. Q_m, Q_1 and Q_2 are the required medium volume flow rate to the splitter, the volume flow rates of pumps P1 and P2, respectively. r_m^V is the percentage at which the medium pumped to the splitter is returned to the PSS circuit without entering the DMC separation process. The control variables $u_1(t)$ and $u_2(t)$ are the on/off status of P1 and P2:

$$u_1(t) = \begin{cases} 0, \text{ P1 is off;} \\ 1, \text{ P1 is on.} \end{cases} \qquad u_2(t) = \begin{cases} 0, \text{ P2 is off;} \\ 1, \text{ P2 is on.} \end{cases}$$

Daily kWh energy consumption of the pumps in the PSS, E_{PSS}^{day}, is calculated by [66]:

$$E_{PSS}^{day} = \int_0^T \frac{Q_1 \rho_m g h_1 u_1(t) + Q_2 \rho_m g h_2 u_2(t)}{1000 \eta_p} dt, \tag{2.2}$$

where T represents the time of a day, ρ_m is the density of the medium, g is the gravitational acceleration, h_1 and h_2 are the differential heads of P1 and P2, respectively. η_p is the combined efficiency of the

pump and its drives. It is assumed that the pumps are properly sized in the PSS configuration and are of the same class of efficiency. It is also noted that h_1 satisfies

$$h_1 = h_0 + \Delta h, \tag{2.3}$$

where h_0 is the differential head of the existing corrected medium pump and Δh is the height of S3 (see Fig. 2.2). In case a cylindrical sump is used, this can be calculated by

$$\Delta h = \frac{4V_3^{max}}{\pi d_T^2}, \tag{2.4}$$

in which d_T is the diameter and V_3^{max} is the capacity of S3.

2.4.2 Operational constraints

For the PSS presented, operational constraints include capacity limits on S2 and S3 and the binary integer control variables for the on/off status of the pumps aligning to the assumptions made.

$$\begin{aligned} V_2^{min} \leq V_2 \leq V_2^{max}, \\ V_3^{min} \leq V_3 \leq V_3^{max}, \\ u_1(t), u_2(t) \in \{0,1\}. \end{aligned} \tag{2.5}$$

Remark 1 The PSS presented in Fig. 2.2 can actually be adopted into two practical options for the plant, as detailed in [64]. In case addition of S3 is impossible owing to space and/or geographical limits, S3 can be replaced with a small tank that merely serves the purpose of re-mixing the medium pumped by P1 and P2. This results in PSS Option 1 that includes only one main secondary storage sump, S2. If a large size of S3 can be used, the PSS can be referred to as PSS option 2. Generally, Option 2 is superior to Option 1 in terms of energy efficiency improvement, as the storage capacity of S3 can be used to shift the electricity demand of the pumps out of peak period. Both options presented in this section are motivated by recirculating the dense medium in an added loop with a shorter differential head in comparison to the existing configuration. The energy savings are achieved by the reduced pump power due to the reduced differential head. The energy cost savings can also be obtained from the optimal operation of the system. The system can be operated in such a way that the over-pumped medium is stored to shift load from a high tariff period to a low tariff period to cope with electricity shortage in peak hours. A choice of one of the two options should be made according to practical situations.

Remark 2 The medium might settle in the added tank, which will influence the relative density of the medium and therefore the product quality. This problem is not studied here because the settlement can

be avoided by engineering methods. For instance, the medium can be supplied to a magnetite separator before entering the storage tank. The water outlet of the magnetite separator can be stored in the added tank and the magnetite can be stored in an extra container. When the stored medium is required to be supplied to the DMC process, the magnetite and water can be blended again to form the medium with the specified density.

2.5 OPTIMAL OPERATION UNDER TIME-BASED ELECTRICITY TARIFFS

Time-base electricity tariffs such as a time-of-use (TOU) tariff are commonly used all over the world nowadays to alleviate grid pressure during peak demand periods by imposing a relatively high price for the electricity consumed during peak hours in comparison to that during low demand hours [67]. Therefore, the same energy consumption is charged differently according to the time-specific load profile. The optimal operation of the proposed PSS in coal beneficiation plant is formulated under such a tariff to minimize electricity cost in order to maximize the revenue of the plant.

The objective of the optimization is to minimize energy cost while maintaining the normal production process. Therefore, the following objective function is used

$$J = \int_0^T \frac{Q_1 \rho_m g h_1 u_1(t) + Q_2 \rho_m g h_2 u_2(t)}{1000 \eta_p} p(t) dt, \tag{2.6}$$

where $p(t)$ is the electricity price at time t.

The operation optimization problem for the PSS is therefore formulated as a binary integer programming problem: minimize (2.6) subject to (2.1) and (2.5).

2.6 LIFE CYCLE COST ANALYSIS

The economic benefit of the PSS that is introduced is evaluated by comparing its LCC to that of the existing system in order to verify its effectiveness and financial viability. In this section, the LCC models for pre- and post-implementation of the PSS scheme are developed. The present value method is employed to estimate the LCC, as it is widely used in economics to compare cash flows at different times and in engineering practice to evaluate the feasibility of a proposed design [68, 69, 70, 71].

2.6.1 Post-implementation of PSS

The simple LCC of the PSS scheme without considering the time value of money introduced can be calculated as

$$\text{LCC} = CC + OC + MC - SV,$$

where CC, OC, MC and SV are, respectively, capital cost, operating cost, maintenance cost and salvage value.

Adopting the present value model yields the following [71]:

$$\text{LCC} = CC + \sum_{i=1}^{n} \frac{OC_i + MC_i}{(1+r)^i} - SV,$$

where i is the number of years, n denotes the project lifetime and r is the discount rate.

Operating cost in this study is electricity cost due to running of pumps, therefore operating cost during the i-th year of the project can be obtained by

$$OC_i = 365 n_c \int_0^T \frac{Q_1 \rho_m g h_1 u_1(t) + Q_2 \rho_m g h_2 u_2(t)}{1000 \eta_p} p_i(t) dt, \tag{2.7}$$

where

$$p_i(t) = (1+q)^i p(t)$$

denotes the electricity tariff in the i-th year, q is the percentage of annual electricity price increase and n_c is the number of DMC modules in the plant. 365 is the number of days in a year because it is assumed that the plant is operating throughout the year and the process is repeated on a daily basis.

Maintenance cost and salvage value are calculated by [68, 72]

$$MC_i = mCC,$$

$$SV = \frac{(1-d)^n CC}{(1-r)^n},$$

where m is the maintenance ratio and d is the annual deprecation ratio of the facilities.

2.6.2 Pre-implementation of PSS

As the baseline, the cost of the existing system during the life cycle of the PSS scheme is calculated as follows to ensure a fair comparison between the PSS and the existing system.

$$\mathrm{LCC}^0 = \sum_{i=1}^{n} \frac{OC_i^0 + MC_i^0}{(1+r)^i} - SV^0,$$

where $OC_i^0 = 365 n_c \int_0^T P_1 p_i(t) dt$, $SV^0 = \frac{CC^0(1-d)^n}{(1+r)^n}$, in which CC^0 is the costs of pumps in the existing system.

2.6.3 Payback period

Payback period is commonly used in economic analysis for its simplicity. It is a measure of the time in which the initial cash outflow of an investment is expected to be recovered from the cash inflows generated by the investment. To take the time value of money into consideration, the discounted payback period is employed to evaluate the proposed system's financial viability and feasibility [73]. The following formula is used to calculate the payback period:

$$\text{Payback period} = n_y + \frac{\sum_{i=1}^{n_y} \left(\mathrm{LCC}^0(i) - \mathrm{LCC}(i)\right)}{\mathrm{LCC}(n_y+1)},$$

where n_y is the last year with a negative cumulative cash flow.

Note that cash flow in this study is the difference between the LCC pre-implementation of the PSS options and the LCC post-implementation of the PSS options.

2.7 CASE STUDY

To demonstrate the feasibility and effectiveness of the proposed system, case studies are done based on the situation of a real coal washing plant. The operation optimization problem is solved in Matlab using the CPLEX[1] toolbox function *cplexbilp*, which solves binary integer programming problems.

[1] ILOG 2008, CPLEX 11.0 User's Manual.

Table 2.1. PSS parameters

Q_m (m^3/s)	h_1 (m)	h_2 (m)	η_p
0.0859	60	20	0.8

2.7.1 Project configurations and parameters

The operational status of a coal washing plant in South Africa is used without losing generality. Under different plant parameters, the performance of the proposed approach will vary in terms of the absolute savings but the energy and cost saving potential will not be affected. The studied mine operates two coal washing plants with 15 cyclone modules in total. Regarding the over-pumping effect of the corrected medium pump, only 25% of the medium pumped to the distributor flows into the DMC feed sump, while the remaining 75% simply flows back to the corrected medium sump. The plant runs for 16 hours every day from 06:00 to 22:00.

Other parameters are listed in Table 2.1. To align with the current plant operational status, the sampling period of the system T_s is set to 0.5 hour.

Both energy savings and electricity cost savings are calculated in comparison with the original configuration (current practice) in the following sections. The originally used pumps delivers a fixed volume flow rate at 0.0859 m^3/s.

In terms of electricity cost, Eskom's TOU tariff for large industrial users is used. The off-peak period is from 01:00 to 06:00 and 23:00 to 24:00, peak period is from 08:00 to 10:00 and 19:00 to 20:00. Other time falls in the standard period. The electricity prices for off-peak, standard and peak period are R0.3558/kWh, R0.5948/kWh and R2.0538/kWh, respectively. The currency unit R used in this study represents the South African rand (average exchange rate of rand to US dollar in 2015 was $1=R12.77).

Results of the PSS are presented in the following context with respect to two practical options of the PSS, as mentioned in Section 2.4.

2.7.2 Results of PSS Option 1

In this subsection, the impacts of the added returned medium sump are investigated. With the capacity limit of S2 set to $V_2^{max} = 160$ m^3 and $h_2 = 20$ m, the simulation results are shown in Fig. 2.3. In this case, Q_2 is set equal to Q_m as the idea is to reduce the running time of P1. In the period P1 is switched off, P2 is responsible for supplying the required medium to the DMC process at the same flow rate (Q_m).

According to the results obtained, the total operational time of P1 is four hours; it is switched off to save energy during the other 12 hours when the added P2 is responsible for the medium supply. It can be seen that the secondary pump P2 is turned on as long as possible because it consumes less power because of the reduced differential head compared to the existing pump P1. The three-to-one operational time of P2 and P1 can be explained by the 75% over-pumping of P1 as $(16-4)/16 = 0.75$.

Regarding the load shifting effect, it can be observed from the first subplot that the secondary pump P2 is switched on most of the time; P1 is switched on only when the medium stored in the returned medium sump S2 is insufficient to supply the cyclone process.

The energy consumption and electricity cost decreased by 50.00% and 51.71%, respectively with this option. This yields a daily R1715 electricity cost reduction per DMC module.

2.7.3 Results of PSS Option 2

In this configuration, a start-up procedure is presented to minimize the size of S2 for the following reasons.

Firstly, P2 cannot start working before there is some medium in S2. That is to say, if there is no medium in S2 when the plant starts to operate, P2 must be kept off in the first sampling period. Secondly, if the P2 is kept off during the first sampling period, the storage capacity of the S2 must be at least $r_m^V Q_m T_s$ according to (2.1). As the flow rate of the over-pumped medium by P1 is high, it requires a large volume S2 to store the over-pumped medium during a sampling period. In practice, the larger S2 is, the higher investment and maintenance cost are, which is undesirable.

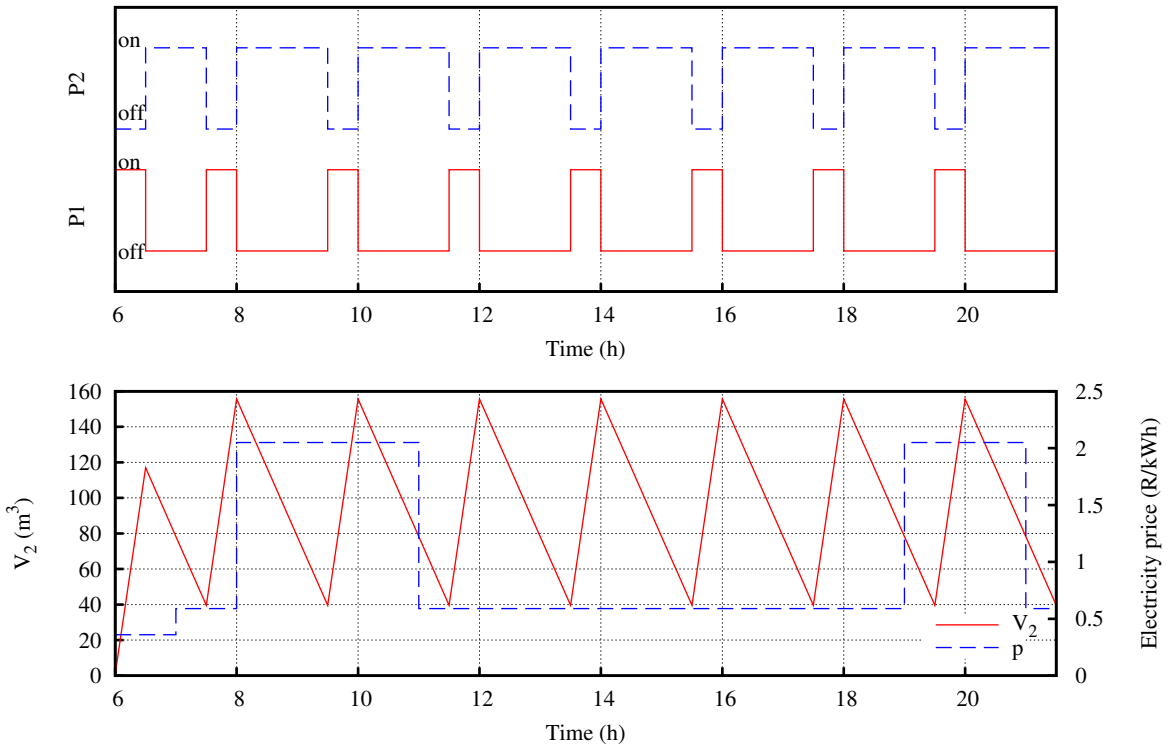

Figure 2.3. Results of Option 1 with $V_2^{max} = 160$ m^3

In order to reduce the size of S2, a simple start-up procedure is introduced. At start-up, P1 is turned on and P2 is kept off to allow S2 to store medium; after $\frac{0.8V_2^{max}}{r_m^V Q_m}$ seconds, P2 is switched on and the optimal schedule of the two pumps is implemented.

In the simulation $Q_2 = r_m^V Q_m$, $V_2^{max} = 1$ m^3 and $V_3^{max} = 160$ m^3. The height of S3 in this case is 0.91 m. Simulation results are shown in Fig. 2.4. The start-up procedure is shown in a zoomed-in plot in Fig. 2.5.

Energy consumption saving is 50.05% and electricity cost saving is 52.23% in this case.

In comparison with the result of Option 1, more electricity cost savings are achieved. Specifically, Option 2 offers 0.52% more electricity cost savings than Option 1. The reason for this 0.52% saving is the energy storage capacity of S3. This enables the DMC process to shift load from the peak period to the off-peak period.

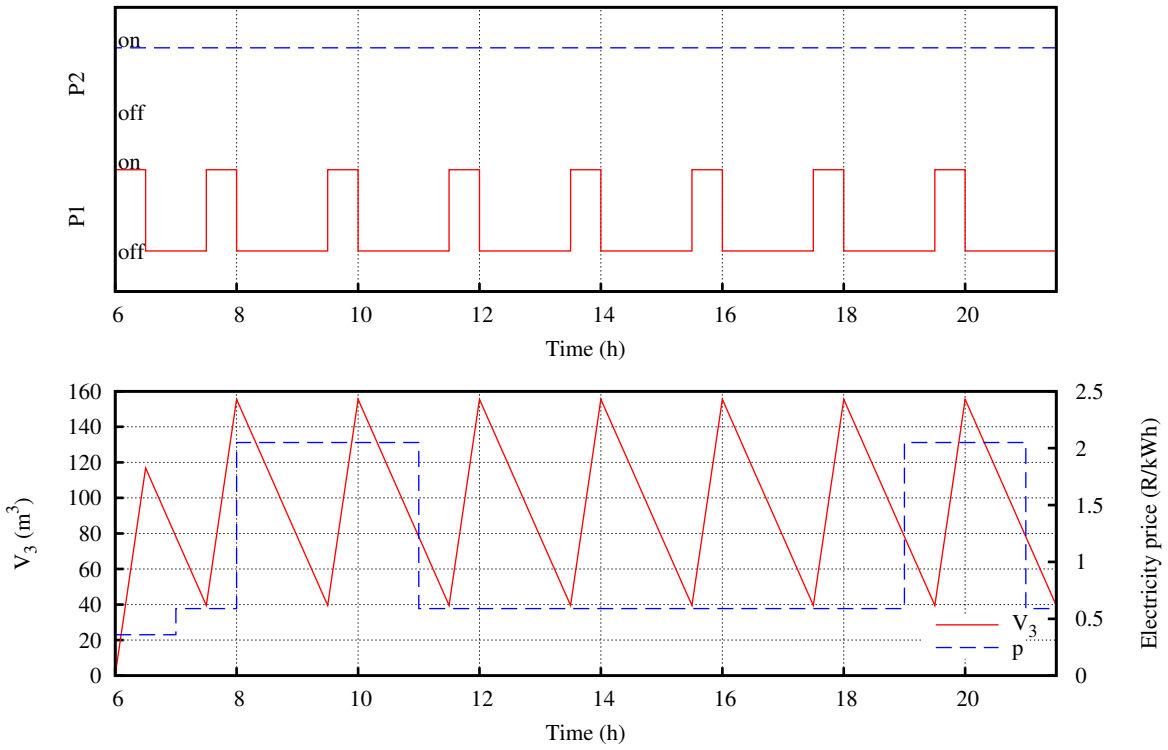

Figure 2.4. Results of Option 2 with $V_3^{max} = 160$ m^3

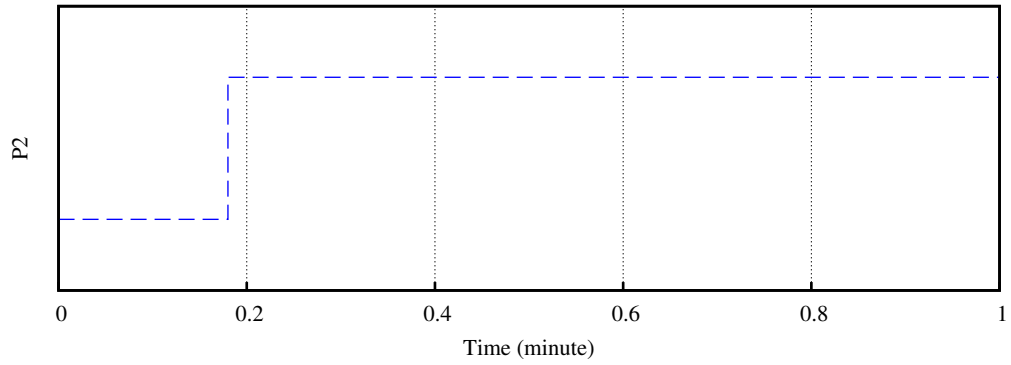

Figure 2.5. Demonstration of the start-up procedure

2.7.4 Results with larger storage capacity

In this subsection, the capacities of the added tanks are increased in order to investigate the impact on load shifting under time-based tariffs.

In Option 1, the capacity of S2 is set to 320 m^3. For Option 2, S2 is kept with $V_2^{max} = 1$ m^3 while the limit of S3 is increased to 320 m^3. The results are depicted in Fig. 2.6 and Fig. 2.7, respectively.

From those figures, it is clear that load shifting is very effective with a large storage tank. In both cases, the original pump P1 is switched off during the peak period.

Energy saving and electricity cost saving from Option 1 are 50.00% and 58.06%, respectively. When compared to the results in Section 2.7.2, it can be seen that the energy saving remains stable while the electricity cost saving is 6.35% more. This is because the required medium at the mixing box is the same. On the one hand, the medium pumped up to the medium splitter is the same, which results in the same amount of time of the on state of P1; as P2 is working opposite to P1, it then leads to the same energy consumption as the result in Section 2.7.2. On the other hand, because of the increased storage capacity of S2, the operation of P1 can be switched off during peak periods to save energy cost.

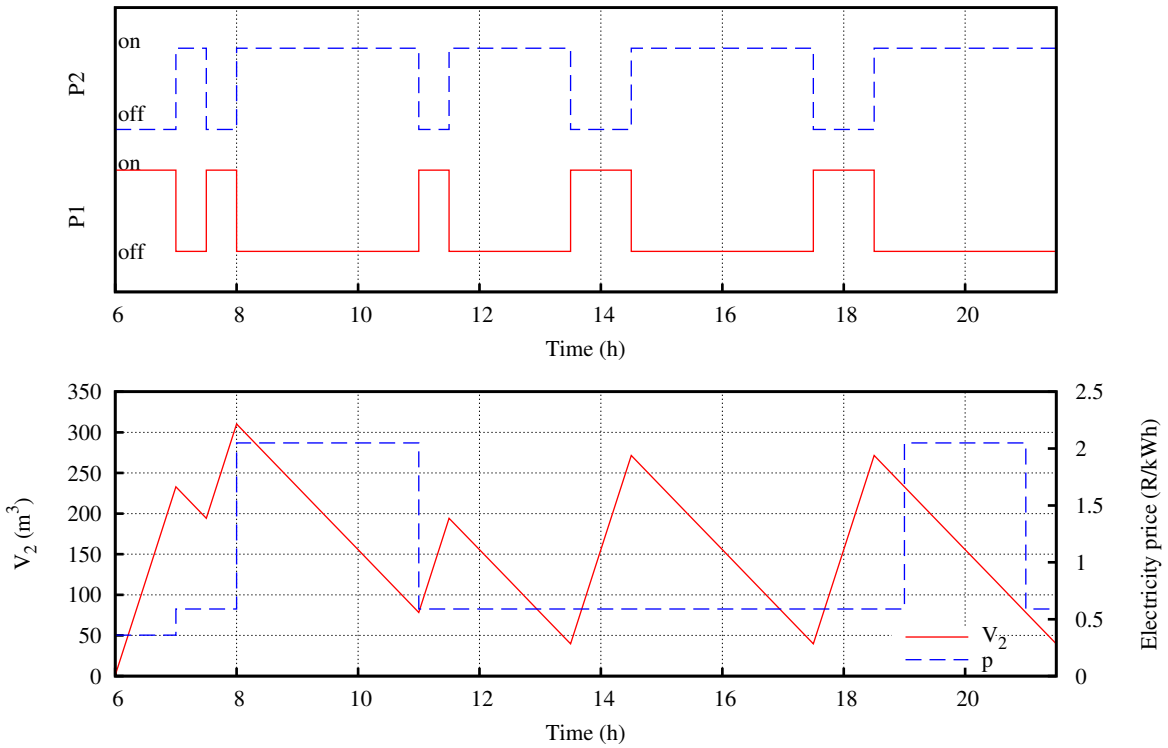

Figure 2.6. Results of Option 1 with $V_2^{max} = 320$ m^3

As for the results of the PSS Option 2, energy consumption decreases by 49.68% in comparison to the existing configuration (no tank, only P1), energy cost reduction reached 61.70%. More energy is consumed than in the case of a smaller tank with 160 m^3 volume because of the increased height of S3 (see equation (2.4)). By contrast, the electricity cost is further reduced as a result of the load shifting with the larger storage capacity.

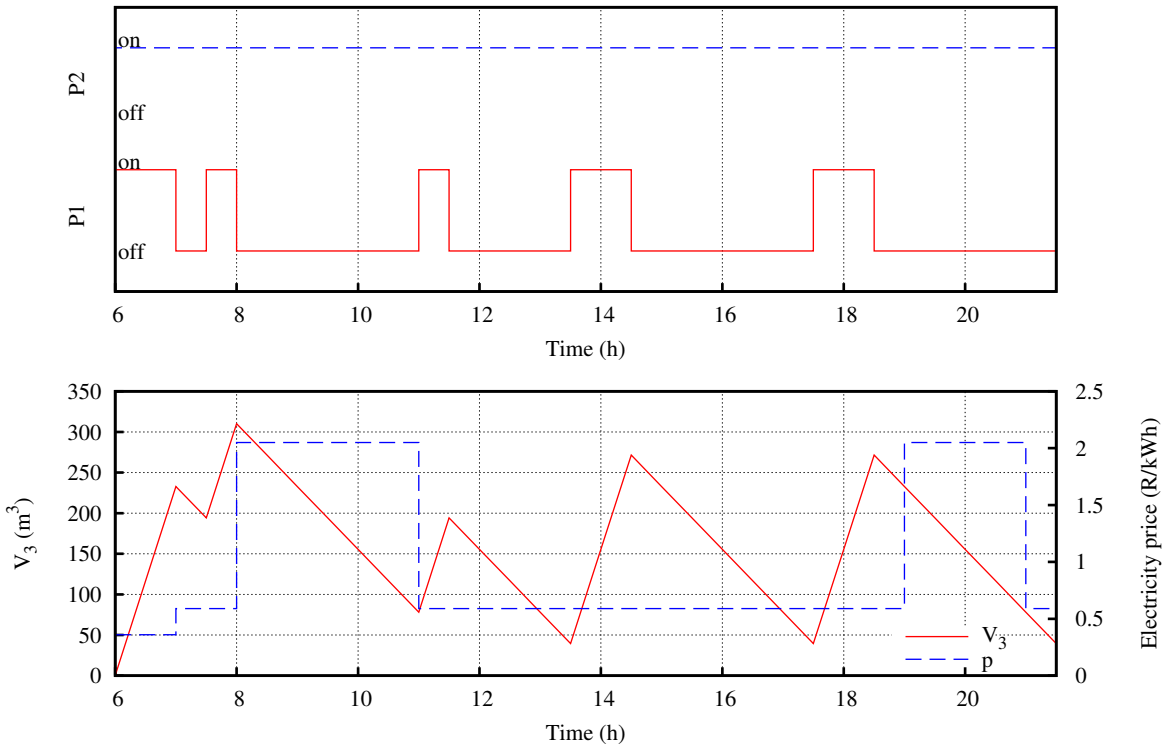

Figure 2.7. Results of Option 2 with $V_3^{max} = 320$ m^3

In summary, electricity cost savings increase with an increase in the capacity of the storage tank, while energy consumption remains stable in Option 1 and a slight increase is witnessed for Option 2.

The influence of the location of the returned medium sump, $h_2 - \Delta h$, and the diameter of S3 on the energy and cost savings are investigated and plotted in Fig. 2.8, in which C_s and E_s are the percentage reduction of energy consumption and cost, respectively. Note that this simulation is run with the larger capacity of 320 m^3.

As depicted in Fig. 2.8, both energy consumption and energy cost savings decrease when h_2 increases in the two proposed configurations. However, the two options (with and without S3) have distinct performance differences. Firstly, the smaller the $h_2 - \Delta h$, the smaller the difference between Option 1 and Option 2. It is noted that the advantage of Option 2 becomes noticeable when $h_2 - \Delta h$ increases. This is evidenced by the effect that the energy cost saving drops faster without S3 when $h_2 - \Delta h$ increases. Nevertheless, the energy consumption saving resulting from the two options share the same rate of change.

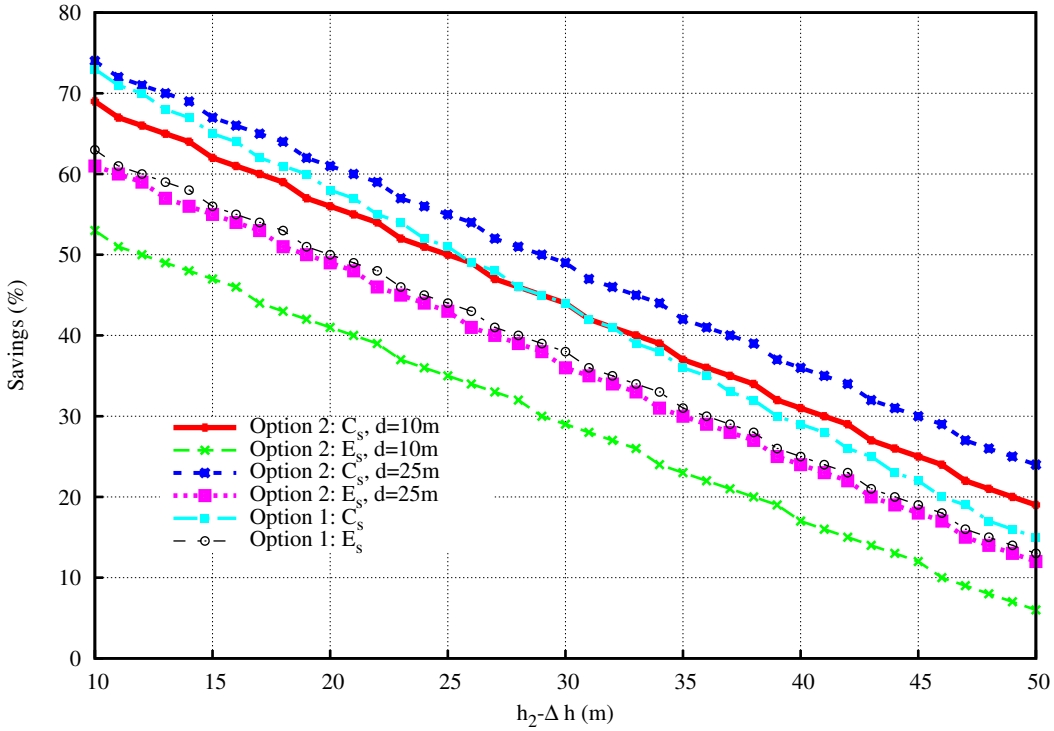

Figure 2.8. Saving ratios relationship to $h_2 - \Delta h$

Moreover, the energy consumption saving yield from Option 2 depends on the diameter of S3; the bigger the diameter, the more energy consumption savings. It is also interesting to note that if $h_2 - \Delta h$ can be small enough, the performance of the Option 2 will be worse than that of Option 1 in terms of both energy consumption saving and energy cost saving, similar to the case when $h_2 - \Delta h < 15$ m and $d_T = 5$ m in Fig. 2.8.

Therefore, the two options proposed should be used according to the specific situation of the plant. Generally, Option 2 is able to outperform Option 1, but if there are limits on the selection of the S3 and if the plant owner prefers energy consumption savings to energy cost savings, Option 1 may offer a better solution.

2.7.5 Life cycle cost analysis

In order to show the economic viability of the proposed schemes, the following LCC analysis is given. To be conservative, the results from the smaller tank size in Section 2.7.2 and Section 2.7.3 are used in this analysis.

Table 2.2. Summary of economic data

	Existing	Option 1	Option 2
Project lifetime (years)	–	10	10
CC (million rands)	2.25[1]	24.41	26.26
MR(%)	120	24.54[2]	25.63[2]
r (%)	10		
d (%)	50		
q (%)	24		

[1] This is the cost of the currently used pumps since there is no initial capital cost for the existing system.

[2] The maintenance ratios after implementation of the proposed schemes are lower than that of the existing system because the maintenance ratio for tanks is much lower than for pumps.

The economic data of the project are shown in Table 2.2. The capital costs of the project are based on the practical data on the installation costs of pumps and water tanks and are given in the second row of Table 2.2. For the maintenance rate, the mine under investigation replaces the slurry pumps every seven months because of performance degradation. Therefore, the maintenance for the existing system is to replace the slurry pumps every seven months, which results in a high maintenance rate (120%). In the proposed schemes, this pump replacement rate is kept the same as in the existing system, while the maintenance rate for tanks is 40%, which yields the results shown in the third row of Table 2.2.

The breakdown of the results is depicted in Table 2.3. Although the initial capital cost and maintenance cost are increased in the proposed schemes, the operating cost is decreased. In this 10-year LCC analysis, the average annual cost savings obtained by PSS Option 1 and PSS Option 2 are R150.03 million and R145.56 million, respectively.

Moreover, the LCC analysis shows that the proposed change in the beneficiation plant can result in positive economic effects on the plant, with a relatively short payback period (2.68 years for the proposed Option 1 and 3.30 years for Option 2).

In this LCC analysis, the results show that Option 1 is better than Option 2 in terms of economic

Table 2.3. Summary of 10-year LCC analysis results (rand)

	Existing	Option 1	Option 2
CC	2 250 000	24 412 275	26 262 483
OC	372 109 617	179 701 589	177 777 562
MC	16 590 331	36 812 065	41 359 556
SV	847	9 191	9 888
Accumulated saving	–	150 032 364	145 559 388
Payback period	–	2.68 years	3.30 years

benefit. However, the benefits of Option 1 and Option 2 may be different in different situations, as shown in the energy consumption and cost analysis part. Therefore, the performance of the two options must be compared before implementation according to given conditions of the plant to which the PSS options are applied.

2.8 CONCLUSION

A PSS is introduced to coal washing plants to improve their energy efficiency. A unified PSS configuration is presented and modeled mathematically. Thereafter, the optimal operation of the PSS is formulated into an optimization problem and solved by a binary integer programming method. It is then pointed out that the PSS presented actually provides two practical options for coal washing plants under different scenarios. Case studies based on a South African coal mine are conducted to validate the benefits of the PSS options. The results obtained verified the effectiveness of the proposed system in terms of energy consumption and cost reduction. In addition, LCC analysis is done to investigate the economic benefits of the scheme change. It is shown that both options are able to produce financial savings with short payback periods.

CHAPTER 3 FEED-FORWARD CONTROL FOR SEPARATION EFFICIENCY

3.1 CHAPTER OVERVIEW

A feed-forward controller is designed in this chapter to improve the separation efficiency of the DMC coal cleaning process, taking advantage of geographically sampled composition measurements of ROM coal from the mining pits. To facilitate the controller design, mathematical models of the DMC-related processes are presented first in Section 3.3, followed by the design of a feed-forward controller in Section 3.4. Simulations are given in Section 3.5 to demonstrate the effectiveness of the controller that was designed.

3.2 INTRODUCTION

While the energy efficiency of the DMC coal cleaning process is addressed in Chapter 2, the separation efficiency of the same process has not been investigated so far. This is the main objective of this chapter, which focuses on designing controllers to deal with the separation efficiency of the process. In particular, a feed-forward controller is designed to improve the separation efficiency of the DMC coal washing process where only geographically sampled measurements from the ROM are available. Development of this controller is motivated by the fact that the composition of ROM coal is measured according to the geographical location from where it is mined. This is common practice for coal mines and measurement of the compositions of the yield from the output of the DMC is not usually done because of the high cost associated with it. Therefore, the feed-forward controller designed in this chapter will bring about improvements in the cleaning efficiency of the DMC circuit in comparison to the current industrial practice of empirical control methods. In particular, the feed-forward controller

is a model-based control designed according to an advanced optimal control concept and it takes the measurements from the ROM coal into account to optimize the performance of the DMC process. It is noticed that although there are many parameters, including the DMC geometry, medium rheology and stability, the medium to coal volume ratio, etc., all play a role in determining the efficiency of the DMC separation process [74]. In this study, however, we have only considered the density of the medium used in the process, assuming that all other parameters are properly designed for the specific application. In addition, the feed-forward controller designed in this chapter lays the foundations for the closed-loop controller design process detailed in Chapter 4.

3.3 MODEL OF THE SEPARATION PROCESS

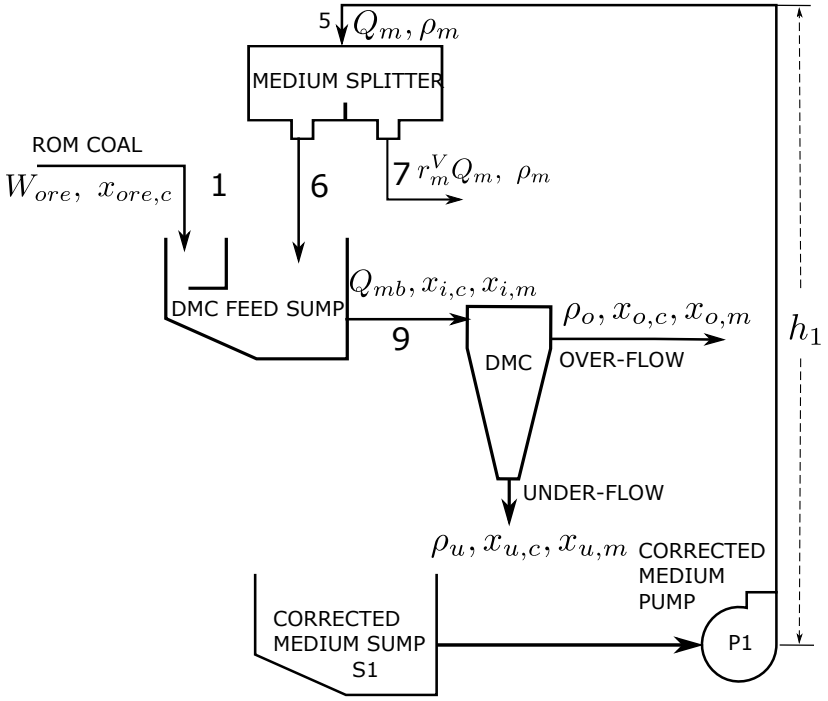

Figure 3.1. Simplified DMC separation efficiency control circuit

The separation-relevant components of the DMC circuit shown in Fig. 1.1 are depicted in Fig. 3.1. The basic operation principles of the DMC coal beneficiation process can be explained in three steps [13]. Firstly, ROM coal is mixed with a slurry whose density is adjusted by the percentages of water and magnetite contents in it. This slurry is usually referred to as a dense medium because it has a relative density higher than one and is used in DMC circuits to enhance the separation. After being blended, the ROM coal and the medium are fed to the DMC, in which swirling occurs. Lastly, because of centrifugal forces, the impurities and carbon content of the ROM coal start to separate inside the DMC

and exit the DMC in two different directions. The impurities, which have a higher density, are thrown to the wall of the DMC by centrifugal force and drop out the DMC at the bottom, while the fine coal that is lighter flows upward in the center and exits the DMC at the top. It is the relative density of the medium used that controls the separation efficiency of this process. Mathematical modeling of this process is difficult and expensive, as swirling is involved.

According to the literature study, the DMC model identified to be suitable for controller design has been developed in [62]. A brief review of this model is provided here.

3.3.1 The DMC feed sump

Mixing of ROM and the dense medium occurs inside the DMC feed sump, as shown in Fig. 3.1. In order to obtain the characteristics of the slurry entering the DMC (flow stream 9), the quality of the ROM coal is required. This quality is best represented by percentages of different components in the ROM coal $x_{ore,c}$, which is a vector consisting of elements defined by

$$x_{ore,c} = [x_{ore,ash}, x_{ore,S}, x_{ore,H_2O}, x_{ore,vol}]^T,$$

where $x_{ore,ash}$, $x_{ore,S}$, x_{ore,H_2O}, $x_{ore,vol}$ represent the mass percentages of ash, sulfur, moisture, and volatile matter within the ROM coal, respectively.

The subscript c representing a set $\{ash, S, H_2O, vol\}$ will be used in the rest of the modeling process to simplify notation. The percentages of those compositions,

$$x_{i,c} = [x_{i,ash}, x_{i,S}, x_{i,H_2O}, x_{i,vol}]^T,$$

and the percentage of the dense medium, $x_{i,m}$, in the mixed slurry from the output of the DMC feed sump (flow stream 9) that is fed into the DMC can be calculated by the following equations [62].

$$\dot{\rho}_{mb} = -\frac{Q_{mb}}{V_{mb}}\rho_{mb} + \frac{Q_m}{V_{mb}}\rho_m + \frac{1}{V_{mb}}W_{ore}, \tag{3.1}$$

$$x_{i,c} = \frac{x_{ore,c}W_{ore}}{Q_{mb}\rho_{mb}}, \tag{3.2}$$

$$x_{i,m} = \frac{Q_m\rho_m}{Q_{mb}\rho_{mb}}, \tag{3.3}$$

where ρ_{mb} is the density of the mixed slurry. V_{mb}, Q_m, ρ_m and W_{ore} are, respectively, the volume of the DMC feed sump, the medium flow rate, the medium density, and the mass flow rate of coal feed to the DMC feed sump. Q_{mb} is the flow rate of the mix to the DMC.

3.3.2 The DMC

After being mixed in the DMC feed sump, the slurry then enters the DMC where the separation occurs. Compositions of slurries that exit the DMC are determined by those of the slurry entering and the characteristics of the DMC. The dynamics of the DMC is modeled in [62]. A brief introduction to this model is given in the following. In particular, the final DMC model is given by the following equations.

$$\begin{aligned}\dot{x}_{o,c} =& \frac{1}{V_o\rho_o}\big[W_i x_{i,c} - Q_o\rho_o x_{o,c} - Q_u\rho_u x_{u,c} - V_o x_{o,c}\dot{\rho}_o \\ & - V_u x_{u,c}\dot{\rho}_u - K_{u,c}V_u\rho_u(\rho_c - \rho_m)(x_{i,c} - x_{u,c})\big],\end{aligned} \tag{3.4}$$

$$\begin{aligned}\dot{x}_{u,c} =& \frac{1}{V_u\rho_u}\big[W_i x_{i,c} - Q_o\rho_o x_{o,c} - Q_u\rho_u x_{u,c} - V_o x_{o,c}\dot{\rho}_o \\ & - V_u x_{u,c}\dot{\rho}_u - K_{o,c}V_o\rho_o(\rho_m - \rho_c)(x_{i,c} - x_{o,c})\big],\end{aligned} \tag{3.5}$$

$$\begin{aligned}\dot{x}_{o,m} =& \frac{1}{V_o\rho_o}\big[W_i x_{i,m} - Q_o\rho_o x_{o,m} - Q_u\rho_u x_{u,m} - V_o x_{o,m}\dot{\rho}_o \\ & - V_u x_{u,m}\dot{\rho}_u - K_{u,m}V_u\rho_u(\rho_{o,m} - \rho_m)(x_{i,m} - x_{u,m})\big],\end{aligned} \tag{3.6}$$

$$\begin{aligned}\dot{x}_{u,m} =& \frac{1}{V_u\rho_u}\big[W_i x_{i,m} - Q_o\rho_o x_{o,m} - Q_u\rho_u x_{u,m} - V_o x_{o,m}\dot{\rho}_o \\ & - V_u x_{u,m}\dot{\rho}_u - K_{o,m}V_o\rho_o(\rho_m - \rho_{u,m})(x_{i,m} - x_{o,m})\big],\end{aligned} \tag{3.7}$$

$$\dot{\rho}_o = \frac{1}{V_o}\left[W_i - Q_o\rho_o - Q_u\rho_u - K_u V_u(\rho_u - \rho_m)x_{i,ash}\right], \tag{3.8}$$

$$\dot{\rho}_u = \frac{1}{V_u}\left[W_i - Q_o\rho_o - Q_u\rho_u - K_o V_o(\rho_o - \rho_m)x_{i,C}\right], \tag{3.9}$$

where $x_{o,c}$ and $x_{u,c}$ are again 4×1 vectors representing the percentages of different compositions (ash, sulfur, moisture and volatile) in the overflow and underflow of the cyclone, respectively:

$$x_{o,c} = [x_{o,ash}, x_{o,S}, x_{o,H_2O}, x_{o,vol}]^T,$$

$$x_{u,c} = [x_{u,ash}, x_{u,S}, x_{u,H_2O}, x_{u,vol}]^T.$$

ρ_o and ρ_u are the densities of slurries exiting at the overflow and underflow of the cyclone. ρ_c is also a 4×1 vector containing the densities of ash, sulfur, moisture and volatile:

$$\rho_c = [\rho_{ash}, \rho_S, \rho_{H_2O}, \rho_{vol}]^T.$$

$x_{o,m}$ and $x_{u,m}$ represent the percentage of dense medium contained in the DMC overflow and underflow, respectively. $W_i = Q_{mb}\rho_{mb}$ is the slurry feed rate to the cyclone. $x_{i,C}$ denotes the percentage of carbon content in the slurry feeding to the DMC. V_o and V_u denote the volume of slurry that reports to the overflow and underflow of the DMC, respectively. These two parameters are calculated according to a constant split ratio of the volume of slurry inside the DMC, V_s, according to [62]:

$$V_o = \frac{\alpha}{1+\alpha}V_s, \tag{3.10}$$

$$V_u = \frac{1}{1+\alpha} V_s. \tag{3.11}$$

Similarly, Q_o and Q_u are the flow rates to the overflow and underflow of the cyclone that are split by the same ratio α of Q_{mb}. K_o, K_u, $K_{o,m}$ and $K_{u,m}$ are DMC-specific constants and. $K_{o,c}$ and $K_{u,c}$ are DMC-specific constant vectors: $K_{o,c} = [K_{o,ash}, K_{o,S}, K_{o,H_2O}, K_{o,vol}]^T$ and $K_{u,c} = [K_{u,ash}, K_{u,S}, K_{u,H_2O}, K_{u,vol}]^T$.

The percentages of fixed carbon in the cyclone overflow and underflow after medium recycling process, $x_{o,C}$ and $x_{u,C}$, are obtained by the following equations.

$$x_{o,C} = 1 - \frac{\mathbf{1}^T x_{o,c}}{1 - x_{o,m}}, \tag{3.12}$$

$$x_{u,C} = 1 - \frac{\mathbf{1}^T x_{u,c}}{1 - x_{u,m}}, \tag{3.13}$$

where $\mathbf{1}$ is a 4×1 column vector of ones.

Assumptions made in the modeling process are [62]:

- The volume of the mix in DMC is constant at V_s m^3.
- The volumes of the overflow V_o and underflow V_u slurries in the cyclone are split at a constant ratio α. That is, $V_o = \frac{\alpha}{1+\alpha} V_s$ and $V_u = \frac{1}{1+\alpha} V_s$.
- The volume flow rates of the overflow Q_o and underflow Q_u are also split at the constant ratio α.
- Only carbon, ash, sulfur, moisture and volatile compositions in the feed are considered. In other words, $x_{ore,C} + \mathbf{1}^T x_{ore,c} = 1$, where $x_{ore,C}$ is the percentage of carbon content in the ROM.
- The rates of change in the percentages of components to the overflow ($\dot{x}_{o,c}$) and underflow ($\dot{x}_{u,c}$) are proportional to the difference in their component densities (ρ_c) to the magnetite medium density ρ_m and the difference in their component percentages ($x_{o,c}$, $x_{u,c}$) to their corresponding feed percentages to the DMC.

The model represented by equations (3.1)—(3.13) is derived from the model developed in [62]. Advantages of this model are threefold. Firstly, the percentages of different components in the cyclone

products and rejects can be obtained directly, which facilitates the controller design. Secondly, it only involves differential equations, which take much less time to solve compared to CFD models. This makes it possible to apply a controller designed with this model in a real-time environment. Thirdly, accuracy of this model is validated with experiments to be more than 95%, which is much better than that of empirical models used for control purposes in current practice [52].

3.4 CONTROLLER DESIGN

In order to maintain the coal quality at a specified level, a well designed controller is required. Since the DMC process model is intrinsically nonlinear, a nonlinear model predictive controller is proposed to control the relative density of the medium.

To facilitate controller design, the DMC model is discretized using the Runge–Kutta method as follows:

$$x(k+1) = f(x(k), u(k)), \tag{3.14}$$

where the state of the DMC process at time kT_s is $x(k) = [x_{o,c}^T(k), x_{u,c}^T(k), x_{o,m}(k), x_{u,m}(k), \rho_o(k), \rho_u(k)]^T$, in which T_s is the sampling period. $f(\cdot)$ is the nonlinear functions that represent the DMC model. The control variable is

$$u(k) = \rho_m(k).$$

The concept for controlling the dense medium circuit is depicted in Fig. 3.2. In coal preparation plants, the raw coal mined from different locations is sampled and analyzed [75]. This analysis provides the coal washing plant with prior information about the percentages of different compositions in the raw coal. Measurement of the same information of fines after DMC separation is not practiced for control purposes because accurate measurement and analysis take a long time and are very costly.

Under such circumstances, the measured composition percentages in the coal feed $x_{ore,c}$ and the coal feed rate W_{ore} are used as feed-forward signals for the controller, as shown in Fig. 3.2. The control law is determined by using this feed-forward information and the cyclone circuit process model [76, 77]. In other words, the control is to ensure the quality of the fine coal product by optimizing the relative density of dense medium according to feed-forward measurement.

As for performance indicators of the control system designed, the following objectives are considered:

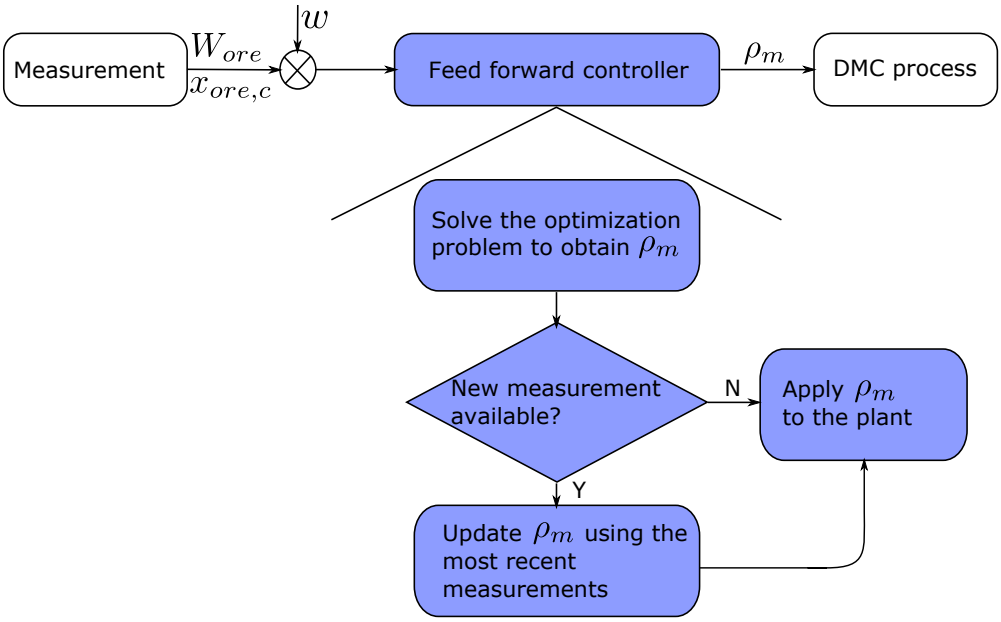

Figure 3.2. Work flow of the feed-forward controller

1. Keep the percentage of the fixed carbon content in the fines stable.

2. Minimize energy consumption of the circuit while ensuring carbon content in the fines within the prescribed interval.

The primary goal of controlling the DMC process is to maintain the quality of the coal. With the sharp increase in the electricity price in recent years, improving the energy efficiency of the DMC plant is also of vital importance for the economic benefit of the plant owner. Therefore, reducing energy consumption is treated as the secondary objective of the controller. As a result, the following objective function is adopted.

$$J = \sum_{k=1}^{T/T_s} \left[k_p(x_{o,C}(k) - x_r(k))^2 + k_e u(k)^2\right], \tag{3.15}$$

where $x_r(k)$ is the desired percentage of fixed carbon in the fines, T is the operating time of the DMC circuit. For simplicity, T is a multiple of T_s. Weights k_p and k_e are used to tune the controller and are chosen by users according to the preference for coal quality and energy consumption.

The first and second terms in this function represent, respectively, the indicators of coal quality and energy consumption. The rationale for using u^2 as an indicator for energy consumption lies in the fact that the dense medium is pumped to the mixing box. The energy consumed by the DMC circuit is

mainly the pumping cost, which is a linear function of the medium density. Therefore, u^2 can be used in the objective function to adequately penalize the energy usage.

Physical constraints of the DMC process include the maximum and minimum limits of the density of the medium, and limits on the percentages of the compositions in the mixture. Operational constraints are the limits on the rate of change of the medium density. In summary, the constraints are given in the following inequalities.

$$0 \leq x_{o,c}(k) \leq 1, \tag{3.16}$$

$$0 \leq x_{u,c}(k) \leq 1, \tag{3.17}$$

$$0 \leq x_{o,C}(k) \leq 1, \tag{3.18}$$

$$0 \leq x_{u,C}(k) \leq 1, \tag{3.19}$$

$$|\rho_m(k) - \rho_m(k-1)| \leq \Delta\rho_m, \tag{3.20}$$

$$\rho_m^l \leq \rho_m(k) \leq \rho_m^u. \tag{3.21}$$

Inequalities (3.16), (3.17), (3.18), and (3.19) naturally exist as the percentages are from 0% to 100%. Constraints (3.20) and (3.21) represent the limits on the rate of change and range of the medium density. $\Delta\rho_m$, ρ_m^l and ρ_m^u are, respectively, the limits on the rate of change, and the lower and upper limits of the density of the medium.

The first term in the objective function (3.15) presents a soft constraint on the proportion of carbon content in fines to track a set value. To ensure that the coal quality is within acceptable levels, a hard constraint on the variation of carbon content in the fine product is also included in (3.22).

$$x_{o,C}^l \leq x_{o,C}(k) \leq x_{o,C}^u, \tag{3.22}$$

where $x_{o,C}^l$ and $x_{o,C}^u$ are the allowable lower and upper bounds of the carbon percentage in fines.

In practice, the percentages of compositions in the ROM coal, as well as the feed rate are measured. Therefore, the feed-forward controller solves the nonlinear optimization problem, minimizing (3.15) subject to (3.14) and (3.16)–(3.22), with help of these measurements.

Because the component percentages of ROM are sampled and measured, the control action optimized by the controller is implemented during the period when no new measurement is available. That is

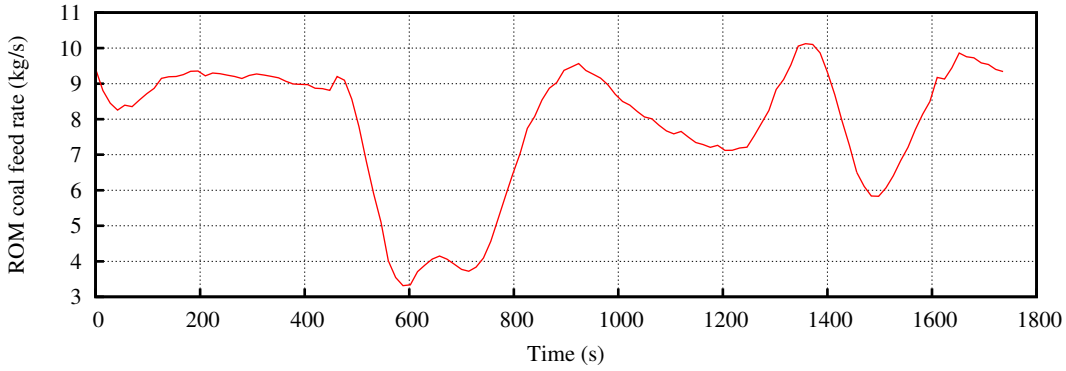

Figure 3.3. Coal feed rate

to say, the control action is implemented according to the most recent measurement and the action is updated whenever a new feed-forward measurement is available. Fig. 3.2 demonstrates the working principles and implementation implications of the controller designed.

3.5 SIMULATION

Based on plant measurements from a South African coal mine, simulations are carried out to verify and evaluate the feasibility and effectiveness of the control strategy proposed. The optimization problem is solved using the standard sequential quadratic programming method and simulations are carried out using Matlab. The DMC process-related parameters and result analysis are given below.

3.5.1 Parameters

The model parameters used are listed in Table 3.1 [62]. In addition, the same plant configuration as given in Section 2.7 is used. That is, there are 15 DMC modules operating 16 hours per day. The limits for the control variable ρ_m are, $\rho_m^l = 1200$ (kg/m^3), $\rho_m^u = 1620$ (kg/m^3) and $\Delta\rho_m = 0.3571$ (kg/m^{3}s), respectively.

At the beginning, the ash, sulfur, moisture, and volatile percentages in the coal feed are 17.6%, 2.5%, 1.59%, and 12.6%, respectively. At time t =600 s, new measurements of these percentages are available as 16.2%, 2.8%, 1.59%, and 13.0%. At time t =1200 s, these percentages are changed back to 17.6%,

Table 3.1. Cyclone separation circuit model parameters

Variable	Value	Unit
V_{mb}	0.16	m^3
Q_m	0.495	m^3/s
Q_{mb}	0.500	m^3/s
α	2	
V_s	0.38	m^3
K_o	0.22	m^2s
K_u	0.22	m^2s
$K_{o,ash}$	2.00×10^{-4}	m^3/kgs
$K_{o,S}$	3.90×10^{-4}	m^3/kgs
K_{o,H_2O}	1.50×10^{-4}	m^3/kgs
$K_{o,vol}$	8.90×10^{-4}	m^3/kgs
$K_{o,m}$	4.80×10^{-2}	m^3/kgs
$K_{u,ash}$	0.77×10^{-4}	m^3/kgs
$K_{u,S}$	3.90×10^{-4}	m^3/kgs
K_{u,H_2O}	0.30×10^{-4}	m^3/kgs
$K_{u,vol}$	8.90×10^{-6}	m^3/kgs
$K_{u,m}$	3.90×10^{-2}	m^3/kgs
ρ_{ash}	2000	kg/m^3
ρ_S	1920	kg/m^3
ρ_{H_2O}	1000	kg/m^3
ρ_{vol}	1100	kg/m^3

2.5%, 1.59%, and 12.6%. As for the coal feed rate, the measured values shown in Fig. 3.3 are used in all simulations.

In simulations, the nonlinear DMC dynamics is solved by the fourth-order Runge-Kutta method. According to industrial practice and information obtained from [62], the sampling period of the controller is set to 14 s. The optimization problem is solved by the *fmincon* function of the Matlab optimization toolbox[1].

[1] MathWorks®. Optimization Toolbox™ documentation.

3.5.2 Results analysis

The simulation results are given in this section along with some analysis.

3.5.2.1 Results with $k_p = 5000, k_e = 0$

In this simulation, the desired carbon percentage in the fine coal is set to a constant value of 72%. Allowing a $\pm 1\%$ deviation from this set target, $x^l_{o,C}$ and $x^u_{o,C}$ are therefore set to 71% and 73%, respectively. The controller is tuned such that only tracking of the carbon percentage in the fines is considered (k_e set to 0). The results are shown in Fig. 3.4, in which the first subplot shows the manipulated medium density ρ_m and densities of the cyclone overflow and underflow slurries. Percentages of fixed carbon and ash content in the fines and rejects are sketched in the second subplot.

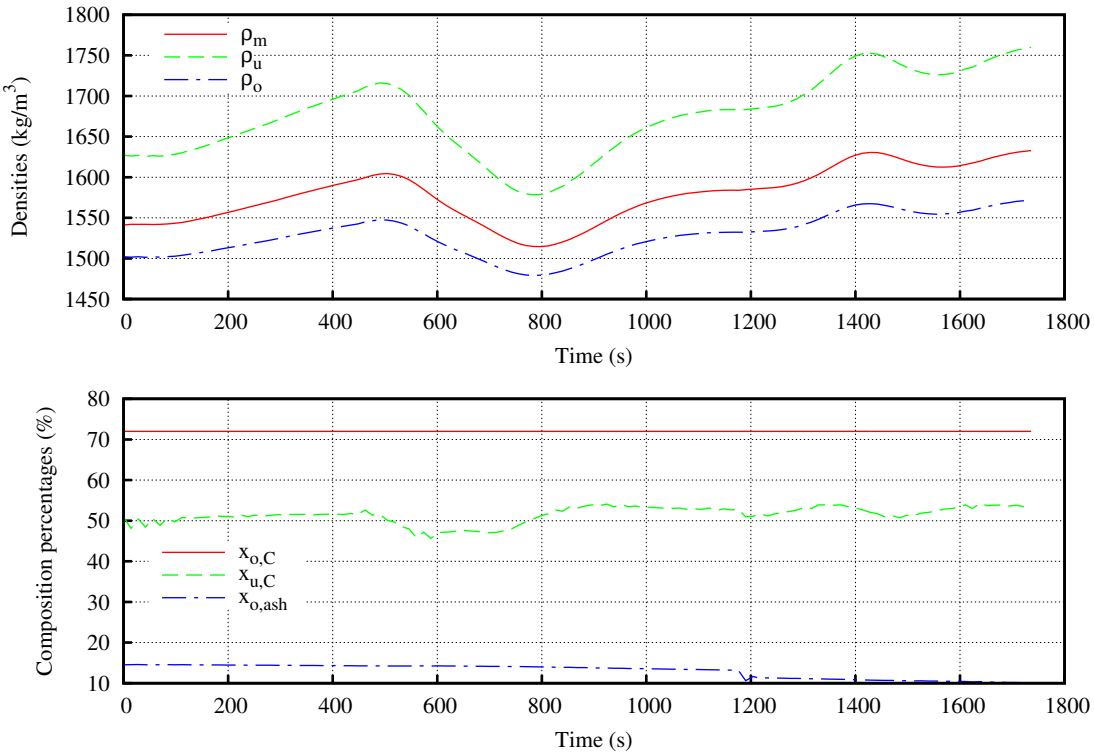

Figure 3.4. Results with $k_p = 5000$ and $k_e = 0$

It can be observed from Fig. 3.4 that the control strategy can maintain the set carbon percentage in the cyclone overflow all the time regardless of the feed coal characteristic changes. The controller

is able to adjust the density of the medium ρ_m to keep the carbon percentage in fines as close to the set value as possible when the coal feed rate changes. In this case, the simulated mean value of the carbon percentage in the overflow of the cyclone is 72.00% with zero tracking error. This verifies the effectiveness of the control strategy presented for the DMC process. The energy consumption of the DMC modules resulting from this control during the simulation period is calculated according to the pumping energy:

$$E = 15 \int_0^T \frac{Q_m \rho_m g h_1}{1000 \eta_p} dt,$$

where η_p is the efficiency of the pumping system, which is set to 0.8 considering the pumps in operation and h_1 is the differential head of the corrected medium pump as seen in Fig. 3.1.

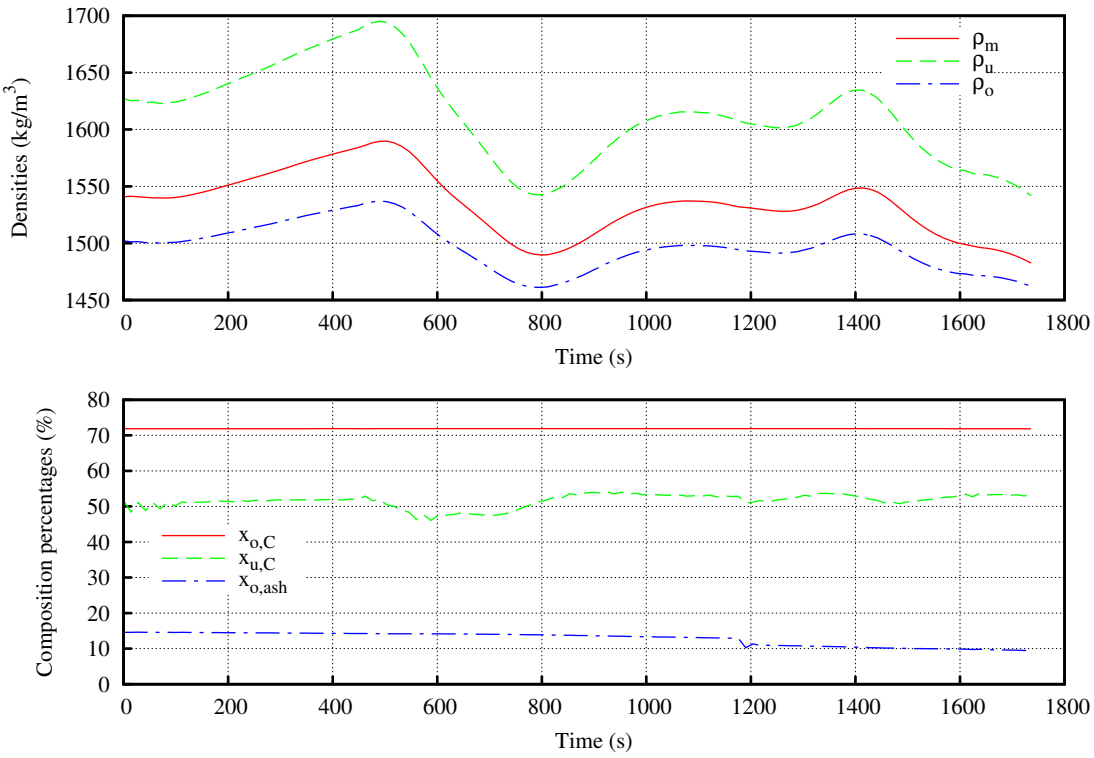

Figure 3.5. Results with $k_p = 5000$ and $k_e = 0.08$

In this case, the energy consumption $E = 6.98$ MWh.

3.5.2.2 Results with $k_p = 5000, k_e = 0.08$

Fig. 3.5 gives an illustration of the results when both carbon content tracking and energy consumption of the DMC process are accounted for. The results of this simulation show that the energy consumption of the DMC process can be reduced with minimal sacrifice of DMC separation efficiency. The mean

Table 3.2. Results with various weights

Weights	$\lvert\overline{e}\rvert$	E (MWh)
$k_p = 5000, k_e = 0$	0.00%	6.98
$k_p = 5000, k_e = 0.08$	0.16%	6.79
$k_p = 5000, k_e = 0.1$	0.21%	6.74
$k_p = 5000, k_e = 0.12$	0.26%	6.68

proportion of carbon content in the fines is 71.88% with a relative tracking error $|\overline{e}| = \frac{\overline{x}_{o,C} - x_r}{x_r} = 0.16\%$. Energy consumption of the DMC process in this case is 452.73 kWh.

In comparison with the case when $k_e = 0$, the carbon content tracking error increased from 0 to 0.16%, while the energy consumption decreased by 2.74%.

In order to study the effects of tuning weights on the controller designed, four scenarios with different weighting factors are shown in Table 3.2 where $|\overline{e}|$ and E represent the relative absolute tracking error from the set carbon percentage and energy consumption, respectively. In the table, it can be seen clearly that the energy consumption of the DMC process decreases when k_e increases. By contrast, the absolute mean tracking error of the carbon content elevates during this process. Specifically, when k_e increases from 0 to 0.1, the energy consumption of the DMC process falls by 3.54% and $|\overline{e}|$ rises from 0 to 0.21%.

On the one hand, the coal washing plant studied operates 16 hours per day with 15 DMC modules; the 4.30% energy reduction when k_e increases from 0 to 0.12 translates to a daily energy saving of 9.95 MWh under the same operating condition. This amounts to an annual energy saving of 3.63 GWh. According to the local electricity tariff (see Section 2.7), annual energy cost savings resulting from this reduction are 4.48 million South African rand (approximately equivalent to 0.35 million US dollar). On the other hand, the deviation of carbon percentage in the fines increases by a minimal percentage of 0.26%.

In addition, comparing Figs. 3.4 and 3.5, it is clear that when larger k_e is used, the medium density is manipulated to be lower to reduce the pumping energy. This also leads to changes in the densities of

the DMC overflow and underflow slurries, which ultimately affect the carbon percentages in the fines and rejects.

The effects of the tuning weights suggest that the plant operators should choose the weights according to their preference for the tracking of carbon content in fines and the corresponding energy cost. Therefore, a trade-off must be made.

3.5.3 Influence of measurement uncertainties

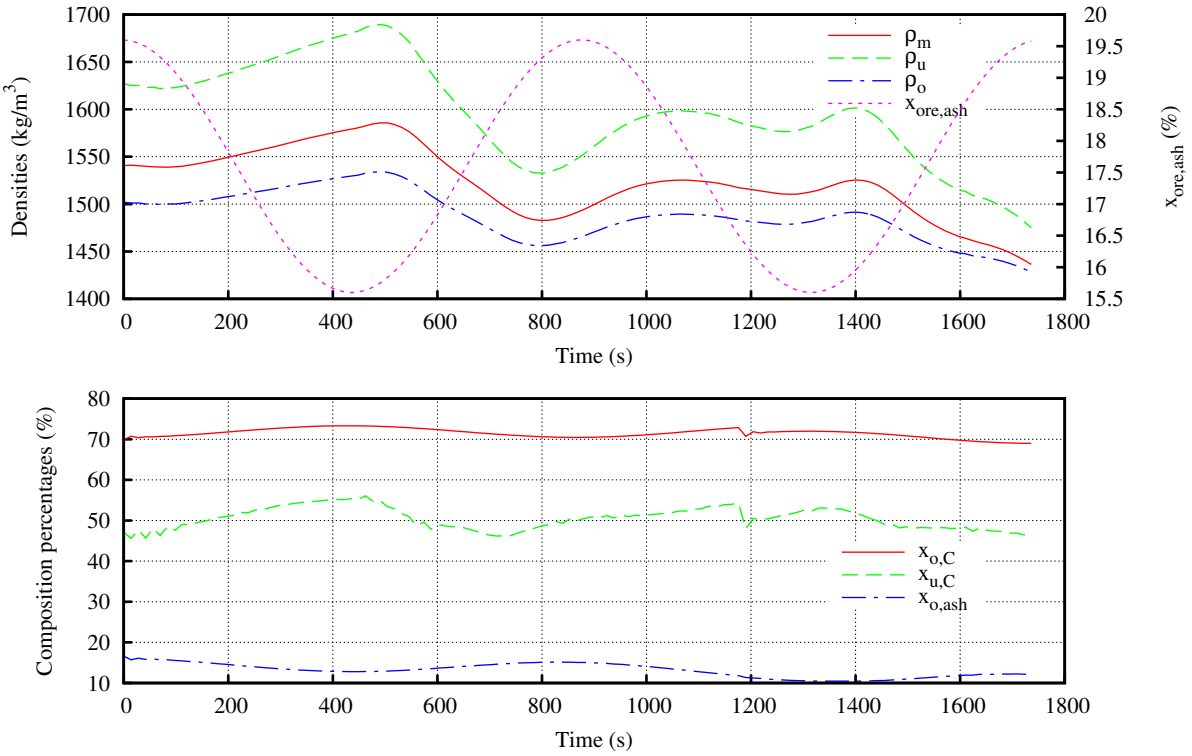

Figure 3.6. Influence of feed ash content

Because of the sample-based measurement of component percentages in the ROM coal, uncertainties brought about by this measurement are unavoidable. To investigate the robustness of the feed-forward controller designed against the measurement uncertainties, the simulation described below is conducted.

A sinusoidal changing disturbance with a magnitude of 2, $w = 2\sin t$, is added to the ash content in the ROM coal, as shown in Fig. 3.2. While the density of the medium optimized according to the available measurements is still implemented, the results are shown in Fig. 3.6 (tuning weights are set

to $k_p = 5000$ and $k_e = 0.1$). The mean percentage of carbon content in the fines resulting from this simulation is 71.46%, incurring a relative tracking error of 0.75% and the energy consumed in this case is 6.74 MWh.

In Fig. 3.6 the time-varying ash content is shown in the first subplot as a dotted line. The carbon tracking results verify that the controller is effective under measurement uncertainties.

In comparison to the situation when no measurement uncertainties are considered (the results given in the fourth row of Table 3.2), the carbon content tracking error increased from 0.21% to 0.75% while energy consumption remains the same.

3.6 CONCLUSION

A model-based control strategy for coal washing dense medium cyclone circuits is proposed. The objective of the control is to guarantee the fine coal quality from DMC output while minimizing energy consumed by the DMC separation process. The controller is designed based on a DMC model derived from mass flow balance and is a feed-forward controller because of the limited measurement available. Simulations are carried out to verify the feasibility and effectiveness of the control approach proposed. The results demonstrate that controlling the density of the medium used for enhancing the separation efficiency of the DMC enables improvement of the desired efficiency of the DMC circuit in terms of improving fine coal quality and reducing energy cost. According to numerical analysis of the results obtained, it is possible to maintain the required coal quality and reduce the annual energy cost of 4.48 million South African rand (0.35 million USD equivalent) for a plant considered in the case study (with 15 DMC modules operating for 16 hours per day). It is also affirmed by simulations that the proposed controller is able to work under measurement uncertainties.

CHAPTER 4 CLOSED-LOOP CONTROL FOR SEPARATION EFFICIENCY

4.1 CHAPTER OVERVIEW

This chapter presents the design of a closed-loop controller for the DMC coal beneficiation process in order to improve its separation efficiency in view of the presence of model-plant mismatch (MPM) and external disturbances. In particular, the DMC model adopted is validated against experimental data to reach an accuracy of the 95%, indicating a 5% mismatch with respect to the actual DMC dynamics. In addition, as an ordinary industrial process, external disturbances are unavoidable in the DMC process. The main motivation for using the closed-loop controller is thus to ensure the robustness of the controller designed under such MPM and external disturbances.

The controller is designed to take advantage of sampled and delayed measurements from the yield of the DMC circuit to close the loop. Details of the controller design, including the challenge incurred in dealing with the sampled and delayed measurements, are shown in Section 4.3. Numerical simulation of the controller designed is presented in Section 4.4. Conclusions are drawn in Section 4.5

4.2 INTRODUCTION

Whereas the feed-forward controller presented in Chapter 3 makes use of feed-forward information to optimize the DMC performance, it is essentially an open loop controller. No feedback information on the quality of the fines processed by the DMC circuit was taken into account because measurement of the required information at the DMC output takes hours and is very costly. Recently, driven by the market demand for better coal quality, coal mining companies have been looking for opportunities to

improve the separation efficiency of the DMC processes by investing in equipment that measures the quality of the yield of the DMC process. However, the new equipment available on the market is only capable of measuring the coal quality with a long delay. In addition, it only gives sampled results, *i.e.*, the measurement device first takes a sample from the output of the DMC circuit and the sample is then analyzed by the the device for a long time before the results can be obtained. A second sample can only be taken after the analysis of the previous sample has been completed. Both the sampled measurement and the long time delay pose technical problems for the design of a feedback solution. On the one hand, it requires the controller to be able to deal with sampled and delayed measurement feedback. On the other hand, controls by sampled and delayed output measurement are of acute control theoretical interest [78, 79, 80], little effort is made to test these new ideas. It is therefore a great challenge to the controller design task.

In this study, a closed-loop MPC approach is employed to optimize the behavior of the DMC plant. Motivations for adopting MPC include its predictive control nature, which helps to deal with sampled measurements [81], its ability to cope with constraints in the design process [82, 83], and its robustness against MPM and external disturbances that inevitably exist [84, 85, 86, 87]. To this end, the controller that is presented takes into account not only the feed-forward measurements but also the feedback measurements from both the output of the DMC and the PSS circuit to ensure its robustness. As discussed in many classical textbooks, closed-loop model predictive controllers inherently possess the property of robustness against modelling uncertainties and external disturbances. This is further evidenced by the fact that MPC is one of the most frequently used control methods in industrial and commercial systems [88, 89, 39]. In particular, application of MPC to address problems raised from energy systems has been studied extensively with great success. For instance, MPC was used in controlling pumping systems [33, 90], trains [91, 92], solar power systems [93] and economic power dispatching [94, 95, 96, 97], etc. In short, MPC has some intrinsic properties that make it suitable for this application. For instance, its state prediction ability is highly desirable for the DMC control under measurement delays. To be exact, with the delayed and sampled measurement, the state of the DMC predicted by an emulation approach is used by the MPC when no actual measurement is available.

The closed-loop control is introduced to determine the optimal control based on the results of the feed-forward controller presented in Chapter 3 such that the performance of the DMC can be improved, especially in the presence of MPM and process disturbances. In such a way, both feed-forward and

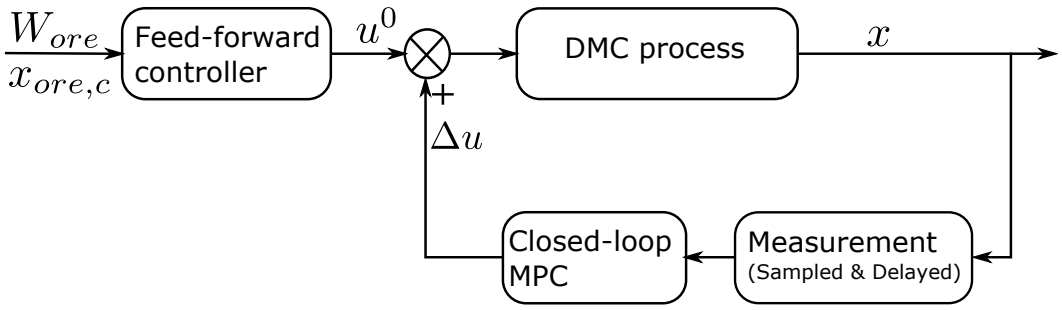

Figure 4.1. Diagram of the closed-loop controller

feedback information on coal quality are taken into account to reach the desired DMC behavior. Results of the feed-forward optimal controller designed in Chapter 3 are used as the baseline to demonstrate the advantages of this design.

The benefits of this design can be summarized as follows:

- Feed coal characteristics are taken into account, which makes the proposed controller robust against variations of the ROM coal quality.
- A closed-loop controller is designed so that performance of the DMC circuit can be maintained despite disturbances and MPM.
- The controller is applicable to similar DMC circuits because it is designed based on a general DMC model.
- It provides a test platform for a delayed and sampled control system.

4.3 CLOSED-LOOP MPC FOR DMC CIRCUITS

The same discretized DMC model shown in equation (3.14) is used for the closed-loop controller design. The DMC state and control achieved by the feed-forward controller are denoted as x^0 and u^0, and the carbon content in the fine product (yield) of the DMC circuit is denoted as $x^0_{o,C}$; the closed-loop MPC is to maintain the carbon content, taking advantage of feedback information x by introducing Δu change to u^0.

Therefore, the objective function for the closed-loop MPC is derived from (3.15) and given as follows

$$\begin{aligned} J = \sum_{i=1}^{N_p} \Big(& k_p \Delta x_{o,C}^2(k+i|k) + k_e \Delta u(k+i-1|k)^2 \\ & + 2k_p [x_{o,C}^0(k+i) - x_r(k+i)] \Delta x_{o,C}(k+i|k) \Big) \\ & + \sum_{i=1}^{N_c} \Big(2k_e u^0(k+i-1) \Delta u(k+i-1|k) \Big), \end{aligned} \tag{4.1}$$

where N_p is the optimization horizon, N_c is the control horizon, k denotes the current time kT_s, $|k$ means that the predicted value is based on the information available from $t = 0$ up to $t = kT_s$, and $\Delta x_{o,C} = x_{o,C} - x_{o,C}^0$ is the change of carbon content resulting from Δu.

As for the constraints, they are transformed into

$$h(\Delta x(k+1|k), \ldots, \Delta x(k+N_p|k), \Delta u(k|k), \ldots, \Delta u(k+N_c-1|k)) \leq \gamma, \tag{4.2}$$

where $\Delta(k+i|k) = x(k+i|k) - x^0(k+i)$ is the change in the state variable with respect to the state reached by the feed-forward controller, the nonlinear function $h(\cdot)$ represents the constraints (3.16)—(3.21) and γ represents the limits derived therein.

As depicted in Fig. 4.1, the feed-forward controller is an open loop controller that optimizes the performance of the DMC, taking into account the feed coal characteristics (W_{ore} and $x_{ore,c}$). Feedback information from the output of the cyclone is used by the closed-loop MPC controller to improve the behavior of the DMC under MPM and external disturbances. The optimal medium density is obtained by adding up the solutions of the feed-forward and the feedback controllers:

$$u = u^0 + \Delta u. \tag{4.3}$$

Therefore, the MPC forms a state feedback control that solves the problem: minimize (4.1) subject to (4.2) and (3.14), iteratively.

To close the loop, measured feedback from the output of the DMC is required. This measurement for the DMC plant is obtained by the new sensor, which yields sampled values at discrete time instances with less than one hour time delay (indicated in Fig. 4.1). This sampled and delayed measurement causes a time interval within which there is no feedback information from the DMC circuit. As a result, the state of the DMC during this period is predicted by the DMC model and updated whenever new measurement is available. Fig. 4.2 shows the scheme of the state prediction.

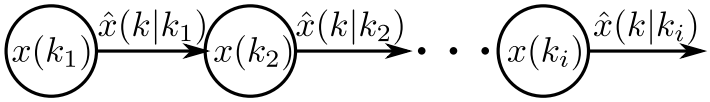

Figure 4.2. State prediction under sampled and delayed measurement

Assume that the measurements are only available at sampling instances $k_1, k_2, \ldots, k_i, \ldots, k_n$, the state of the DMC during the interval (k_i, k_{i+1}) is predicted making use of the most recent measurement, $x(k_i)$ and the controls according to equation (3.14). In other words, the state at next sample instant $k_i + 1$ is simulated by

$$\hat{x}(k_i + 1|k_i) = f(x(k_i), u(k_i|k_i)), \tag{4.4}$$

where $\hat{x}(k_i + 1|k_i)$ represents the predicted state of the DMC process at sampling instance $k_i + 1$ according to the measurements at sampling instance k_i. The same mechanism is used to update the state of the DMC until the next measurement at k_{i+1} is received by the controller.

During the time interval within which no measurement is received, the state predicted based on the most recent measurement according to (4.4) is used by the controller. The measured data are the feedback for the controller to: 1) calibrate the modeling error and 2) improve the behavior of the DMC process according to the actual state. Under process disturbances and MPM, this feedback information is essential to ensure the robustness of the control system.

The work flow of the proposed nonlinear MPC controller is depicted in **Algorithm 1**, where the procedure of state feedback, optimization and control are demonstrated.

4.4 SIMULATION

The same operational data used in Section 3.5.1 are used here. Sampling period T_s is taken as 14 seconds. The optimization and control horizon N_p and N_c are set to 5 and 3, respectively. The set carbon percentage in the fine coal is kept constant as 75% in this chapter instead of 72% to demonstrate the effectiveness of the controllers designed with respect to different set values. The weighting factors for product quality and energy consumption are chosen as $k_p = 5000$ and $k_e = 0.1$. The optimization is done over a simulation period of T, equal to 4.9 hours.

Algorithm 1 Nonlinear closed-loop MPC for DMC circuits

Input: model parameters, x_r, N_p and N_c.

Set $k := 1$.

while $kT_s < T$ **do**

  if *feedback measurements from the yield available* **then**
    Update state prediction according to (4.4).

  end

  Solve the optimization problem within the optimization horizon to obtain the feedback control vector $\Delta u = [\Delta u(k|k), \ldots, \Delta u(k+N_c-1|k)]$.

  Apply the control variable $u^0(k) + \Delta u(k|k)$ to the DMC plant.

  Set $k := k+1$.

end

The feed-forward controller is essentially an open loop controller and its results are taken as reference to investigate the advantages of the designed control approach. In simulations, the results of the feed-forward controller are referred to as open loop results, which take five minutes of a PC with Intel i7-2600 core to solve with Matlab 2010b.

To demonstrate the effectiveness of the proposed control strategy, the MPC results without MPM and disturbances are shown in Fig. 4.3. As this is the ideal case, it shows that the density of the medium is varied in such a way that the carbon percentage in the product is kept almost constant at the set value. The key factor that affects the medium density in this case is the feed rate of the ROM coal.

4.4.1 Model-plant mismatch

In practice, the model used for controller design can usually not capture the exact behavior of the plant accurately and there are always disturbances from other processing occurring at the mine. Both the modeling uncertainties and external disturbances can be represented by

$$x(k+1) = f(x(k), u(k)) + d(k+1), \tag{4.5}$$

where $d(k+1)$ is the term denoting the compounded effect of the modeling uncertainties and external disturbances.

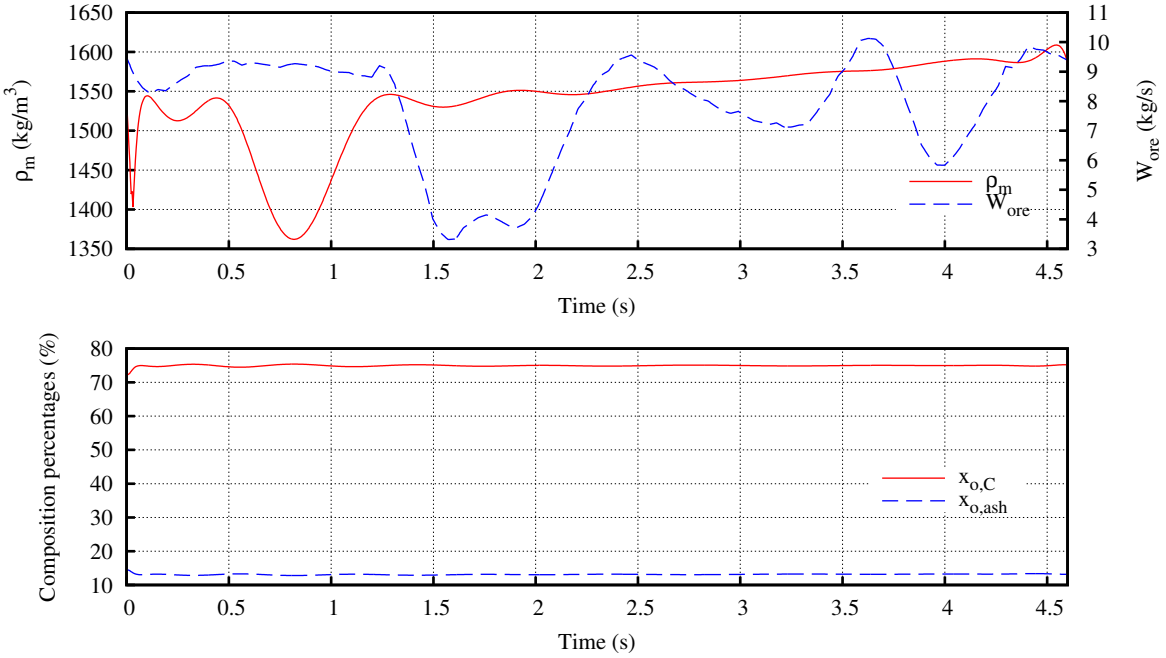

Figure 4.3. Closed-loop MPC results under ideal case

Under the sampled and delayed measurement, the state predicted according to the most recent measurement, $\hat{x}(k|k_i)$, is used in the optimal control during the time interval $[k_iT_s,\ k_{i+1}T_s)$. This means that during the period $[k_iT_s,\ k_{i+1}T_s)$ the control is not based on the actual plant state, which results in control errors. In the closed-loop approach, the measurement data are used to eliminate prediction errors from the model and consequently eliminate control errors and improve the performance of the DMC.

A 5% modeling error is considered, since it has been verified by [62] that the DMC model developed is able to predict the plant behavior within 5% error. Specifically, the error d is assumed to be:

$$d(k) = 0.05x(k)(-1+2\delta(k)), \tag{4.6}$$

where δ is a vector with uniformly distributed random numbers on [0,1].

A comprehensive comparison of the DMC performance between the closed-loop MPC approach and the open loop controller is shown in Fig. 4.4, in which the 5% model-plant mismatch is present for all circumstances. $|\overline{e}|$ in the figure stands for absolute mean tracking error of the controller (as defined in Section 3.5).

According to the results, it is clear that the open loop control strategy for the DMC plant suffers from

carbon percentage deviation in the fine product. 2.09% mean deviation from the set value is observed during the 4.9 hour simulation. To improve this, a closed-loop approach is desirable. All closed-loop results are better than the open loop results, as demonstrated in Fig. 4.4. For instance, the MPC results with one hour measurement delay cause 0.70% deviation in the carbon percentage, which is one third of that with the open loop control.

4.4.2 Measurement delay

Measurement of coal quality from the DMC process usually takes several hours. The mine under investigation is planning to install a new sensor that could shorten this delay to less than one hour. Consequently, to ensure the applicability and effectiveness of the controller, the controller's tolerance on the measurement delay is investigated. Up to two hours' measurement delays are investigated, which is sufficient for practical application as the measurement delay in practice is less than one hour.

As illustrated in Fig. 4.4, one can see that the larger the measurement delay, the worse the performance of the controller. $|\overline{e}|$ of those results show a decreasing trend with the decrease in the measurement delay. Specifically, the tracking error with open loop control is largest (2.09%), while it is smallest with a five-minute measurement delay (0.04%).

Considering that the measurement delay is less than one hour in practice, the closed-loop MPC approach achieves the goal of keeping the carbon content constant with less than or equal to 0.7% tracking error. In comparison with the open loop strategy, the MPC reduces the tracking error by more than 66.5%. This verifies that, even though the DMC feedback information is measured in a sampled and delayed manner, the proposed MPC strategy can improve the performance of the DMC plant significantly.

4.4.3 Implementation disturbance

Disturbance from implementing optimal control is considered here. For the DMC plant, the valve control for the water and make-up medium addition module in the DMC plant results in disturbances in

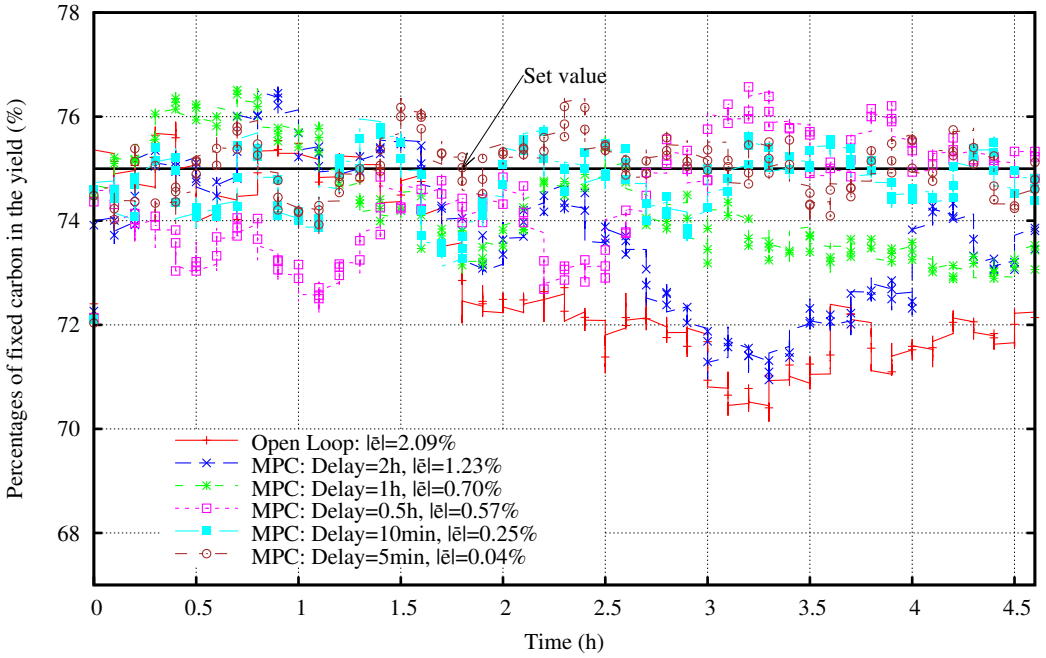

Figure 4.4. Performance comparison under MPM and varying measurement delay

the optimized density of the medium. Therefore, robustness against actuator disturbances is essential for the control approach proposed. Simulations are conducted in this section to verify this.

In simulations, an implementation disturbance is introduced to the control signal, which leads to

$$u_d = u + w,$$

where w is a white Gaussian noise.

The disturbed control signal u_d instead of the optimized u is implemented to the DMC plant under such a situation. The performance of the closed-loop MPC controller and the open loop controller are again compared to investigate the robustness of the closed-loop MPC controller.

It is observed from Fig. 4.5 that, not surprisingly, the closed-loop MPC approach is more effective in achieving the desired DMC performance in comparison to the open loop control. Note that the 5% MPM is also considered in this simulation.

The mean values of the deviations from the specified 75% carbon content in the fines are 2.34% and 1.06% with the open loop controller and the closed-loop MPC with one hour measurement delay, respectively. This verifies that the closed-loop MPC approach is capable of keeping the carbon

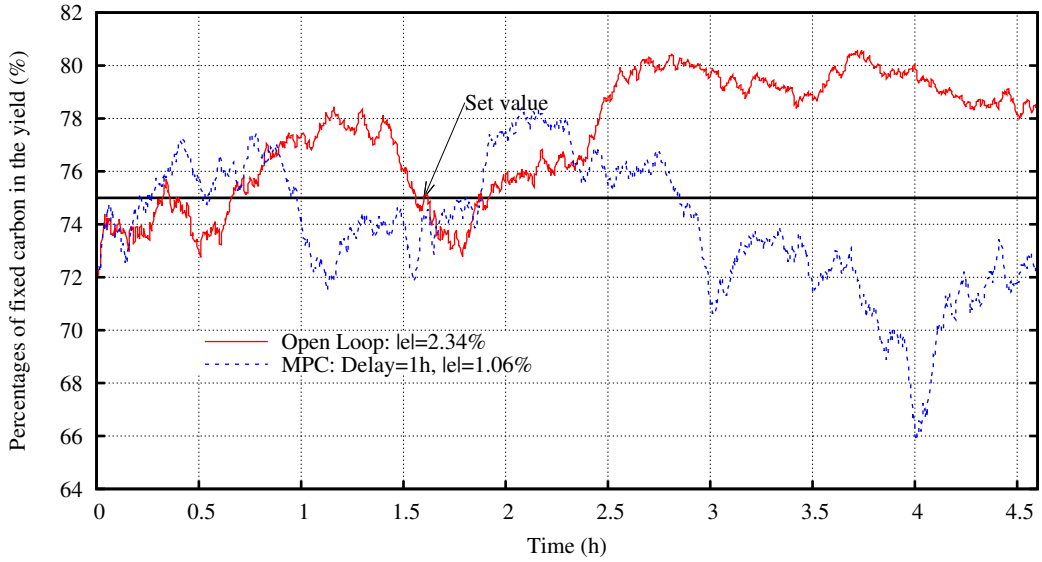

Figure 4.5. Closed-loop MPC vs. open loop control under disturbances

content in the fines to the desired level under the disturbance from implementation of the optimized control.

4.5 CONCLUSION

This study investigates the feasibility and advantages of designing a closed-loop controller to improve the separation efficiency of coal beneficiation dense medium cyclones in the presence of sampled feedback measurements with large delays. A model predictive control approach, which takes advantage of both the feed-forward information on the run-of-mine quality and the sampled and delayed fine coal quality measurement, is proposed to improve the efficiency of the dense medium cyclone plant. The density of the heavy medium used to enhance the separation is taken as the control variable. It is illustrated by simulations that the controller can achieve the desired performance with up to two hours' measurement delay. In addition, the controller is designed based on a general cyclone model, which ensures its applicability to similar dense medium cyclone circuits.

CHAPTER 5 INTEGRATED CONTROL FOR ENERGY AND SEPARATION EFFICIENCY

5.1 CHAPTER OVERVIEW

This chapter presents an integrated control system for the DMC coal washing circuit including control of the medium density profile and control of the medium supply system. Whereas the part of medium density control is an extension of the closed-loop controller designed in Chapter 4, the controller for the medium supply circuit is newly designed in this chapter. Moreover, the medium density control and the medium supply circuit control are integrated together into a dual closed-loop control (DCLC) architecture that features optimization of the medium density profile by the outer loop control using feed-forward and feedback measurements and direct actuator manipulation by the inner loop control in a closed-loop manner. Further, the control system designed in this chapter considers the structural change to the DMC circuit introduced in Chapter 2, which was not considered in the preceding two chapters focusing on separation efficiency improvement. In summary, a complete control system is designed to improve energy and separation efficiency simultaneously for the DMC coal cleaning process.

The DMC coal cleaning process with a PSS is briefly elaborated on in Section 5.3. Mathematical modeling of the medium supply system is shown in Section 5.4. The design of the DCLC is given in Section 5.5. Simulations are presented in Section 5.6. Finally, conclusions are given in Section 5.7.

5.2 INTRODUCTION

So far, the energy efficiency and separation efficiency of the DMC coal beneficiation process have been studied separately, in Chapter 2 and Chapters 3-4, respectively. In particular, PSS was introduced in Chapter 2 to improve energy efficiency. Feed-forward control was designed in Chapter 3 and closed-loop control was designed in Chapter 4 to improve separation efficiency. However, the interplay between the two has not been investigated.

In addition, the two controllers, the open loop one [98] and the closed-loop one [99], only deal with optimization of the density profile of the medium used. A control system for the medium solution preparation process to track the optimized density profile was only studied in a more recent paper published by the author of this thesis and others [100]. While the closed-loop controller is a step forward from the open loop one and the control of the medium preparation circuit helps to complete the control system for the DMC coal cleaning process, the interactions between the DMC process and medium solution preparation process are ignored in the design of all the three controllers. Therefore, a complete design is urgently required to facilitate implementation of the required control. This is one of main purposes of controller design presented in this chapter, from separation efficiency point of view.

From the energy efficiency perspective, the PSS scheme presented in [64] has not been considered by the preceding DMC process controllers designed [98, 99]. Therefore, another aim of the control system designed in this chapter is to take advantage of the PSS scheme to improve the energy efficiency of the DMC coal cleaning process.

With the help of on-site measurement devices/equipment [101] and the PSS structural change, an integrated control system is designed in this chapter to optimize the energy and separation efficiency simultaneously. In particular, the control system designed takes into account the PSS for energy efficiency improvement and considers all measurements available to improve the separation efficiency of the process. The control required is first divided into two layers. The top layer focuses on optimizing the medium density profile according to sampled measurements from the ROM coal (feed-forward) and the output of the DMC (feedback). The lower level aims to track the density set by the upper level controller by means of manipulating actuators, including a water addition valve and a screw conveyor for magnetite addition. These two layers form a dual loop control architecture with the upper level

being the outer loop and the lower level being the inner loop. The plant to be controlled by the outer loop is the DMC, which determines the quality of the fine coal obtained, and the plant to be controlled by the inner loop is the PSS circuit, which supplies medium with proper density to the DMC.

To design such a dual closed-loop controller, mathematical models of both the DMC and the PSS circuit are prerequisites. While the DMC model used in previous chapters of this thesis is still used by the outer loop control, the magnetite circulation circuit is modeled from first principles according to mass flow balance equations.

Another contribution of this design is to display a real industrial system to which the well-known design approach based on feedback decoupling and linearization [102, 103, 104, 105, 106] can be applied.

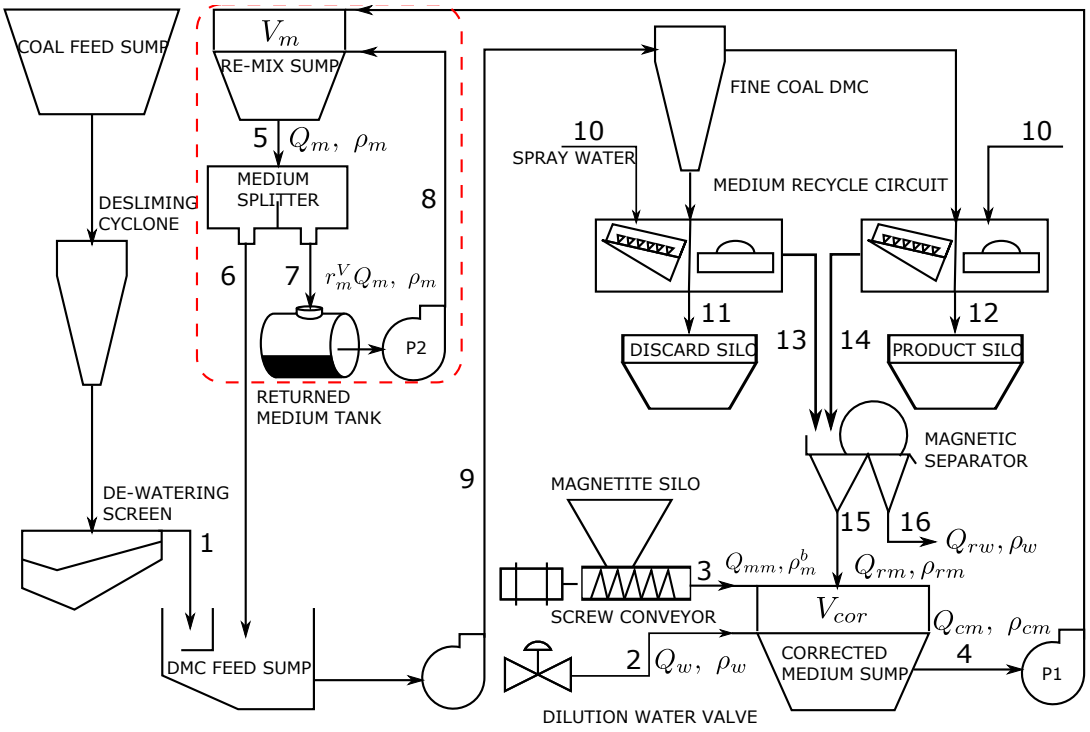

Figure 5.1. DMC coal cleaning process with PSS

5.3 THE DMC COAL CLEANING PROCESS WITH PSS

Fig. 5.1 shows the schematic diagram of a DMC coal washing process operating with the PSS presented in Chapter 2. For ease of readability, this process is briefly described again in this section. Before

entering the DMC process, the ROM coal is first processed by a de-slimming cyclone and de-watering screen, after which it (flow stream marked as 1 in Fig. 5.1) is fed to the DMC feed sump where it is blended with the dense medium (flow stream 6). This mixed coal and medium slurry (flow stream 9) is then fed to the DMC for separation. In the DMC, the carbon content and impurities of the ROM coal are separated and exit at the top and bottom of the DMC, respectively. These two streams of slurries from the output of the DMC are subject to drain and rinse screens to remove magnetite from the product and the discard. The final outputs are stored in the product silo and discard silo respectively for further processing and the diluted medium slurries (flow streams 13 and 14) are then collected and sent to a magnetic separator for magnetite recovery.

The recovered medium (flow stream 15) is in the form of condensed magnetite and is fed to a corrected medium sump, where extra magnetite and water are added to formulate the required medium solution with the proper density. The valve used to add water and the screw conveyor used to add magnetite to the corrected medium sump are the actuators that can be controlled to adjust the density of the medium and therefore determine the fine coal quality. The whole process starts with the in-flows, flow streams 1, 2 and 3, to the DMC circuit and ends at flow stream 15, which enters the corrected medium sump. This process is repeated constantly with new ROM coal being beneficiated.

The PSS scheme is integrated into the controller design of this chapter such that energy efficiency and separation efficiency of the DMC coal beneficiation process can be improved simultaneously. Consequently, the process to be controlled in this chapter is the DMC coal preparation process with a PSS that operates similar to the original configuration but with an extra medium circulation loop that decreases the energy consumption of the process without risking the quality of fine coal, as shown in Fig. 5.1, where a tank is used to store the returned medium, which is pumped back to the re-mix sump.

To facilitate the dual-loop controller design, mathematical models of the DMC, the medium supplying circuit, and the medium recycling process must be established. Whereas the DMC model defined in equation (3.14) is still used, the models of the PSS and the magnetite recycle process are developed in this chapter before the controller design is discussed. In particular, modeling of the magnetite recovering process is shown in Section 5.4.1 and modeling of the slurry flows in the PSS circuit is done in Section 5.4.2.

5.4 MODELING OF THE MEDIUM SUPPLY SYSTEM

Mathematical models of the magnetite recycling process and the PSS circuit supplying dense medium to the DMC are presented in this section. This is first done for the magnetite recycle process and then for the PSS.

5.4.1 The magnetite recycling process

The medium trapped in the under- and overflows of the DMC outputs is subject to drain and rinse screens for magnetite recycling. The diluted medium collected under the screens is then sent to the magnetic separator for subsequent magnetite recovery, as shown in Fig. 5.1. Studies have shown that in the DMC circuit, the medium entering the DMC can only be recycled by a certain percentage because of losses in the circulation [107]; therefore, the mass flow rate of condensed magnetite from the output of the magnetic separator can be obtained by considering magnetite losses and the mass flow balance of the magnetic separator. In this modeling process, the following assumptions are made:

1. Magnetite loss due to the drain and rinse screens is a fraction of the magnetite entering the DMC process. In other words, β percent of the magnetite entering the DMC will reach the magnetic separator for magnetite recovery.

2. The separation efficiency of the magnetic separator is a constant η_s, meaning that η_s percent of the magnetite entering the separator will be separated from the diluted medium slurry.

3. The processing delay inside the magnetic separator is negligible.

4. The condensed magnetite from the outlet of the magnetic separator has a stable density, ρ_{rm}.

Since the interest here is to determine the amount of magnetite recovered, the dirty water from the outlet of the magnetic separator is not considered in the modeling process.

With the above assumptions, one can calculate the mass flow rate of magnetite carried in the diluted medium that reaches the magnetic separator according to the following process. Firstly, according to

the composition of the medium entering the DMC, it can be found that

$$\begin{cases} Q_{cm}\rho_m = \rho_m^p Q_m^p + \rho_w Q_w, \\ Q_{cm} = Q_m^p + Q_w, \end{cases} \tag{5.1}$$

which leads to

$$Q_m^p = \frac{Q_{cm}(\rho_m - \rho_w)}{\rho_m^p - \rho_w}, \tag{5.2}$$

where Q_m^p and ρ_m^p represent the volume flow rate and density of the magnetite particles carried in the dense medium. Q_w and ρ_w represent the volume flow rate and density of water contained in the medium solution.

$$Q_{cm} = (1 - r_m^V)Q_m$$

is the volume flow rate of the medium flowing into the DMC process.

Therefore, the mass flow rate of magnetite reaching the magnetic separator can be obtained by

$$m_m = \beta Q_m^p \rho_m^p = \frac{\beta \rho_m^p Q_{cm}(\rho_m - \rho_w)}{\rho_m^p - \rho_w}, \tag{5.3}$$

where m_m denotes the mass flow rate of the magnetite reaching the magnetic separator according to assumption 1 above.

Following equation (5.3) and assumptions 2-4, the volume flow rate of the condensed medium can be obtained as

$$Q_{rm} = \frac{\eta_s \beta Q_{cm} \rho_m^p (\rho_m - \rho_w)}{\rho_{rm}(\rho_m^p - \rho_w)}. \tag{5.4}$$

This equation will be used in the design process of the controller for the inner loop controller for medium supplying circuit incorporated with the PSS model.

5.4.2 The PSS

The PSS scheme is shown in Fig. 5.2, in which the two circulation loops of the medium are clearly shown. The PSS option introduces an extra loop (the PSS LOOP shown in Fig. 5.2) to improve energy efficiency of the plant. To facilitate controller design, the densities of slurry flows within the PSS scheme must be mathematically modeled. This is achieved by using mass flow balance method.

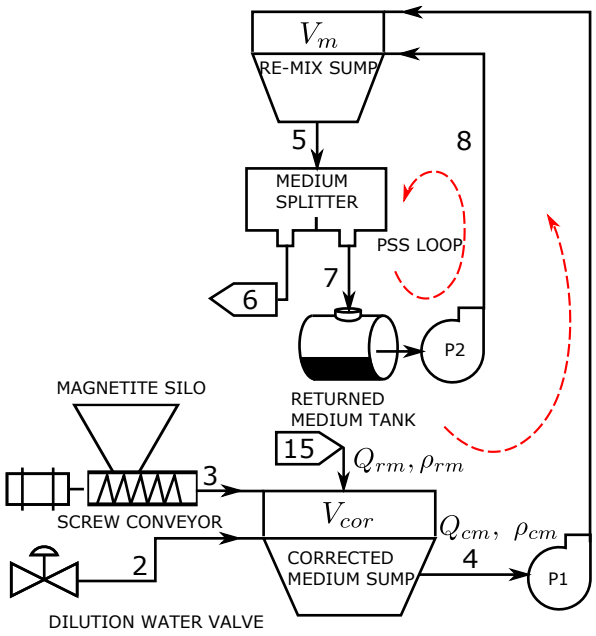

Figure 5.2. PSS scheme

According to the mass balance of the re-mix sump, the density of medium that enters the DMC feed sump and DMC thereafter can be modeled by the following equation:

$$V_m \frac{d\rho_m}{dt} = -Q_m\rho_m + r_m^V Q_m \rho_m + Q_{cm}\rho_{cm}, \tag{5.5}$$

where $Q_{cm} = (1 - r_m^V)Q_m$ is the volume flow rate of the corrected medium (it also equals the flow rate of medium that enters the DMC, as explained in the preceding subsection), ρ_{cm} is the density of the corrected medium from the corrected medium sump, and V_m is the volume of the re-mix box, where the medium flows back and the corrected medium are mixed.

In Fig. 5.2, the circuit to control the density of the medium supplied to the DMC process, ρ_m, is also shown in the left bottom part. As stated earlier, it is the density of the medium supplied to the DMC that affects the quality of fine coal obtained. Proper control of this density is therefore essential. To obtain better control, it is proposed that a screw conveyor to be used to fulfill the purpose of magnetite addition to the circuit. The main benefit of using a screw conveyor is the improved precision of the magnetite addition compared to the conventional split box module. The density ρ_m is adjusted by controlling the volume flow rates of water, Q_w, and magnetites, Q_{mm}, to the corrected medium sump. The density of the corrected medium can be obtained using

$$V_{cor} \frac{d\rho_{cm}}{dt} = -Q_{cm}\rho_{cm} + Q_{rm}\rho_{rm} + Q_w\rho_w + Q_{mm}\rho_m^p, \tag{5.6}$$

where V_{cor} is the volume of medium in the corrected medium sump, Q_{rm} and ρ_{rm} are the volume flow

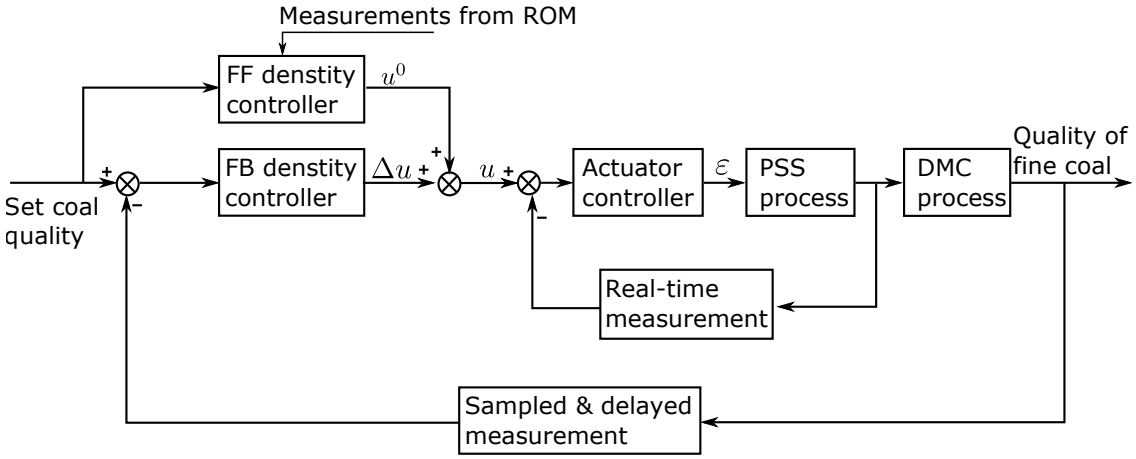

Figure 5.3. Diagram of the dual-loop controller

rate and density of the magnetite recovered by the magnetic separator (flow stream 15 in Fig. 5.2). Q_{mm} is the volume flow rate of the make-up magnetite particles added by the screw conveyor, respectively. The volume change of the medium in the corrected medium sump is described by

$$\frac{dV_{cor}}{dt} = Q_{rm} + Q_w + Q_{mm} - Q_{cm}. \tag{5.7}$$

Both actuators, the screw conveyor and the water addition valve, are linear devices. In particular, the volume flow rate of the linear valve is a function of the fluid density and valve position. The following equation is used to relate the volume water flow rate to the valve position:

$$Q_w = C_w l_w \sqrt{\frac{\Delta P}{\rho_w}}, \tag{5.8}$$

where C_w is the valve coefficient, l_w is the valve position in percentage, and ΔP is the pressure drop across the valve.

The speed of the motor driving the screw conveyor belt can be related to the volume flow rate of the magnetite particles by the following equation [108]:

$$Q_{mm} = Q_0 \frac{\rho_m^b}{\rho_m^p} N, \tag{5.9}$$

where Q_0 is a conveyor belt capacity related constant, ρ_m^b is the bulk density of the magnetite and N is the speed of the motor in rpm.

5.5 CONTROLLER DESIGN

The diagram of the control system designed in this chapter is depicted in Fig. 5.3, where the dual-loop control is clearly shown. In this figure, the FF density controller and the FB density controller refers to the feed-forward control and feedback control of the outer loop controller, respectively.

Algorithm 2 Outer loop control

Input: model parameters, x_r, N_p and N_c.

Set $k := 1$.

while $kT_s < T$ **do**

Feed-forward control:

if *measurements from ROM available* **then**

Solve feed-forward control problem to obtain $u^0 = [u^0(k), u^0(k+1), \ldots, u^0(k+\frac{T}{T_s}-1)]$.

end

Closed-loop MPC:

if *measurements from output of DMC available* **then**

Update state prediction according to (4.4).

end

Solve closed-loop MPC to obtain $\Delta u(k+i|k)$ for $i = 0, 1, \ldots, N_c - 1$.

Calculate $u(k+i|k) = u^0(k+i) + \Delta u(k+i|k)$.

Send $u(k+i|k)$, $i = 0, 1, \ldots, N_c - 1$, to the inner loop controller and execute **Algorithm 3**.

Set $k := k+1$.

end

5.5.1 Outer loop controller

For the outer loop, the controller designed in Chapter 4 is used with a slight modification. This is due to the fact that the DMC process itself is not affected by the PSS circuit introduced and that the same measurements of the feed ore quality and fines yield from the output of the DMC are available. To be exact, the FF and FB density controllers shown in Fig. 5.3 are the feed-forward controller designed in Chapter 3 and the closed-loop controller designed in Chapter 4, respectively.

To fit in the dual-loop architecture, the controller designed in Chapter 4 is modified to work in the way given in **Algorithm 2**, where the complete procedure of the outer loop control incorporating both the feed-forward and feedback control is demonstrated.

5.5.2 Inner loop controller

The primary aim of the inner loop controller is to track the optimal density profile set by the outer loop controller by manipulating the actuators, namely the water addition valve and the magnetite addition conveyor. This essentially requires the design of a controller for the PSS circuit. In Section 5.5.2.1, a state-space model of the PSS circuit (together with the magnetite recovery process model) is developed, followed by a detailed design of the inner loop controller.

5.5.2.1 PSS state-space model

To facilitate the inner loop controller design, the equations developed in Section 5.4 are modified to a state space model. The state space model is then used to design the inner loop controller to adjust the density of medium to track the density profile set by the outer loop controller.

If one denotes the state variable of the PSS as

$$\zeta = [\dot{V}_{cor}, V_{cor}, \dot{\rho}_{cm}, \rho_{cm}, \rho_m]^T,$$

and the control variables as

$$\varepsilon = [\dot{l}_w, \dot{N}]^T,$$

the following equations can be derived from equations (5.5)–(5.9):

$$\dot{\zeta}_1 = \frac{\eta_s \beta \rho_m^p (1-r_m^V)^2 Q_m^2}{V_m \rho_{rm} (\rho_m^p - \rho_w)} (\zeta_4 - \zeta_5) + C_w \sqrt{\frac{\Delta P}{\rho_w}} \varepsilon_1 + \frac{\rho_m^b}{\rho_m^p} Q_1 \varepsilon_2, \tag{5.10}$$

$$\dot{\zeta}_2 = \zeta_1, \tag{5.11}$$

$$\dot{\zeta}_3 = \frac{1}{\zeta_2}\left[-(1-r_m^V) Q_m \zeta_3 + \frac{\eta_s \beta \rho_m^p (1-r_m^V)^2 Q_m^2}{V_m (\rho_m^p - \rho_w)} (\zeta_4 - \zeta_5) - \zeta_1 \zeta_3 + C_w \sqrt{\Delta P \rho_w} \varepsilon_1 + Q_1 \rho_m^b \varepsilon_2 \right], \tag{5.12}$$

$$\dot{\zeta}_4 = \zeta_3, \tag{5.13}$$

$$\dot{\zeta}_5 = \frac{(1-r_m^V) Q_m}{V_m} (\zeta_4 - \zeta_5). \tag{5.14}$$

Take

$$\phi = [\phi_1, \phi_2]^T = [\zeta_2, \zeta_5]^T$$

as output, these equations can be represented by a nonlinear state-space model

$$\begin{aligned} \dot{\zeta} &= h(\zeta, \varepsilon), \\ \phi &= l(\zeta), \end{aligned} \tag{5.15}$$

where $h(\cdot)$ and $l(\cdot)$ are nonlinear functions representing the PSS circuit model.

5.5.2.2 Inner loop controller design

It can be seen that (5.15) is a non-linear model. It can, however, be decoupled and linearized using state feedback, as shown in this section [102, 103].

Introduce the following coordinate transformation

$$z = T(\zeta) = \begin{bmatrix} z_1 \\ z_2 \\ z_3 \\ z_4 \\ z_5 \end{bmatrix} = \begin{bmatrix} \phi_1 \\ \dot{\phi}_1 \\ \phi_2 \\ \dot{\phi}_2 \\ \ddot{\phi}_2 \end{bmatrix},$$

where $\dot{\phi}$ and $\ddot{\phi}$ represent the first and second derivatives of ϕ, respectively.

It then follows that

$$\begin{aligned} \dot{z}_1 &= z_2, \\ \dot{z}_2 = \dot{\zeta}_2 = \zeta_1 &= \frac{\eta_s \beta \rho_m^p (1 - r_m^V)^2 Q_m^2}{V_m \rho_{rm} (\rho_m^p - \rho_w)} (\zeta_4 - \zeta_5) + C_w \sqrt{\frac{\Delta P}{\rho_w}} \varepsilon_1 + \frac{\rho_m^b}{\rho_m^p} Q_1 \varepsilon_2, \\ \dot{z}_3 &= z_4, \\ \dot{z}_4 &= z_5, \\ \dot{z}_5 &= \phi_2^{(3)}, \end{aligned}$$

where $\phi_2^{(3)}$ is the third derivative of ϕ.

Denote

$$\Theta = \frac{\eta_s \beta \rho_m^p (1 - r_m^V)^2 Q_m^2}{V_m \rho_{rm} (\rho_m^p - \rho_w)} \text{ and } \Theta_m = \frac{(1 - r_m^V) Q_m}{V_m},$$

$\phi^{(3)}$ can be found by following

$$\dot{\phi}_2 = \dot{\zeta}_5 = \Theta_m(\zeta_4 - \zeta_5),$$

which yields

$$\ddot{\phi}_2 = \ddot{\zeta}_5 = \Theta_m(\dot{\zeta}_4 - \dot{\zeta}_5) = \Theta_m\left[\zeta_3 - \Theta_m(\zeta_4 - \zeta_5)\right],$$

which gives

$$\begin{aligned}
\phi_2^{(3)} &= \frac{d\ddot{\phi}_2}{dt} = -\Theta_m\left[\dot{\zeta}_3 - \Theta_m(\dot{\zeta}_4 - \dot{\zeta}_5)\right] \\
&= \frac{\Theta_m}{\zeta_2}\left[-(1-r_m^V)Q_m\zeta_3 + \Theta\rho_{rm}(\zeta_4 - \zeta_5) - \zeta_1\zeta_3 + C_w\sqrt{\Delta P\rho_w}\varepsilon_1 + \rho_m^b Q_1\varepsilon_2\right] \\
&- \Theta_m^2\left[\zeta_3 - \Theta_m(\zeta_4 - \zeta_5)\right] \\
&= \Theta_m^3(\zeta_4 - \zeta_5) - \Theta_m^2\zeta_3 + \frac{\Theta_m}{\zeta_2}\left[-(1-r_m^V)Q_m\zeta_3 + \Theta\rho_{rm}(\zeta_4 - \zeta_5) - \zeta_1\zeta_3\right] \\
&+ \frac{\Theta_m}{\zeta_2}\left[C_w\sqrt{\Delta P\rho_w}\varepsilon_1 + \rho_m^b Q_1\varepsilon_2\right]
\end{aligned}.$$

Now denote the derivatives of $\dot{z}_2$ and $\dot{z}_5$ as the new input variables

$$v = \begin{bmatrix} \dot{z}_2 \\ \dot{z}_5 \end{bmatrix},$$

The original system (5.15) can be transformed into a new linear system in z coordination as follows:

$$\begin{aligned}
\dot{z} &= Az + Bv, \\
\phi &= Cz,
\end{aligned} \tag{5.16}$$

where

$$A = \begin{bmatrix} 0 & 1 & 0 & 0 & 0 \\ 0 & 0 & 0 & 0 & 0 \\ 0 & 0 & 0 & 1 & 0 \\ 0 & 0 & 0 & 0 & 1 \\ 0 & 0 & 0 & 0 & 0 \end{bmatrix}, B = \begin{bmatrix} 0 & 0 \\ 1 & 0 \\ 0 & 0 \\ 0 & 0 \\ 0 & 1 \end{bmatrix}, \text{ and } C = \begin{bmatrix} 1 & 0 & 0 & 0 & 0 \\ 0 & 0 & 1 & 0 & 0 \end{bmatrix}.$$

v is the new control variable in the z coordination defined by

$$v = F(\zeta) + T\varepsilon, \tag{5.17}$$

where

$$F(\zeta) = \begin{bmatrix} \Theta(\zeta_4 - \zeta_5) \\ \Theta_m^3(\zeta_4 - \zeta_5) - \Theta_m^2\zeta_3 + \frac{\Theta_m}{\zeta_2}[(r_m^V - 1)Q_m\zeta_3 + \Theta\rho_{rm}(\zeta_4 - \zeta_5) - \zeta_1\zeta_3] \end{bmatrix},$$

$$T = \begin{bmatrix} C_w\sqrt{\frac{\Delta P}{\rho_w}} & \frac{\rho_m^b}{\rho_m^p} \\ \frac{\Theta_m C_w}{\zeta_2}\sqrt{\Delta P\rho_w} & \frac{\Theta_m\rho_m^p Q_1}{\zeta_2} \end{bmatrix}.$$

It is straightforward that the new linear system shown in equation (5.16) is controllable and in a Brunovsky canonical form [102]. Therefore, the original nonlinear system can be controlled by designing the new control variable v. After v has been found, the original control ε can be determined by

$$\varepsilon = T^{-1}(-F(\zeta)+v). \tag{5.18}$$

Note that the inverse of T exists since the determinant of T

$$\det T = \frac{C_w\sqrt{\frac{\Delta P}{\rho_w}}\rho_m^b Q_1}{\zeta_2}\left(1-\frac{\rho_w}{\rho_m^p}\right) \neq 0,$$

because $\rho_w \neq \rho_m^p$.

After the model has been linearized, it is further discretized to be

$$\begin{aligned} z(k+1) &= A_d z(k) + B_d v(k), \\ \phi(k) &= C_d z(k), \end{aligned} \tag{5.19}$$

where A_d, B_d and C_d are matrices obtained by applying the zero-order holder method with sampling period of T_s^{in} to the continuous model (5.16). Note that $T_s^{in} \leq T_s$ must hold in order for the dual-loop control to work properly.

A model predictive controller is again designed based on (5.19) to complete the inner loop controller design. With the main aim of tracking the set density profile and the secondary aim of minimizing control effort, the following stage objective function is adopted for this inner loop model predictive controller:

$$J^{in} = \sum_{i=1}^{N_p^{in}} [\phi(k+i|k) - r(k+i|k)]^T \begin{bmatrix} k_v & 0 \\ 0 & k_d \end{bmatrix} [\phi(k+i|k) - r(k+i|k)] + \sum_{j=0}^{N_c^{in}-1} k_c \varepsilon(k+j|k)^2, \tag{5.20}$$

where k_v, k_d and k_c are weighting factors, N_p^{in} and N_c^{in} are the predictive horizon and control horizon of the inner loop MPC, respectively.

$$r(k+i|k) = \begin{bmatrix} V_{set} \\ u(k+i-1|k) \end{bmatrix}$$

is the vector consisting of the set volume of medium in the corrected medium sump and density set by the outer loop controller. It is noticed that the following relationship:

$$N_p^{in} T_s^{in} \leq N_c T_s,$$

should hold all the time because the optimal density profile set by the outer loop control is defined over the interval $[kT_s,\ (k+N_c-1)T_s]$.

The constraints are those of the upper and lower limits of the state variable and the control variable:

$$\begin{aligned} \zeta_{min} \leq \zeta(k) \leq \zeta_{max}, \\ \varepsilon_{min} \leq \varepsilon(k) \leq \varepsilon_{max}, \end{aligned} \tag{5.21}$$

where the subscripts *min* and *max* denote the lower and upper limits, respectively.

Therefore, the inner loop MPC control solves the problem minimize (5.20) subjective to (5.21) iteratively. The solution obtained at each sampling instant is implemented in the receding horizon control manner as shown in **Algorithm 3**.

Algorithm 3 Inner loop control

Initialization: model parameters, N_p^{in} and N_c^{in}.

Set $k^{in} := 1$.

Get $u(k+i|k)$, $i = 0,1,\ldots,N_c-1$ from the outer loop controller.

while $k^{in}T_s^{in} < T_s$ **do**

1. Obtain state feedback measurements from the PSS circuit.
2. Solve the inner loop control problem to obtain $\varepsilon(k^{in}+j|k^{in})$, $j = 0,1,\ldots,N_c^{in}-1$.
3. Send $\varepsilon(k^{in}|k^{in})$ to the actuators for implementation.
4. Set $k^{in} := k^{in}+1$.

end

5.6 SIMULATION

Simulations in this chapter are done based on the same coal processing plant used in the previous chapters together with a PSS introduced in Chapter 2. That is, 15 coal washing DMC modules run 16 hours per day. The same set of parameters shown in Table3.1 are used. Additional parameters introduced in this chapter are shown in Table 5.1.

$T_s = 14$s is used to discretize the DMC model for the outer loop control as discussed in the preceding two chapters and $T_s^{in} = 0.01$s is used to discretize the PSS circuit model for the inner loop control.

Table 5.1. Parameters of DMC circuit with a PSS

Variable	Value	Unit
ρ_m^b	2580	kg/m^3
ρ_m^p	3500	kg/m^3
r_m^V	0.75	–
β	0.97	–
η_s	0.98	–
V_{cor}^{max}	2	m^3
V_m	1	m^3
h_1	60	m
h_2	20	m
η_p	0.8	–
g	9.80	kg/s
C_w	0.2×10^{-3}	m^3/h·Pa
ΔP	100	kPa
Q_1	1.18×10^{-5}	m^3/s

5.6.1 The benchmark

The designed control system is compared to the open loop feed-forward control designed in Chapter 3, which is used as a benchmark. The reason for this is that the current practices of coal beneficiation plants use rule-of-thumb based control for separation efficiency, which differs from time to time and from case to case. Unified results can therefore not be obtained for comparison purposes. In addition, PSS is not introduced to coal washing plants. This choice of the baseline is also in accordance with the principles of energy efficiency measurement and verification [109, 65]. Lastly, using the open loop control as benchmark shows the improvements presented in this chapter compared to the author's previous work.

Performance of this open loop controller will be presented together with that of the DCLC in the following section. It is therefore not listed separately to avoid repetition (refer to Chapter 3 for more details). It should be noted that since this benchmark already uses an improved controller, performance

improvements reported in this chapter are not a direct comparison between the designed system and the industrial practice. It only gives a very conservative indication of the potential energy and separation efficiency improvements.

5.6.2 Performance indicators

Performance indicators with respect to which the control system designed will be compared to benchmark control are the separation efficiency and energy efficiency. In particular, fine coal quality, measured by carbon content deviation from the set value in the fines, is used as separation efficiency indicator and is defined as

$$QI = [e_{min}, e_{ave}, e_{max}],$$

where e_{min}, e_{ave} and e_{max} are the minimum, mean and maximum deviation from the set value of the carbon content in the fine coal, respectively.

Daily energy consumption of the 15 DMC modules is used as energy efficiency indicator. For the benchmark, this energy (kWh) is calculated by

$$E_B = 15 \int_0^T \frac{u(t) Q_m g h_1}{3600000 \eta_p} dt,$$

where T is the daily operational time, g is gravitational acceleration, h_1 is the differential head of the corrected medium pump, and η_p is the combined efficiency of the corrected medium pumping system. The number 3600000 is a unit conversion factor.

For the system proposed in this study, the daily energy consumption (kWh) is calculated by

$$E_{DCLC} = 15 \int_0^T \left(\frac{\rho_{cm}(t) Q_{cm} g h_1 + u(t) r_m^V Q_m g h_2}{3600000 \eta_p} \right) dt,$$

where h_2 is the differential head of the secondary pump severing the PSS.

5.6.3 Dual closed-loop control

In addition to parameters provided at the beginning of this section, the predicting and control horizons of the outer loop and inner loop controllers are set as $N_p = 7$, $N_c = 5$, $N_p^{in} = 8$, and $N_c^{in} = 4$. In addition, the coal feed rate to the DMC circuit is kept constant at $W_{ore} = 9.42$ kg/s in simulations to verify the effectiveness of the DCLC.

5.6.3.1 Robustness against MPM and disturbances

One of the properties of closed-loop control is its ability to deal with disturbances and MPM. This is demonstrated here. In particular, the model used for controller design can usually not capture the exact behavior of the plant accurately and there are always disturbances from other processing at the mine. It has been explained in Section 4.4.1 that both the modeling uncertainties and external disturbances can be represented by equation (4.5). The same disturbance signal is used in the following simulations to demonstrate the robustness of the controller that was designed.

Since the disturbances introduced by (4.5) are random in nature, the average performance indicators of 20 simulation runs of the DMC with the designed control system and the benchmark controller are compared to provide a fair comparison. The performance indicators, as well as graphs, in the following sections will be focusing on the average figures.

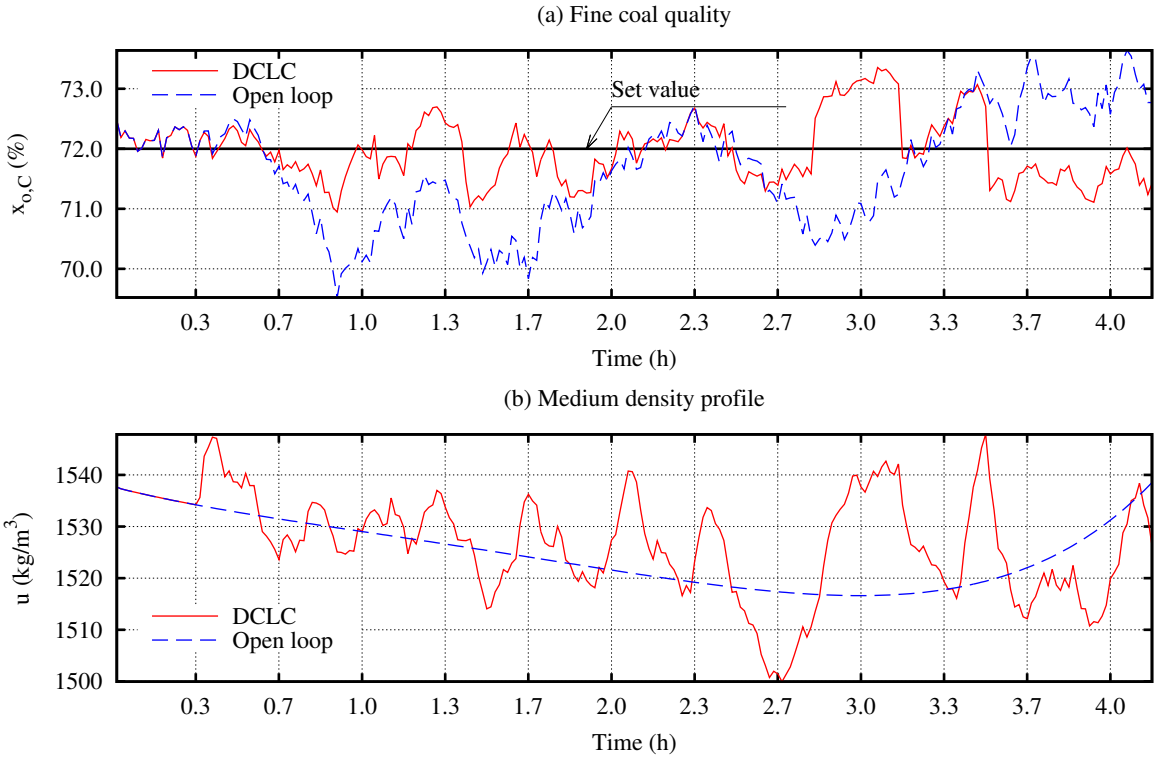

Figure 5.4. Comparing the DCLC to the benchmark: outer loop control

Figs. 5.4–5.5 show the comparison between the designed DCLC and the benchmark control system subject to 5% disturbance in case of 20 minutes of measurement delay. Fig. 5.4 presents the average

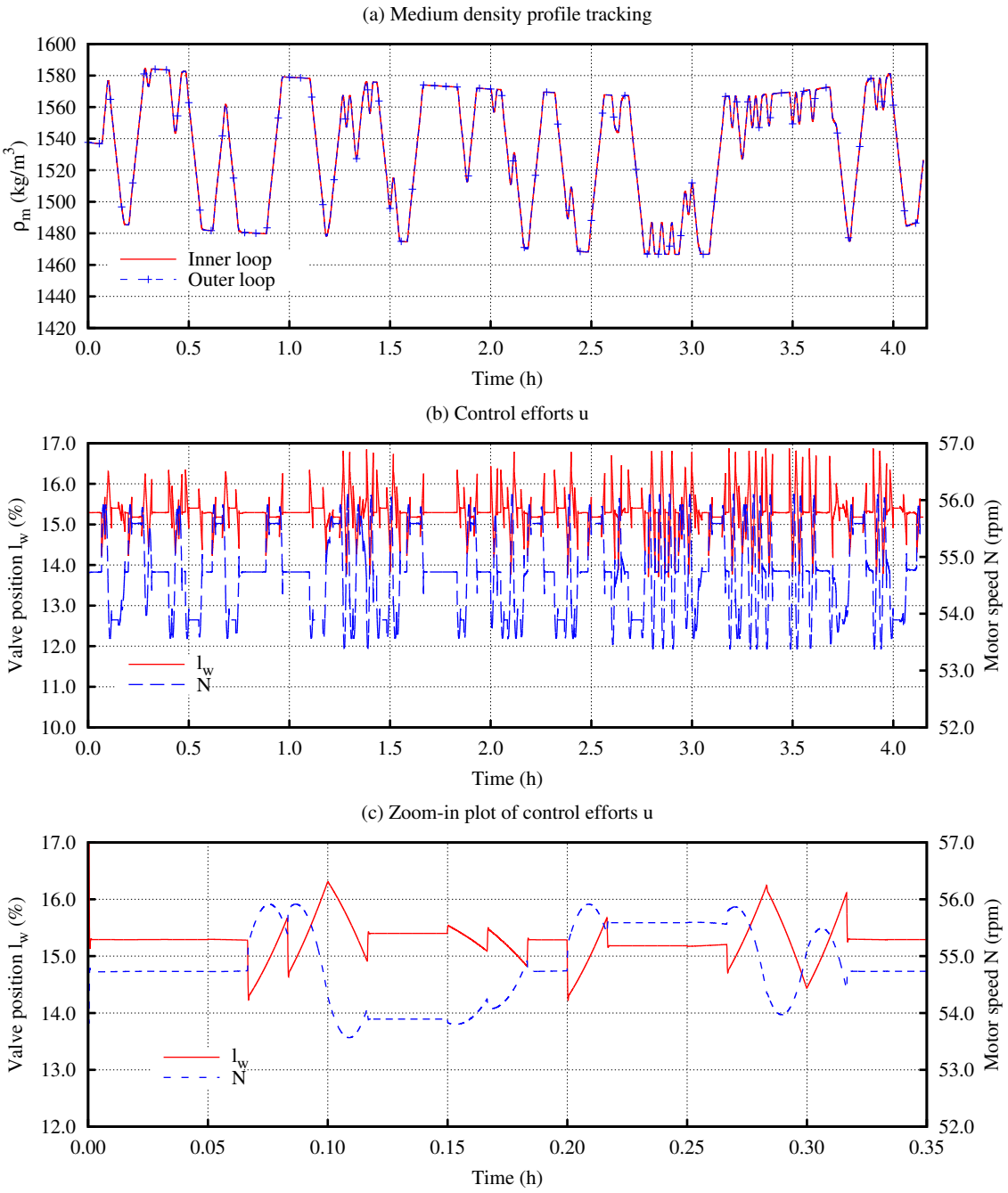

Figure 5.5. Performance of inner loop control

fine coal quality indicator and the medium density profile obtained by the DCLC and the benchmark controller, respectively.

From these figures, one can conclude that the DCLC is superior to the benchmark controller in terms of improving fine coal quality from the output of the DMC circuit. It can be seen that while the coal quality deviates from the set level during the period without feedback measurement, the DCLC is able to correct this deviation whenever new measurement is received. For ease of readability, the horizontal grid in Fig. 5.4 is set to be the same as the measurement delay (20 minutes). It is clear that in the case the DCLC is used, the percentage of carbon content in the fine coal is driven to shift closer to the set value every 20 minutes. By contrast, the benchmark controller does not have the capability, as indicated by the dotted line in the first subplot of Fig. 5.4. Detailed quantitative analysis of the result achieved is presented in the following section.

Fig. 5.5 is presented to demonstrate that the inner loop controller is able to realize the optimal medium density profile set by the outer loop control. In this figure, the first subplot reveals that the inner loop is capable of tracking the medium profile set by the outer loop control with high accuracy. The second subplot shows the actuator actions to realize the medium profile in the first subplot. A zoomed-in plot of the second subplot for the time period [0, 0.35 h] is given in the third subplot for a clearer view. The minimum and maximum deviations between the optimal density set by the outer loop controller and that achieved by the inner loop control are, respectively, 0.208×10^{-2} kg/m^3 and 0.37 kg/m^3 with the mean and standard deviations at 1.58×10^{-6} kg/m^3 and 2.28×10^{-4} kg/m^3.

5.6.3.2 Impact of the measurement delay

In addition to disturbances, measurement delay incurred for the feedback measurement is another key parameter that affects the performance of the controller designed. It is essential to investigate the impact of measurement delays on the performance of the DMC circuit. Therefore, performance indicators are compared under varying sampling delays to reveal the impact of the measurement delay.

A detailed comparison is shown in Table 5.2. It is again noticed that these results are obtained with the same disturbance introduced in the preceding section and the reported figures are average values of 20

simulation runs to be representative.

Table 5.2. Performance indicators under varying measurement delays

Measurement delay (min)	QI_{DCLC} (%)	QI_B (%)	E_{DCLC} (kWh)
5	[-6.18, -0.00, 4.77]	[-67.03, -0.32, 13.66]	4069.34
20	[-12.56, -0.02, 6.13]	[-67.07, -0.32, 13.66]	4122.81
30	[-4.60, -0.08, 2.58]	[-8.51, -0.49, 5.02]	4072.14
60	[-5.79, -0.17, 3.85]	[-10.61, -0.81, 6.12]	4075.60
120	[-27.19, -0.18, 9.29]	[-100.00, -1.98, 10.92]	4073.70

The daily energy consumption with the benchmark control is not listed in Table 5.2 because it is a constant value of $E_B = 8172.18$ kWh, since the control is open loop and feedback measurement has no effect on the control inputs. From data presented in Table 5.2, it can be seen that in general the shorter the delay is, the better the performance indicators are. Specifically, the mean deviation from the set value achieved by the DCLC varies from 0% to 0.18% when the measurement delay increases from five minutes to two hours. More significantly, the magnitude of the minimum deviation, which is of the utmost concern for the quality of the coal, increased from 6.18% to 27.19% in the course. In particular, there is a sharp increase when the delay increases from one hour to two hours (369.60%). This essentially suggests that an on-site measurement device that is able to take measurements with less than one hour delay will lead to dramatic quality improvement in the yield of the DMC circuit. Looking at the results reached by the benchmark control, the fine coal quality achieved is of a more random nature, as evidenced by the fact that the minimum deviation changes without a clear trend linked to the measurement delay. This is mainly due to the random nature of the disturbances and the open loop characteristics of the control.

In addition to the data shown in Table 5.2, Fig. 5.6 gives a visual demonstration of the performance of the DCLC under measurement delays together with the disturbances. It can be seen that before the first feedback measurement is received by the DCLC, the DMC process follows the open loop feed-forward control (the benchmark). After that, the DCLC corrects the carbon content deviation according to the feedback measurement. As clearly indicated in the figure, after the point of measurement delay, the percentage of carbon content in the fines becomes closer to the set value. This percentage then again deviates from the set value during the period without measurement because of the sampled measurement. However, this is again corrected as soon as the new measurement becomes available.

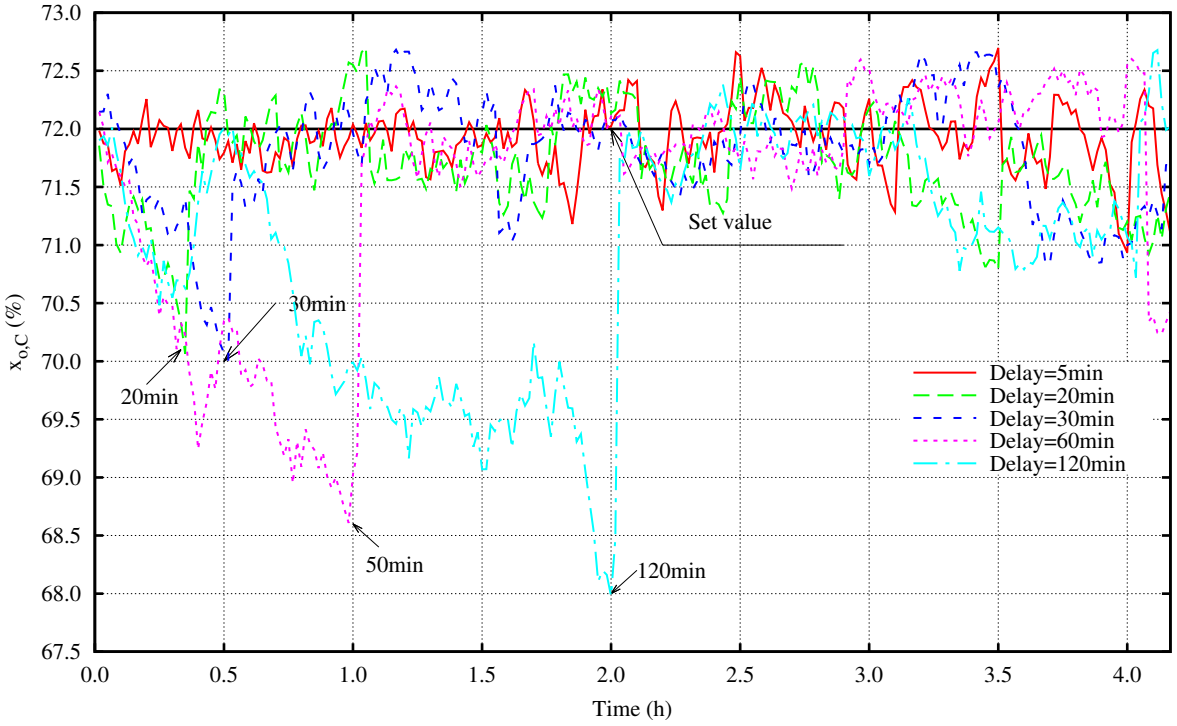

Figure 5.6. Performance comparison under varying delays

5.7 CONCLUSION

The controller designed in this study has several advantages over existing control methods for dense medium coal cleaning processes. Firstly, the controller is designed using advanced approaches such as feedback decoupling, linearization and MPCs. Secondly, the controller presented is capable of making use of both feed-forward and feedback measurements to control the operation of the process optimally, combining the power of open loop feed-forward control and closed-loop feedback control. Thirdly, the controller is designed considering a pumped-storage system in order to reduce energy consumption/cost of the plant, enabling it to improve the energy efficiency and the separation efficiency of the dense medium coal beneficiation process simultaneously. Lastly, the controller designed consists of two loops, with each loop dedicated to its own functionality. Results obtained from a case study verify that the controller presented is superior to the benchmark control in terms of improving both the separation efficiency and energy efficiency of the process.

CHAPTER 6 CONCLUSION AND FUTURE WORK

This thesis focuses on two aspects of a dense medium cyclone coal beneficiation process, namely energy efficiency and separation efficiency, because of the interest in emission reduction, resource conservation and efficient utilization. These two aspects have been fully studied and solutions to improve them are presented. In particular, a pumped-storage scheme is presented to address energy efficiency improvement and control systems are designed to improve the separation efficiency of the process. In this section, the major contributions of this thesis are summarized, together with a brief look into future research activities in this area.

6.1 CONCLUSION

It has been found that improving the energy and separation efficiency of the DMC coal washing circuit is an integrated task although the efficiency of the two can be improved separately. Both individual and integrated approaches to address the efficiency of the both have been proposed in the preceding four chapters (from Chapter 2 to Chapter 5). The main contributions and findings of these chapters are summarized in the following section.

For energy efficiency improvement, a unified pumped-storage system offering two practical options is presented in Chapter 2. It is found that the PSS can effectively reduce energy consumption as well as energy cost for the DMC coal cleaning process. A reduction of more than 50% in energy consumption and the associated cost can be achieved with proper design and operation strategy presented. It is also noted that the PSS scheme has the potential to reduce the energy cost of the process under time-of-use based electricity tariffs by means of shifting power demand from peak hours to off-peak hours. Life cycle cost analysis of the application of the PSS in a case study demonstrated that the PSS

scheme proposed is an economically viable option for energy efficiency improvement of the DMC coal beneficiation process.

For separation efficiency improvement, two types of controllers, one open loop and one closed-loop, are designed in Chapter 3 and Chapter 4, respectively. While both of these controllers that have been designed are superior to the current industrial practice of medium density control of the DMC circuit, it is expected that these two controllers will find their best application in coal processing plants according to different scenarios. The open loop feed-forward controller will suit the case where measurement on the quality of the fines yield from the output of the DMC circuit is not available. The closed-loop controller is recommended for cases where measurement of the fine coal quality is practiced because it will result in better separation efficiency than open loop control. Simulations conducted based on operational data from a real-world coal washing plant validated the effectiveness of the two controllers. It is concluded that whereas both controllers can improve the separation efficiency of the process under consideration, taking into account model-plant mismatch and external disturbances, the closed-loop one is superior to the open loop one because it can further improve the performance of the DMC, taking advantage of feedback measurements. In addition, the measurements available to the controllers are all sampled and delayed, posing challenges for controller design. The controllers designed in these two chapters are based on advanced model predictive control method, which is able to predict the future behavior of the DMC to combat this challenge. To this end, it can be concluded that model predictive control is a suitable control method for the DMC coal cleaning process.

Lastly, an integrated control system to address both the energy efficiency and separation efficiency of the DMC process is designed in Chapter 5. This integrated control system takes into account the interplay between energy and separation efficiency and offers a way to improve both of them simultaneously. To achieve this, a dual closed-loop control system is designed, with the outer loop taking care of the separation efficiency by optimally determining the density profile of the medium supplied to the DMC and the inner loop focusing on actuator manipulation to track the density profile set by the outer loop. In the meantime, the PSS scheme developed in Chapter 2 is adopted to improve energy efficiency of the process. The medium flows in the PSS and the magnetite recovery circuit of the DMC coal washing circuit are mathematically modeled for the controller design. The inner loop PSS circuit controller and a modified version of the closed-loop controller designed in Chapter 4 together form a dual closed-loop control system that provides a complete solution to the DMC coal beneficiation process in terms of energy and separation efficiency improvement. This dual closed-loop

control is again verified by a case study to show its effectiveness.

6.2 FUTURE WORK

Moving forward, the research presented in this thesis can be further improved in the following aspects:

1) New structural changes to the DMC coal beneficiation process can be investigated to further improve the energy- and cost-effectiveness of the circuit. For instance, it is noticed in the study that the medium supplying circuit adjusts the medium density at the bottom of the plant by adding magnetite and water to the corrected medium sump. The medium with corrected density is then pumped up to the DMC process by the corrected medium pump. The energy efficiency of this process can be further improved by introducing another structural change to the DMC circuit. That is, mount the corrected medium sump at the same height in the DMC process. In this manner, the pump will only be responsible to pump the diluted medium from the medium recovery circuit, thus reducing pumping energy consumption. To supply make-up magnetite to the corrected medium sump, a conveyor belt can be used. The benefit of doing this is threefold. Firstly, the energy efficiency of the conveyor belt is usually better than that of slurry pumps, which leads to further energy efficiency improvement. Secondly, the conveyor belt will have much lower maintenance cost compared to that of the slurry pumps, thus offering economic benefits. Thirdly, the conveyor belt can be used in conjunction with a magnetite storage device to shift electricity demand from the peak period to the low period. Supplying water to this newly allocated corrected medium sump can be done by a normal water pump, which is less expensive than slurry pumps. Therefore, there is a need to study and investigate the feasibility and benefits of this kind of new structural changes to the DMC coal beneficiation process.

2) The DMC model adopted in this thesis has an accuracy of 95%. Therefore, it will be beneficial to investigate possible improvements to this model in terms of modeling accuracy in order to improve controllers designed in this thesis further.

3) It is also possible to investigate the optimization of the ratio of ROM coal and medium feed into the DMC in order to improve the separation efficiency of the process. A preliminary attempt to study

this effect was made in [110]. However, in-depth study of this aspect of the DMC coal beneficiation process is needed. A combined control system approach to control both the medium density and the ROM coal feed rate is therefore a possible way forward for future research.

4) A systematic energy management system for plant-wide optimization of the coal beneficiation plant is another way forward for future study. This mainly includes plant-wide scheduling of the throughput of the system components, such as the ROM coal feeding conveyor belt, and optimal control of the DMC process, taking into account the varying ROM coal feed rate to minimize the energy cost of the plant.

The topics listed above are, in the author's opinion, some aspects of the DMC coal beneficiation process that need further investigation in terms of energy efficiency and separation efficiency.

REFERENCES

[1] U.S. Energy Information Administration, "Annual energy outlook 2015," U.S. Department of Energy, Tech. Rep. DOE/EIA-0383(2015), 2015.

[2] J. L. Kohler, J. Sottile, and D. S. Placha, "Process control of heavy-media systems for coal-preparation plants," *IEEE Transactions on Industry Applications*, vol. IA-23, no. 2, pp. 382–388, 1987.

[3] G. H. Luttrell, J. N. Kohmuench, and R.-H. Yoon, "An evaluation of coal preparation technologies for controlling trace element emissions," *Fuel Processing Technology*, vol. 65-66, pp. 407 – 422, 2000.

[4] V. Gupta and M. Mohanty, "Coal preparation plant optimization: A critical review of the existing methods," *International Journal of Mineral Processing*, vol. 79, no. 1, pp. 9 – 17, 2006.

[5] K. Vatopoulos, D. Andrews, J. Carlsson, I. Papaioannou, and G. Zubi, "Study on the state of play of energy efficiency of heat and electricity production technologies," European Commission, Tech. Rep. EUR 25406 EN, 2012.

[6] R.-H. Yoon, G. T. Adel, and G. H. Luttrell, "Process and apparatus for separating fine particles by microbubble flotation together with a process and apparatus for generation of microbubbles," Virginia Tech Intellectual Properties, Inc., US patent US4981582 A, 1988.

[7] G. H. Luttrell, "Hydrodynamic studies and mathematical modeling of fine coal flotation," Ph.D. dissertation, Virginia Polytechnic Inst. and State Univ., Blacksburg, USA, 1986.

[8] G. H. Luttrell and R.-H. Yoon, "The collectorless flotation of chalcopyrite ores using sodium sulfide," *International Journal of Mineral Processing*, vol. 13, no. 4, pp. 271 – 283, 1984.

[9] D. Osborne, Ed., *The Coal Handbook: Towards Cleaner Production: Coal Production*, 1st ed. Elsevier, 2013.

[10] A. Noble and G. H. Luttrell, "A review of state-of-the-art processing operations in coal preparation," *International Journal of Mining Science and Technology*, vol. 25, no. 4, pp. 511 – 521, 2015.

[11] P. J. Bethell and G. H. Luttrell, "Coal preparation," in *Encyclopedia of Energy*, C. J. Cleveland, Ed. New York: Elsevier, 2004, pp. 507 – 528.

[12] J. Chen, K. Chu, R. Zou, A. Yu, and A. Vince, "Prediction of the performance of dense medium cyclones in coal preparation," *Minerals Engineering*, vol. 31, pp. 59 – 70, 2012.

[13] K. J. Kindig, "Coal cleaning process," Genesis Research Corporation, US patent EP0608325 A1, 1994.

[14] P. Hines, J. Apt, and S. Talukdar, "Large blackouts in North America: Historical trends and policy implications," *Energy Policy*, vol. 37, no. 12, pp. 5249–5259, 2009.

[15] M. de Nooij, R. Lieshout, and C. Koopmans, "Optimal blackouts: Empirical results on reducing the social cost of electricity outages through efficient regional rationing," *Energy Economics*, vol. 31, no. 3, pp. 342–347, 2009.

[16] C. De Jonghe, B. F. Hobbs, and R. Belmans, "Optimal generation mix with short-term demand response and wind penetration," *IEEE Transactions on Power Systems*, vol. 27, no. 2, pp. 830–839, 2012.

[17] A. Chatterjee, L. Zhang, and X. Xia, "Optimization of mine ventilation fan speeds according to ventilation on demand and time of use tariff," *Applied Energy*, vol. 146, pp. 65 – 73, 2015.

[18] E. M. Wanjiru and X. Xia, "Energy-water optimization model incorporating rooftop water harvesting for lawn irrigation," *Applied Energy*, vol. 160, pp. 521 – 531, 2015.

[19] H. Tazvinga, B. Zhu, and X. Xia, "Optimal power flow management for distributed energy resources with batteries," *Energy Conversion and Management*, vol. 102, pp. 104 – 110, 2015.

[20] Z. Wu, H. Tazvinga, and X. Xia, "Demand side management of photovoltaic-battery hybrid system," *Applied Energy*, vol. 148, pp. 294 – 304, 2015.

[21] B. Numbi and X. Xia, "Systems optimization model for energy management of a parallel HPGR crushing process," *Applied Energy*, vol. 149, pp. 133 – 147, 2015.

[22] X. Ye, X. Xia, L. Zhang, and B. Zhu, "Optimal maintenance planning for sustainable energy efficiency lighting retrofit projects by a control system approach," *Control Engineering Practice*, vol. 37, pp. 1 – 10, 2015.

[23] DOE-SA, "Integrated resource plan for electricity 2010-2030," Department of Energy, Republic of South Africa, Tech. Rep., 2013.

[24] NT-SA, "Carbon tax policy paper–reducing greenhouse gas emissions and facilitating the transition to a green economy," National Treasury, Republic of South Africa, Tech. Rep., 2013.

[25] DOE-SA, "State of renewable energy in South Africa," Department of Energy, Republic of South Africa, Tech. Rep., 2015.

[26] R. Aihara, A. Yokoyama, F. Nomiyama, and N. Kosugi, "Optimal operation scheduling of pumped storage hydro power plant in power system with a large penetration of photovoltaic generation using genetic algorithm," in *2011 IEEE Trondheim PowerTech*, Trondheim, Norway, 19-23 Jun 2011, pp. 1–8.

[27] Á. J. Duque, E. D. Castronuovo, I. Sánchez, and J. Usaola, "Optimal operation of a pumped-storage hydro plant that compensates the imbalances of a wind power producer," *Electric Power Systems Research*, vol. 81, no. 9, pp. 1767–1777, 2011.

[28] X. Zhuan and X. Xia, "Optimal operation scheduling of a pumping station with multiple pumps," *Applied Energy*, vol. 104, pp. 250–257, 2013.

[29] A. Bagirov, A. Barton, H. Mala-Jetmarova, A. Al Nuaimat, S. Ahmed, N. Sultanova, and J. Yearwood, "An algorithm for minimization of pumping costs in water distribution systems using a novel approach to pump scheduling," *Mathematical and Computer Modelling*, vol. 57, no. 3-4, pp. 873–886, 2013.

[30] S. Shu, D. Zhang, S. Liu, M. Zhao, Y. Yuan, and H. Zhao, "Power saving in water supply system with pump operation optimization," in *2010 Asia-Pacific Power and Energy Engineering Conference*, Chengdu, China, 28-31 March 2010, pp. 1–4.

[31] Y. Gong, G. Shen, K. Zuo, and H. S. Shi, "Overview of a few key issues for optimal operation of parallel pumping stations," *Applied Mechanics and Materials*, vol. 212-213, pp. 1217–1222, 2012.

[32] T. Zhao, J. Zhang, and L. Ma, "On-line optimization control method based on extreme value analysis for parallel variable-frequency hydraulic pumps in central air-conditioning systems," *Building and Environment*, vol. 47, pp. 330–338, 2012.

[33] X. Zhuan and X. Xia, "Development of efficient model predictive control strategy for cost-optimal operation of a water pumping station," *IEEE Transactions on Control Systems Technology*, vol. 21, no. 4, pp. 1449–1454, jul 2013.

[34] D. Borkowski, A. Wetula, and A. Bień, "Design, optimization, and deployment of a waterworks pumping station control system," *ISA transactions*, vol. 51, no. 4, pp. 539–49, 2012.

[35] J. Speight, *Handbook of Coal Analysis*. New Jersey: John Wiley & Sons, 2005.

[36] G. Luttrell, G. Adel, and R. Yoon, "Precombustion removal of hazardous air pollutant precursors," Virginia Polytechnic Inst. and State Univ., Tech. Rep. DOE/PC/95154–T7, 1997.

[37] J. Nurkowski, "Coal quality, coal rank variation and its relation to reconstructed overburden, upper cretaceous and tertiary plains coals, Alberta, Canada," *American Association of Petroleum Geologists Bulletin*, vol. 68, no. 285-295, 1984.

[38] A. Kolker, C. Senior, and J. Quick, "Mercury in coal and the impact of coal quality on mercury emissions from combustion systems," *Applied Geochemistry*, vol. 21, no. 11, pp. 1821 – 1836, 2006.

[39] T. Chai, S. Qin, and H. Wang, "Optimal operational control for complex industrial processes," *Annual Reviews in Control*, vol. 38, no. 1, pp. 81–92, 2014.

[40] T. Chai, L. Zhao, J. Qiu, F. Liu, and J. Fan, "Integrated network-based model predictive control for setpoints compensation in industrial processes," *IEEE Transactions on Industrial Informatics*, vol. 9, no. 1, pp. 417–426, 2013.

[41] S. Shah and J. MacGregor, Eds., *Dynamics and Control of Process Systems 2004 (Volume I)*. Elsevier, 2005.

[42] J.-L. Fan, Y.-W. Zhang, and T.-Y. Chai, "Optimal operational feedback control for a class of industrial processes," *Zidonghua Xuebao/Acta Automatica Sinica*, vol. 41, no. 10, pp. 1754–1761, 2015.

[43] W. Dai and T.-Y. Chai, "Data-driven optimal operational control of complex grinding processes," *Zidonghua Xuebao/Acta Automatica Sinica*, vol. 40, no. 9, pp. 2005–2014, 2014.

[44] T. Chai, H. Li, and H. Wang, "An intelligent switching control for the intervals of concentration and flow-rate of underflow slurry in a mixed separation thickener," in *The 19th International Federation of Automatic Control*, Cape Town, South Africa, August 2014, pp. 338–345.

[45] P. Zhou, T. Chai, and J. Sun, "Intelligence-based supervisory control for optimal operation of a DCS-controlled grinding system," *IEEE Transactions on Control Systems Technology*, vol. 21, no. 1, pp. 162–175, 2013.

[46] W. Dai, T. Chai, and S. Yang, "Data-driven optimization control for safety operation of hematite grinding process," *IEEE Transactions on Industrial Electronics*, vol. 62, no. 5, pp. 2930–2941, 2015.

[47] P. Zhou, W. Dai, and T.-Y. Chai, "Multivariable disturbance observer based advanced feedback control design and its application to a grinding circuit," *IEEE Transactions on Control Systems Technology*, vol. 22, no. 4, pp. 1474–1485, 2014.

[48] C. Burgess, "System for controlling separating gravity in dense-media cyclone," Bethlehem Steel Corp., U.S. patent 4470901, 1984.

[49] B. A. Firth, "Dense medium cyclone control – A reconsideration," *International Journal of Coal Preparation and Utilization*, vol. 29, no. 3, pp. 112–129, 2009.

[50] C. Addison, "Development of a multi-stream monitoring and control system for dense medium cyclones," Master's thesis, Virginia Polytechnic Institute and State University, Feb. 2010.

[51] M. Narasimha, M. S. Brennan, and P. N. Holtham, "A review of flow modeling for dense medium cyclones," *Coal Preparation*, vol. 26, no. 2, pp. 55–89, 2006.

[52] T. Napier-Munn, "Modelling and simulating dense medium separation processes – A progress report," *Minerals Engineering*, vol. 4, no. 3C4, pp. 329 – 346, 1991.

[53] M. Narasimha, M. Brennan, P. Holtham, and T. Napier-Munn, "A comprehensive CFD model of dense medium cyclone performance," *Minerals Engineering*, vol. 20, no. 4, pp. 414 – 426, 2007.

[54] K. Chu, B. Wang, A. Yu, A. Vince, G. Barnett, and P. Barnett, "CFD–DEM study of the effect of particle density distribution on the multiphase flow and performance of dense medium cyclone," *Minerals Engineering*, vol. 22, no. 11, pp. 893 – 909, 2009.

[55] K. Chu, B. Wang, A. Yu, and A. Vince, "CFD–DEM modelling of multiphase flow in dense medium cyclones," *Powder Technology*, vol. 193, no. 3, pp. 235 – 247, 2009.

[56] K. Chu, B. Wang, A. Yu, and A. Vince, "Particle scale modelling of the multiphase flow in a dense medium cyclone: Effect of vortex finder outlet pressure," *Minerals Engineering*, vol. 31, pp. 46 – 58, 2012.

[57] L. Shen, Y. Hu, J. Chen, P. Zhang, and H. Dai, "Numerical simulation of the flow field in a dense-media cyclone," *Mining Science and Technology (China)*, vol. 19, no. 2, pp. 225 – 229, 2009.

[58] Y. Tsuji, T. Tanaka, and T. Ishida, "Lagrangian numerical simulation of plug flow of cohesionless particles in a horizontal pipe," *Powder Technology*, vol. 71, no. 3, pp. 239 – 250, 1992.

[59] H. H. Shalaby, "On the potential of large eddy simulation to simulate cyclone separators," Ph.D. dissertation, Chemnitz University of Technology, Jan. 2007.

[60] J. Chen, K. Chu, R. Zou, A. Yu, A. Vince, G. Barnett, and P. Barnett, "How to optimize design and operation of dense medium cyclones in coal preparation," *Minerals Engineering*, vol. 62, pp. 55 – 65, 2014.

[61] D. Sambasivam and A. K. Bhattacharya, "Synthesis of CFD and Monte-Carlo simulations for improved design and operation of dense medium cyclones," *Computers & Fluids*, vol. 96, pp. 47 – 62, 2014.

[62] E. Meyer and I. Craig, "The development of dynamic models for a dense medium separation circuit in coal beneficiation," *Minerals Engineering*, vol. 23, no. 10, pp. 791 – 805, 2010.

[63] G. T. Adel, R.-H. Yoon, and G. H. Luttrell, "Video instrumentation for the analysis of mineral content in ores and coal," Virginia Polytechnic Institute & State University, US patent US5396260 A, 1992.

[64] L. Zhang, X. Xia, and J. Zhang, "Improving energy efficiency of cyclone circuits in coal beneficiation plants by pump-storage systems," *Applied Energy*, vol. 119, pp. 306 – 313, 2014.

[65] Efficiency Valuation Organization (EVO), "International performance measurement and verification protocol: concepts and options for determining energy and water savings," Volume 1, Tech. Rep., 2012.

[66] B. M. A. Bernier and B. Bourret, "Pumping energy and variable frequency drives," *ASHRAE Journal*, vol. 12, pp. 37–40, 1999.

[67] S. Ashok and R. Banerjee, "Load-management applications for the industrial sector," *Applied Energy*, vol. 66, no. 2, pp. 105–111, 2000.

[68] H. Ong, T. Mahlia, H. Masjuki, and D. Honnery, "Life cycle cost and sensitivity analysis of palm biodiesel production," *Fuel*, vol. 98, pp. 131–139, aug 2012.

[69] M. Leckner and R. Zmeureanu, "Life cycle cost and energy analysis of a Net Zero Energy House with solar combisystem," *Applied Energy*, vol. 88, no. 1, pp. 232–241, 2011.

[70] D. G. Cople and E. S. Brick, "A simulation framework for technical systems life cycle cost analysis," *Simulation Modelling Practice and Theory*, vol. 18, no. 1, pp. 9–34, jan 2010.

[71] W. J. Fabrycky and B. S. Blanchard, *Life-Cycle Cost and Economic Analysis*, 1st ed., W. Fabrycky and J. Mize, Eds. Prentice-Hall, 1991.

[72] A. Dell'Isola and S. J. Kirk, *Life Cycle Costing for Facilities*. John Wiley & Sons, 2003.

[73] S. Yard, "Developments of the payback method," *International Journal of Production Economics*, vol. 67, no. 2, pp. 155–167, 2000.

[74] Y. He, "The effects of rheology and stability of magnetite dense media on the performance of dense medium cyclones," Ph.D. dissertation, The university of British Columbia, Apr. 1994.

[75] A. Majumder and J. Barnwal, "Processing of coal fines in a water-only cyclone," *Fuel*, vol. 90, pp. 834–837, 2011.

[76] T. Rabbani, F. Di Meglio, X. Litrico, and A. Bayen, "Feed-forward control of open channel flow using differential flatness," *IEEE Transactions on Control Systems Technology*, vol. 18, no. 1, pp. 213–221, 2010.

[77] C. Schmuck, F. Woittennek, A. Gensior, and J. Rudolph, "Feed-forward control of an HVDC power transmission network," *IEEE Transactions on Control Systems Technology*, vol. 22, no. 2, pp. 597–606, 2014.

[78] T. Ahmed-Ali, I. Karafyllis, and F. Lamnabhi-Lagarrigue, "Global exponential sampled-data observers for nonlinear systems with delayed measurements," *Systems & Control Letters*, vol. 62, no. 7, pp. 539 – 549, 2013.

[79] T. H. Lee, J. H. Park, O. Kwon, and S. Lee, "Stochastic sampled-data control for state estimation of time-varying delayed neural networks," *Neural Networks*, vol. 46, pp. 99 – 108, 2013.

[80] J. Sheng, T. Chen, and S. L. Shah, "Generalized predictive control for non-uniformly sampled systems," *Journal of Process Control*, vol. 12, no. 8, pp. 875 – 885, 2002.

[81] C. García, D. Prett, and M. Morari, "Model predictive control: Theory and practice - A survey," *Automatica*, vol. 25, no. 3, pp. 335–348, 1989.

[82] D. Mayne, J. Rawlings, C. Rao, and P. Scokaert, "Constrained model predictive control: Stability and optimality," *Automatica*, vol. 36, no. 6, pp. 789–814, 2000.

[83] R. Patwardhan, S. Shah, and K. Qi, "Assessing the performance of model predictive controllers," *Canadian Journal of Chemical Engineering*, vol. 80, no. 5, pp. 954 – 966, 2002.

[84] L. Grüne and J. Pannek, *Nonlinear Model Predictive Control: Theory and Algorithms*. Springer-Verlag London Limited, 2011.

[85] J. Gao, R. Patwardhan, K. Akamatsu, Y. Hashimoto, G. Emoto, S. L. Shah, and B. Huang, "Performance evaluation of two industrial MPC controllers," *Control Engineering Practice*, vol. 11, no. 12, pp. 1371 – 1387, 2003.

[86] A. S. Badwe, R. D. Gudi, R. S. Patwardhan, S. L. Shah, and S. C. Patwardhan, "Detection of model-plant mismatch in MPC applications," *Journal of Process Control*, vol. 19, no. 8, pp. 1305 – 1313, 2009.

[87] A. S. Badwe, R. S. Patwardhan, S. L. Shah, S. C. Patwardhan, and R. D. Gudi, "Quantifying the impact of model-plant mismatch on controller performance," *Journal of Process Control*, vol. 20, no. 4, pp. 408 – 425, 2010.

[88] S. J. Qin and T. A. Badgwell, "A survey of industrial model predictive control technology," *Control Engineering Practice*, vol. 11, no. 7, pp. 733–764, 2003.

[89] J. Prakash, S. C. Patwardhan, and S. L. Shah, "State estimation and nonlinear predictive control of autonomous hybrid system using derivative free state estimators," *Journal of Process Control*, vol. 20, no. 7, pp. 787 – 799, 2010.

[90] A. J. van Staden, J. Zhang, and X. Xia, "A model predictive control strategy for load shifting in a water pumping scheme with maximum demand charges," *Applied Energy*, vol. 88, no. 12, pp. 4785 – 4794, 2011.

[91] L. Zhang and X. Zhuan, "Optimal operation of heavy-haul trains equipped with electronically controlled pneumatic brake systems using model predictive control methodology," *IEEE Transactions on Control Systems Technology*, vol. 22, no. 1, pp. 13–22, 2014.

[92] L. Zhang and X. Zhuan, "Development of an optimal operation approach in MPC framework for heavy haul trains," *IEEE Transactions on Intelligent Transportation Systems*, vol. 16, no. 3, pp. 1391–1400, 2015.

[93] B. Zhu, H. Tazvinga, and X. Xia, "Switched model predictive control for energy dispatching of a photovoltaic-diesel-battery hybrid power system," *IEEE Transactions on Control Systems Technology*, vol. 23, no. 3, pp. 1229–1236, 2015.

[94] N. I. Nwulu and X. Xia, "Implementing a model predictive control strategy on the dynamic economic emission dispatch problem with game theory based demand response programs,"

Energy, vol. 91, pp. 404 – 419, 2015.

[95] X. Xia, J. Zhang, and A. Elaiw, "An application of model predictive control to the dynamic economic dispatch of power generation," *Control Engineering Practice*, vol. 19, no. 6, pp. 638 – 648, 2011.

[96] J. Zhang and X. Xia, "A model predictive control approach to the periodic implementation of the solutions of the optimal dynamic resource allocation problem," *Automatica*, vol. 47, no. 2, pp. 358 – 362, 2011.

[97] A. Elaiw, X. Xia, and A. Shehata, "Application of model predictive control to optimal dynamic dispatch of generation with emission limitations," *Electric Power Systems Research*, vol. 84, no. 1, pp. 31 – 44, 2012.

[98] L. Zhang, X. Xia, and J. Zhang, "Medium density control for coal washing dense medium cyclone circuits," *IEEE Transactions on Control Systems Technology*, vol. 23, no. 3, pp. 1117–1122, 2015.

[99] L. Zhang and X. Xia, "A model predictive control for coal beneficiation dense medium cyclones," in *The 19th International Federation of Automatic Control*, Cape Town, South Africa, August 2014, pp. 9810–9815.

[100] L. Zhang, X. Xia, and B. Zhu, "Magnetite and water addition control for a dense medium coal washing circuit," in *Chinese Automation Congress (CAC), 2015*, Wuhan, China, 27–29 Nov 2015, pp. 1744–1749.

[101] K. Gordon, "Can coal ash be accurately analyzed using PGNAA?" 2013, Accessed: 11 July 2013. [Online]. Available: http://acceleratingscience.com/mining/can-coal-ash-can-be-accurately-analyzed-using-pgnaa/

[102] L. Hunt, R. Su, and G. Meyer, "Global transformations of nonlinear systems," *IEEE Transactions on Automatic Control*, vol. 28, no. 1, pp. 24–31, 1983.

[103] X. Xia, "Parameterization of decoupling control laws for affine nonlinear systems," *IEEE Transactions on Automatic Control*, vol. 38, no. 6, pp. 916–928, 1993.

[104] D. Cheng and T.-J. Tarn, "Global external linearization of nonlinear systems via feedback," *IEEE Transactions on Automatic Control*, vol. AC-30, no. 8, pp. 808–811, 1985.

[105] R. W. Brockett, "Feedback invariants for nonlinear systems," in *The Seventh Triennial World Congress*, Helsinki, Finland, 12–16 June 1978.

[106] A. Isidori and A. Krener, "on the feedback equivalence of nonlinear systems," *Systems & Control Letters*, vol. 2, no. 2, p. 809, 1982.

[107] R. Sripriya, A. Dutta, P. Dhall, M. Narasimha, V. Kumar, and B. Tiwari, "An analysis of medium losses in coal washing plants," *International Journal of Mineral Processing*, vol. 80, no. 2-4, pp. 177 – 188, 2006.

[108] Conveyor Eng. & Mfg. Co., *Screw Conveyor components & design*, 2012, version 2.20.

[109] X. Xia and J. Zhang, "Mathematical description for the measurement and verification of energy efficiency improvement," *Applied Energy*, vol. 111, pp. 247 – 256, 2013.

[110] L. Zhang and X. Xia, "An optimization model for reducing energy usage of coal washing plants," in *2014 International Conference on Applied Energy*, Taipei, Taiwan, 30 May - 02 June 2014.